ISTC Reports

Illinois Sustainable Technology Center

Spatial and Source Apportionment Analysis of PAH and Metal Contaminants in the Illinois River's Peoria Pool Sediments

Yonghong Zou
Illinois Sustainable Technology Center

Wei Zheng
Illinois Sustainable Technology Center

ILLINOIS SUSTAINABLE TECHNOLOGY CENTER
PRAIRIE RESEARCH INSTITUTE

RR-131
December 2015
www.istc.illinois.edu

RR-131

Spatial and Source Apportionment Analysis of PAH and Metal Contaminants in the Illinois River's Peoria Pool Sediments

Yonghong Zou
Illinois Sustainable Technology Center

Wei Zheng
Illinois Sustainable Technology Center

December 2015

Submitted to the
Illinois Sustainable Technology Center
Prairie Research Institute
University of Illinois at Urbana-Champaign
www.istc.illinois.edu

The report is available on-line at:
http://www.istc.illinois.edu/info/library_docs/RR/RR131.pdf

Printed by the Authority of the State of Illinois
Bruce Rauner, Governor

ACKNOWLEDGMENTS

This research was funded by the Illinois Sustainable Technology Center (ISTC), a part of the Prairie Research Institute at the University of Illinois at Urbana-Champaign (Grant No. SR2). The authors wish to acknowledge the assistance of John C. Marlin (ISTC) for making sediment analysis data available for this report, providing text on the river and sample collection and preparation, and assisting with editing. The sediment cores and data were collected over several years as part of several projects collectively referred to as the Illinois River sediment project. Several divisions of the Prairie Research Institute contributed to the collection and analysis of samples including the Illinois State Water Survey's James A. Slowikowski; the Illinois Geological Survey's Richard A. Cahill, who also provided helpful comments on drafts; and staff at ISTC. Additional support was provided by the Illinois Department of Natural Resources. Monica Mingione and Lindsay Donovan provided assistance with data entry and figure and table preparation. We thank Nancy Holm (ISTC) for supporting this research.

TABLE OF CONTENTS

LIST OF TABLES

LIST OF FIGURES

LIST OF ABBREVIATIONS AND SYMBOLS

AcNe	acenaphthene
AcNy	acenaphthylene
Al	aluminum
An	anthracene
As	arsenic
Ba	barium
BaA	benz[a]anthracene
BaP	benzo[a]pyrene
BbF	benzo[b]fluoranthene
Be	beryllium
BghiP	benzo[ghi]perylene
BkF	benzo[k]fluoranthene
Ca	calcium
Cd	cadmium
Chy	chrysene
CMB	chemical mass balance
Cr	chromium
Co	cobalt
COD	coefficient of determination
cos φ	cosine φ value
Cu	copper
DBahA	dibenz[a,h]anthracene
DR	diagnostic ratio
dw	dry weight
EF	enrichment factor
FA	factor analysis
Fe	iron
Fl	fluorene
FlA	fluoranthene
HDPE	high density polyethylene
Hg	mercury
ICP	inductively coupled plasma spectroscopy
ICP-MS	inductively coupled plasma spectroscopy-mass spectrometry
IDNR	Illinois Department of Natural Resources
Igeo	geoaccumulation index
IP	indeno[1,2,3-cd]pyrene
IRCC	Illinois River Coordinating Council
ISGS	Illinois State Geological Survey

K	potassium
MDL	method detection limit
Mg	magnesium
Mn	manganese
Mo	molybdenum
Na	sodium
Nap	naphthalene
Ni	nickel
NIST	National Institute of Standards and Technology
PAHs	polycyclic aromatic hydrocarbons
Pb	lead
PCA	principal component analysis
PCBs	polychlorinated biphenyls
PEC	probable effect concentration
V	vanadium
PhA	phenanthrene
PMF	positive matrix factorization
POPs	persistent organic pollutants
Py	pyrene
RL	reporting limit
SPSS	Statistical Package for the Social Sciences
SQGs	sediment quality guidelines
TACO	Tiered Approach to Corrective Objectives
TSS	total suspended solid
TEC	threshold effect concentration
USACE	United States Army Corp of Engineers
U.S. EPA	United States Environmental Protection Agency
Zn	zinc
^{137}Cs	Cesium-137
$\sum_{16}PAH$	total 16 PAHs

ABSTRACT

In this study, sediments from the Peoria Pool of the Illinois River were analyzed for the presence and concentrations of polycyclic aromatic hydrocarbons (PAHs) and metals.

The PAH source apportionment analysis utilized 225 PAH profiles from 10 PAH sources collected through a literature search. The analysis suggested that anthropogenic sources contributed the PAHs while the majority of metals originated from the Earth's crust. Higher PAH concentrations were generally found in sediment cores taken close to the main river channel or the mouths of backwater lakes where they join the river, suggesting an association with main river flows. Concentrations of PAHs in the backwater areas varied considerably.

The source apportionment analysis suggested that coal dust; coal and wood combustion soot; asphalt and coal-tar sealcoat; and traffic emissions are the main sources of PAHs in Illinois River sediments. The analysis also indicated coal dust or an aggregated PAH input from several sources contributed approximately 47 ± 7% of total PAHs in the Peoria Pool sediments; coal combustion (soot) contributed 28 ± 4%; traffic emissions (soot) contributed 15 ± 3%; and wood combustion contributed 5%. The combined gas phase of coal and wood combustion and traffic exhaust accounted for another 5% of the total PAHs.

The analysis indicated that the majority of metals (60%) in the Illinois River sediments were derived from crustal material weathering. Beyond that, industrial emissions contributed slightly more than 20% of the total metals, and traffic emissions accounted for the remaining 20%.

1. INTRODUCTION

1.1 BACKGROUND

The Illinois River is a tributary of the Mississippi River. It is formed by the confluence of the Des Plaines River and the Kankakee River southwest of Chicago and joins the Mississippi River at Grafton, IL, spanning a distance of 227 miles. The Illinois River watershed (Figure 1.1) comprises 32,081 square miles, which includes about 44% of the state's area (Marlin, 2002). It provides water, transportation corridors, recreation, tourism sites, and ecological habitat for much of Illinois.

The commercially navigable Illinois Waterway, with a total distance of 333 miles, was originally established through the construction of the Illinois and Michigan Canal, which connected the Illinois River to the Chicago River. The hydrology of the system changed dramatically in 1900 when the flow of the Chicago River was reversed to carry waste from the Chicago metropolitan area down the river system. During the 1930s, federal locks and dams were built to establish a minimum nine-foot channel for commercial navigation. The stretches of river between navigation dams are called pools. These projects increased the volume of water entering the system, increased its depth, and caused the river to expand over much of the original floodplain. As a result, the water surface area of the Illinois River system approximately doubled. The increased depth reduced the number of bottomland lakes in the Illinois River valley from 378 to 135. These changes altered the habitat in the river valley and introduced pollutants from upstream metropolitan sources. The histories of the alterations to the watershed are discussed at length in Bellrose et al. (1983), Demissie (1997), and Marlin (2002). This study is primarily concerned with the Peoria Pool, which extends from the Peoria Lock and Dam at river mile 157.6 near North Pekin, IL, to the Starved Rock Lock and Dam at river mile 230 near Utica, IL.

Sedimentation is generally acknowledged as the greatest threat to the integrity of the Illinois River and its bottomland lakes, which historically were renowned for their fish and wildlife resources. Bellrose et al. (1983) estimated that by 1979 the average depth of bottomland lakes in the Illinois River Valley was only 2 feet (0.62m). By 1985, the depth of the largest lake, Upper Peoria Lake, was also about 2 feet outside the navigation channel (Demissie and Bhowmik, 1986). Overall, the bottomland lakes lost about 72% of their storage capacity by 1990 (Demissie, 1992). The most recent estimate by the Illinois State Water Survey (ISWS) (Demissie and Keefer, 2013) is that 12.8 million tons of sediment were delivered to the river valley annually from tributary streams between 1981 and 2010. Of this, 7.6 million tons were deposited in the backwater lakes, side channels, bottomland lakes, and floodplains.

State and federal agencies have long considered restoring the ecological and economic qualities of the river. Suggestions have included erosion control to reduce future sedimentation into the river, sediment removal from the river, restoration of floodplain functions, and numerous other activities and projects to enhance habitat and other attributes (Bhowmik et al., 2001; USACE, 2007). The Peoria Pool is a likely location for restoration efforts due to its largely intact floodplain and habitat diversity.

The dredging of sediments to restore water depth is a frequently suggested restoration approach. However, this activity would generate large quantities of dredged material. Traditionally, such material was treated as having no value and was disposed of by dumping it in any convenient area or facility that would accept it, including wetlands and backwaters. Since the 1980s, agencies have increasingly sought to find beneficial uses for dredged material. The Illinois Department of Natural Resources (IDNR) has actively sought uses for the mostly fine-grained sediments in the Illinois River and many of the State's other water bodies. This effort is coordinated by the Illinois Sustainable Technology Center (ISTC), which was once an IDNR division. Potential uses for the sediments include island restoration; construction of elevated habitats; use as fill for construction sites; and as reclaimed topsoil at old industrial sites, landfills, and strip mines (Marlin, 2002). Illinois has completed several such projects under the program named "Mud to Parks." The name came from the first large project which transported Lower Peoria Lake sediment to Chicago for use as topsoil at the former US Steel South Works site. This area is now being converted to a lake-front park. Other projects have used sediments from small lakes and a recreational waterway as reclaimed topsoil at various locations.

The potential uses of sediment from a specific area depend upon its physical and chemical characteristics. For example, some fine-grained sediment may have the texture and organic matter characteristics of good topsoil, but may be unsuitable for use as construction fill. An understanding of soil fertility and potential contaminants is important if sediment is to be used as topsoil or in locations where the introduction of elevated levels of contaminants may impact the environmental or human health. Studies of Peoria Pool sediment indicate that its fertility and soil properties are similar to those of central Illinois topsoil (Darmody and Marlin, 2002). Chemical contaminants in and along the Illinois River, primarily in the Peoria Pool backwater lakes, were evaluated by Cahill (2001) and Cahill et al. (2008). Concentrations of phenolic compounds, chlorinated pesticides, and most PCBs were below reporting limits. PAH compounds (polycyclic aromatic hydrocarbons) were detected at a wide range of concentrations, as were several metals including nickel (Ni), copper (Cu), zinc (Zn), arsenic (As), cadmium (Cd), mercury (Hg), and lead (Pb). The concentrations of metals in most samples did not exceed Illinois' Tiered Approach to Corrective Action Objectives (TACO) regulatory levels for residential soil remediation levels (by ingestion). However, some PAH compounds, especially benzo(a)pyrene (BaP), frequently exceeded the objective levels for rural areas (IEPA, 2013). While TACO is not a topsoil use standard, it is sometimes used as a surrogate to help determine if a soil is suitable for use in a particular application.

While largely agricultural, the watershed upstream of the Peoria Pool is also home to many potential sources of contaminants. It contains the Chicago Metropolitan area, which has been home to steel mills, coke plants, metal plating, and many other industries with PAH and metal emissions. Additionally, oil refineries near Joliet, IL, a steel mill near Henry, IL, and a zinc smelter located in DePue, IL, have all introduced waste into the watershed. The Peoria area is home to heavy equipment manufacturing and the metal-working industries that support it. Over time, these industries have decreased their emissions in response to regulations and better understanding of the impacts of many chemicals on human health and the environment. Home heating during much of the region's history was by wood or coal burning, which emits PAHs.

Identifying possible contaminant sources and quantifying the contributions from different sources to the receiving sediments is of great interest to the government, public, and researchers.

This kind of analysis is called source apportionment analysis, and it has been an active research topic for decades. Many source apportionment analysis algorithms and tools exist. The basic concept in source apportionment analysis is based on the assumption that the pollutants released from the same or similar sources maintain stable compositions. The composition of contaminants from a source is called its fingerprint. Comparing the similarity of the fingerprints is one of the most intuitive source apportionment methods, e.g., cosine φ value (Soonthornnonda et al., 2011). There are also variations of this method, such as the diagnostic ratio (DR) of PAHs (Yunker et al., 2002). In some cases, where the possible sources and their fingerprints are known (or assumed to be known), only the contributions of the sources need to be calculated. This analysis can be done by chemical mass balance (CMB) (Malinowski, 1991).

Another approach is to check the correlations between individual contaminants detected in the receiving media (in this case, the Illinois River sediments). The most widely recognized method using this approach is principal component analysis (PCA) (Jolliffe, 2002). Several advanced methods based on PCA have been developed. These include factor analysis with non-negative constraints (Rachdawong and Christensen, 1997), and positive matrix factorization (PMF) (Paatero, 1997). PMF is one of the source apportionment tools that can generate source fingerprints and contributions simultaneously. It generates the source fingerprints and loadings through non-negative matrix rotation controlled by enhanced penalty terms (Paatero, 1997). The non-negative matrix rotation is considered to be able to produce physically meaningful source fingerprints. The PMF program is generally considered an advanced source apportionment tool.

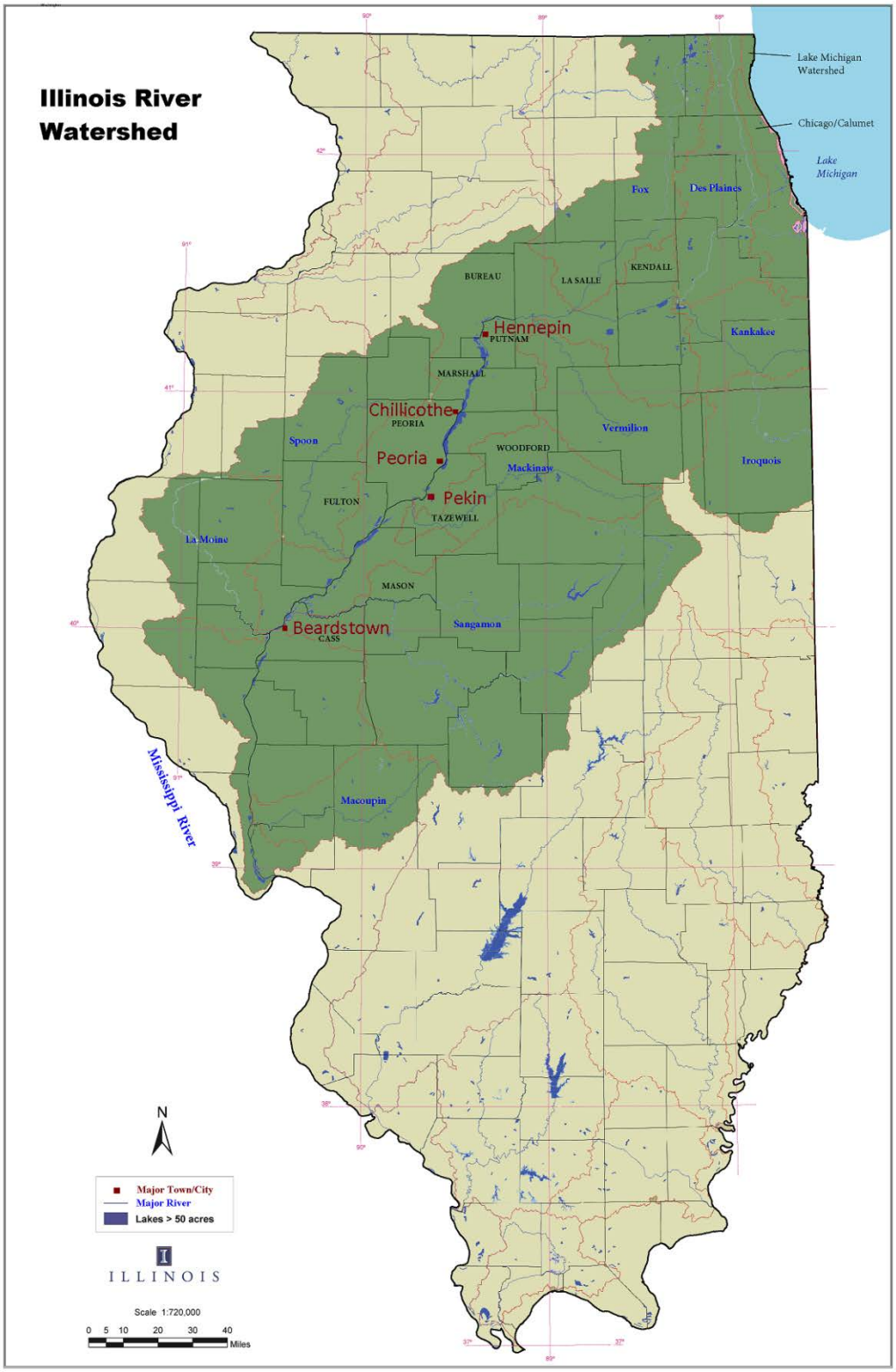

Figure 1.1. Map of the Illinois River watershed.

All these methods have been shown to be applicable in source apportionment analysis of PAH and metal sources in aquatic sediments. Diagnostic ratios derived from a variety of paired PAH compounds have been widely used to determine possible PAH sources (Yunker et al., 2002). PCA is also commonly used in PAH source apportionment analysis (Harrison et al., 1996). Li et al. (2003) applied CMB to estimate PAH sources and contributions in Lake Calumet, Chicago. Christensen and Bzdusek (2005) used factor analysis to estimate PAH sources in sediments of the Black River and the Ashtabula River, OH. However, application of these methods requires insightful understanding of the principles underlying them. Many researchers have concluded that unquestioning application of these models can lead to inappropriate or inaccurate interpretations (Robinson et al., 2006). Therefore, the validation of results is essential for a credible source apportionment analysis, which benefits greatly from good background knowledge.

1.2 STUDY AREAS AND SAMPLE COLLECTION

This report is based on 80 sediment cores collected from the Peoria Pool between 2004 and 2010 (Figures A-1 to A-6) as part of ongoing state and federal river restoration efforts. The majority of the samples were taken from backwater lakes and from the large Upper and Lower Peoria Lakes. A few cores were taken from the navigation channel and a side channel. Several were taken near the boat ramps at the Woodford and Marshall County State Fish and Wildlife Areas. Some cores were collected from locations in portions of bottomland lakes shown on old maps from 1902-1904, prior to the building of navigation dams that resulted in increased water levels (Woermann, 1905). Other sampling locations were on former floodplains, some of which were farmed.

Sediment cores were collected by the Illinois State Water Survey (ISWS) using a vibracore mounted on a pontoon boat. The vibracore uses a steel core tube 10 cm in diameter with high density polyethylene (HDPE) liners. The core tube was designed to obtain cores with a maximum length of about 270 cm, although shorter lengths were obtained when sediment became too dense to penetrate. Details of the vibracore methodology are contained in Slowikowski et al. (2008).

The cores were processed by splitting them in half lengthwise and then dividing them into subsamples for analysis of various parameters. The chemical samples consisted of 2 cm subsample slices of sediment taken every 20 cm, beginning 8 cm from the top of the core. The slices were thoroughly mixed in a stainless steel bowl and sent to the laboratory in a cooler. Whole-core chemical samples contained a mixture of slices from all of the chemical subsamples from a given core. Segment chemical samples contained subsamples from only a portion of a core. For example a core may have a top segment from the first 80 cm of a core and a bottom segment from the remaining 100 cm. In some cases, a whole core sample and one or more segment samples were obtained by using both halves of the split core. In a few instances, a discrete sample was taken. This was usually from a 10 cm section taken for a specific purpose. Had funds not been limited, all cores would have included segment analyses to clearly determine the varying quality of sediment deposited at different times as well as the background material. For this study, data from top segments were used where possible.

1.3 OBJECTIVES

The primary objective of this study was to use several source apportionment methodologies to determine the physical source of PAHs in the sediment. PAHs are found in coal dust and a variety of petroleum and combustion products. Knowing the source of PAHs can help determine the risk associated with their presence. For instance, some PAHs in coal dust may not be available for biological uptake (Meyer et al., 2013). Knowledge of the sources could also help target regulatory efforts. Secondly, the sources of sediment contamination by metals were evaluated. Because there is not as much information on metal fingerprints, metals source apportionment is not as definitive as that for PAHs. However, comparing the metals results with PAH results may help advance future work on metals apportionment. Finally some spatial relationships of contaminants in the pool were examined.

2. POLYCYCLIC AROMATIC HYDROCARBONS (PAHs)

PAHs are a large group of persistent organic pollutants (POPs) containing a structure consisting of two or more fused aromatic rings (Ravindra et al., 2008). PAHs can be released from natural petrogenic materials such as crude oil, oil shale (Ravindra et al., 2008), and coal dust (Stout and Emsbo-Marttingly, 2008). Major anthropogenic sources of PAHs are emissions from pyrogenic processes of carbonaceous materials, especially incomplete combustion (Zhang and Tao, 2009; Shen et al., 2013). These include such materials as soot from coal, wood, diesel, and gasoline combustion (Ravindra et al., 2008), as well as asphalt and coal-tar sealant (Mahler et al., 2005).

Many PAH compounds have been identified. The United States Environmental Protection Agency (USEPA, or simply EPA) has listed 16 priority PAHs, which are acenaphthene (AcNe), acenaphthylene (AcNy), anthracene (An), benz[a]anthracene (BaA), benzo[a]pyrene (BaP), benzo[b]fluoranthene (BbF), benzo[ghi]perylene (BghiP), benzo[k]fluoranthene (BkF), chrysene (Chy), dibenz[a,h]anthracene (DBahA), fluoranthene (FlA), fluorene (Fl), indeno[1,2,3-cd]pyrene (IP), naphthalene (Nap), phenanthrene (PhA), and pyrene (Py). These 16 EPA priority PAHs are frequently targeted in PAH studies. Based on their molecular structures, PAHs are divided into two groups. Lower molecular weight PAHs have two or three rings and include Nap, AcNe, AcNy, Fl, PhA, and An. Higher molecular weight PAHs, which have four or more rings, include FlA, Py, Chy, BaA, BkF, BbF, BaP, DBahA, IP, and BghiP.

The global total annual atmospheric emission of the 16 EPA priority PAHs in 2007 was 504 gigagrams (Gg) (Shen et al., 2013). PAHs have become an environmental concern due to their negative impact on human health, e.g., as carcinogens (ATSDR, 1995; WHO, 2000). Efforts during the last two decades to control PAH releases have led to a reduction of atmospheric emissions from 592 Gg in 1995 to 499 Gg in 2008 (Shen et al., 2013). Even though emissions of PAHs are decreasing, huge amounts of PAHs have accumulated in the environment, resulting in elevated concentrations in air, water, sediments, and soils.

PAHs in sediments are thought to be stabilized by physicochemical association with sediment matrices, and therefore, undergo few changes once combined with sediment (Page et al., 1999; Tobiszewski and Namiesnik, 2012). Thus, PAHs in sediments are often used as a proxy to trace anthropogenic pollutant inputs in the environment (Liu et al., 2013). Information on PAH source identification is of great interest to researchers and regulators. This interest has inspired numerous studies on PAH source apportionment analysis. Widely used source apportionment methods include diagnostic ratios (DR) (Yunker et al., 2002); chemical mass balance (CMB) (Malinowski, 1991); principal component analysis (PCA) (Jolliffe, 2002); factor analysis (FA) with non-negative constraints (Rachdawong and Christensen, 1997); positive matrix factorization (PMF) (Paatero, 1997); and Unmix (Henry, 2003). These methods generally rely on the PAH profile (i.e., proportions of PAH compounds) in samples to identify specific sources.

The fate and transport of PAHs, including their release to the atmosphere and deposition to aquatic sediments, are dynamic and complex. Degradation, gas-particle phase partitioning, and air-water and water-sediment redistribution or mixing during airborne transport and sedimentation will alter PAH compositions. This alteration of the original PAH profiles hinders source apportionment analysis (Robinson et al., 2006; Galarneau, 2008). For example, the DR

method has been widely challenged due to its questionable ability to account for the change of PAH profiles once introduced to the environment (Dvorska et al., 2011; Katsoyiannis et al., 2011; Tobiszewski and Namiesnik, 2012). Another factor that hampers source identification is that PAH profiles from the same category of sources can be dramatically diverse (described below). Alternatively, PAH profiles from different sources might also be very similar. This variability, therefore, leads to difficulty in determining sources when using some methods, e.g., DR and CMB. To overcome these issues, more powerful source apportionment tools are needed.

2.1 PAH ANALYSIS AND DATA PREPARATION

2.1.1 PAH Analysis and Quality Control

Sediment samples were analyzed by Test America Chicago, previously Severn Trent Laboratories. USEPA standard methods were used for the analyses. Sample processing followed USEPA Method 3540C (EPA, 1996b) and chemical analysis followed USEPA method 8270C (EPA, 1996a). The 16 USEPA priority PAHs were analyzed. Quality control concerning PAH sample analysis was conducted according to the USEPA Method 8270C, including laboratory control samples (LCS), matrix spikes, and the appropriate surrogate application.

2.1.2 Data Selection and Pretreatment

The concentrations of some PAHs were below the reporting limit (RL) in some sediment cores. RL is defined as the lowest level that can be achieved within specified limits of precision and accuracy during routine laboratory operating conditions. These imprecise values could introduce uncertainties into the analysis, but complete deletion of these data would have resulted in the loss of some useful information. Core samples in which more than eight of the targeted PAHs were detected below RL were not used for spatial analysis. However, a stricter criterion was adopted when selecting PAH data for source apportionment analysis; samples with more than four target PAHs below RL were not used. Additionally, cores taken from portions of the floodplain above normal pool level, which had very shallow sediment deposits, were also excluded. For the retained sediment samples, the non-detects were replaced by the RL. The actual values ("J" values) provided by the contract lab were used when the detections were less than RL but higher than the method detection limit (MDL). In total, 80 sediment cores were selected for spatial distribution analysis, and 65 sediment cores were retained for source apportionment analysis (n = 1040, data dimensions of 16 (PAHs) × 65 (samples)). The sediment cores from the La Grange Pool of the Illinois River between Pekin and Beardstown, IL, generally had very low PAH concentrations, with most concentrations below the MDL. Therefore, the sediment cores from the La Grange Pool river segment were excluded from this study.

2.2 PAH RESULTS AND DISCUSSION

2.2.1 PAH Concentrations in Sediments

The total concentration of the 16 USEPA priority PAHs ($\sum_{16}$PAH) of 80 individual sediment cores are plotted in Figure 2.1. This figure includes lines indicating the threshold effect

concentration (TEC) and probable effect concentration (PEC) as points of reference. They are consensus-based sediment quality guidelines explained in MacDonald et al. (2000). Contaminant concentrations below the TEC are likely to have no harmful effects on sediment-dwelling organisms. At or above the PEC level, the effects are expected to be negative on some of these benthic organisms. The total PAH values in 3 sediment cores (i.e., 254, 269, and 360) were higher than that of PEC. In contrast, 27 of them were below TEC level. In addition, the total PAHs in 33 of the sediment cores were distributed in a narrow range between TEC and the mean values. The total PAH concentrations in the majority of the sediment cores could be considered to pose low environmental risk.

A total of 20 sediment cores exhibited $\sum_{16}$PAH higher than the mean. Thirteen of these sediment cores were taken from locations close to the main river channel or the mouths of backwater lakes near where they join the main channel; these included sediment cores 284, 347, 349, 272, 269, 266, 280, 362, 361, 360, 357, 382, and 337 (Figures 2.1, and A-1 to A-6). However, there were also high $\sum_{16}$PAH in some cores that were located in other areas, e.g., sediment cores 346, 254, 252, 274, 250, 251, and 354. Six of these high $\sum_{16}$PAH concentration cores were from backwater lakes and one was from the Goose Lake area adjacent to Upper Peoria Lake. Five of these were west of the main channel, including two each from Wightman and Meadow Lakes. Unlike most backwater lakes which are largely separated from the river channel, the segment from Chillicothe to Peoria, IL, consists of wide open water areas comprising Goose Lake (Woodford County, IL), Upper Peoria Lake, and Lower Peoria Lake. The main or navigation channel is within the Peoria Lakes.

The $\sum_{16}$PAH in the selected 80 sediment cores ranged from 389 to 23,323 µg/kg (dry weight, dw), with a mean concentration of 3,702 µg/kg. Note that PAH concentrations are essentially the average value for each whole sediment core or segment. The boxplots of $\sum_{16}$PAH grouped by river segments are shown in Figure 2.2. Overall, the ANOVA test rejected the significant differences hypothesis at $p = 0.05$ ($p = 0.15$), indicating no significant differences in the total PAHs in the sediments between the river segments grouped as Hennepin-Henry (7 cores), Henry-Lacon (8 cores), Lacon-Chillicothe (25 cores), Upper Peoria/Above Spring Bay (9 cores), Upper Peoria/Below Spring Bay (6 cores), and Lower Peoria Lake (22 cores). However, given the variability between individual sediment cores, there were clearly localized differences in total PAH concentrations. Specifically, a t-test suggested that the average total PAH concentration in sediment cores from Upper Peoria Lake/Above Spring Bay was significantly ($p = 0.037$) higher than Lower Peoria Lake.

Some cores in the river segment from Lacon to Chillicothe exhibited higher concentrations. Figure 2.2 also shows boxplots for the cores east and west of the channel and in the north and south halves of this reach. Wightman and Meadow Lakes on the west side appeared to have higher PAH levels than the other sections, as did the portion of Upper Peoria Lake above Spring Bay. Lower Peoria Lake samples were generally lower in PAH concentration and were less variable than those from other segments.

Explanation of the varying PAH concentrations at various locations is beyond the scope of this report and will require further investigation. However, these differences are likely related to such factors as depth and extent of recently deposited sediment, hydrologic conditions, and historic

regional contaminant sources (John Marlin, Illinois Sustainable Technology Center, personal communication).

2.2.2 PAH Profiles

A PAH profile is a representation of the percentages of 16 PAHs in a sample. Four-Ring (BaA, Chy, FlA, Py) and 5-ring (BaP, BbF, BkF) PAHs were dominant in sediments of the Peoria Pool of the Illinois River (Figure 2.3); however, the fraction of 4-ring PAHs is higher than the others. Six-ring PAHs (IP, BghiP) were moderately abundant, while 2- and 3-ring PAHs (Nap, AcNe, AcNy, An, Fl, PhA) were relatively rare. This PAH distribution pattern appears to be similar to that found in the Ammer River (Germany) (Liu et al., 2013). It is somewhat different from that in the Liangtan River (China) (Liu et al., 2013), where higher fractions of 2- and 3-ring PAHs, smaller fractions of 4- and 5-ring PAHs, and higher variance in 6-ring PAHs were found. The PAH profiles in the Ammer River were thought to be typical of those in countries with a long history of industrialization with widespread non-point sources and legacy contamination that is becoming relatively diffuse (Liu et al., 2013). The similarity of the PAH profile in the Peoria Pool to the Ammer River sediments may also indicate early industrial contamination. It is noteworthy that 4-ring PAHs are dominant in low-rank coals (Table D-1) (Stout and Emsbo-Mattingly, 2008), while comparable 4-ring and 5-ring PAHs have been found in coal combustion soot (Table D-2) (Zhang et al., 2008); therefore, the higher fraction of 4-ring PAHs could indicate the presence of local mineral coal dust deposition in Illinois River sediments.

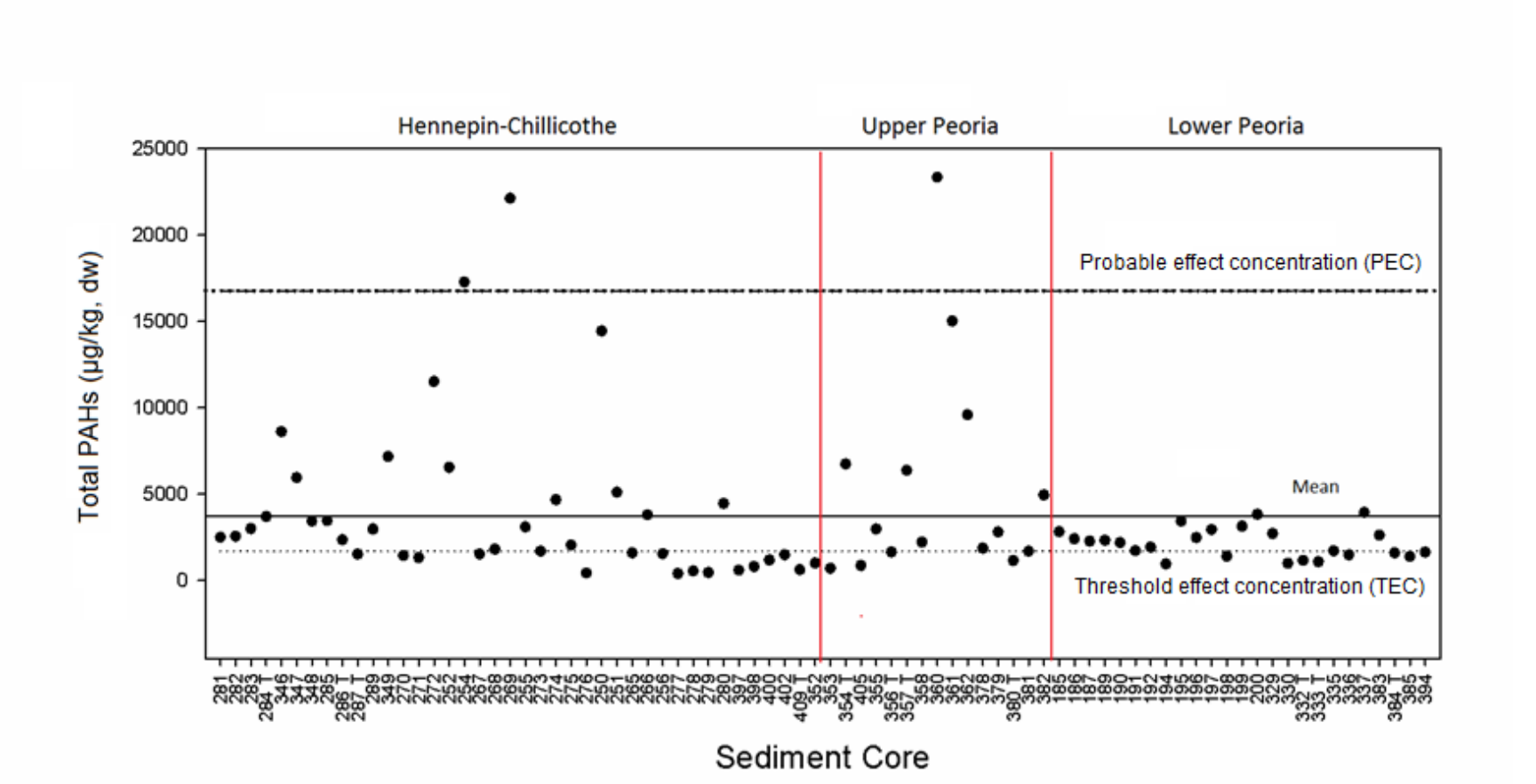

Figure 2.1. Total PAHs for 80 selected sediment cores taken in the Peoria Pool of the Illinois River. River segments were divided as Hennepin-Chillicothe, Upper Peoria, and Lower Peoria. TEC=1,610 (µg/kg, dw), PEC=22,800 (µg/kg, dw). Upper dashed line indicates the probable effect concentration (PEC); solid line represents the mean PAH concentration; and the lower dotted line indicates the threshold effect concentration.

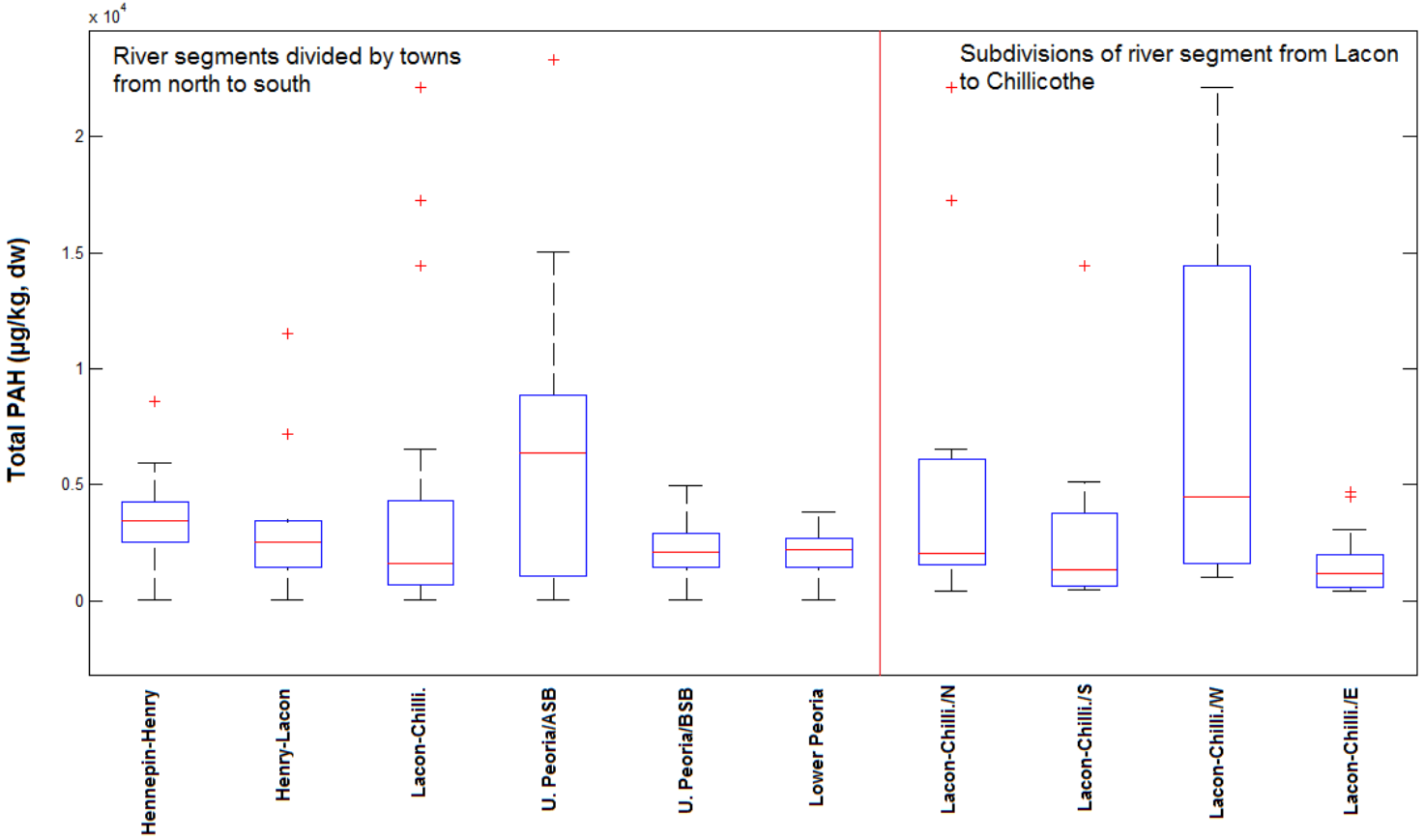

Figure 2.2. Boxplots of total PAHs in divided river segments in the Peoria Pool of the Illinois River. River segments: Hennepin-Henry (7 cores), Henry-Lacon (8 cores), Lacon-Chillicothe (25 cores), Upper Peoria/Above Spring Bay (9 cores), Upper Peoria/Below Spring Bay (6 cores), and Lower Peoria Lake (22 cores). Lacon-Chillicothe/North refers to Lacon to Strawn Creek (11 cores), Lacon-Chillicothe/South refers to Strawn Creek to Chillicothe (14 cores), Lacon-Chillicothe/West refers to Wightman Lake and Meadow Lake and core 352 (10 cores), Lacon-Chillicothe/East refers to Sawyer Slough and Babb Slough (15 cores). The box shows 25 (lower bound, $Q_{25\%}$) and 75 (upper bound, $Q_{75\%}$) percentiles of the data. Red line in the box indicates the median. Dashed tails are whiskers, which are calculated by $Q_{75\%}+1.5(Q_{75\%}-Q_{25\%})$, and $Q_{25\%}-1.5(Q_{75\%}-Q_{25\%})$ respectively. "+" represents outliers.

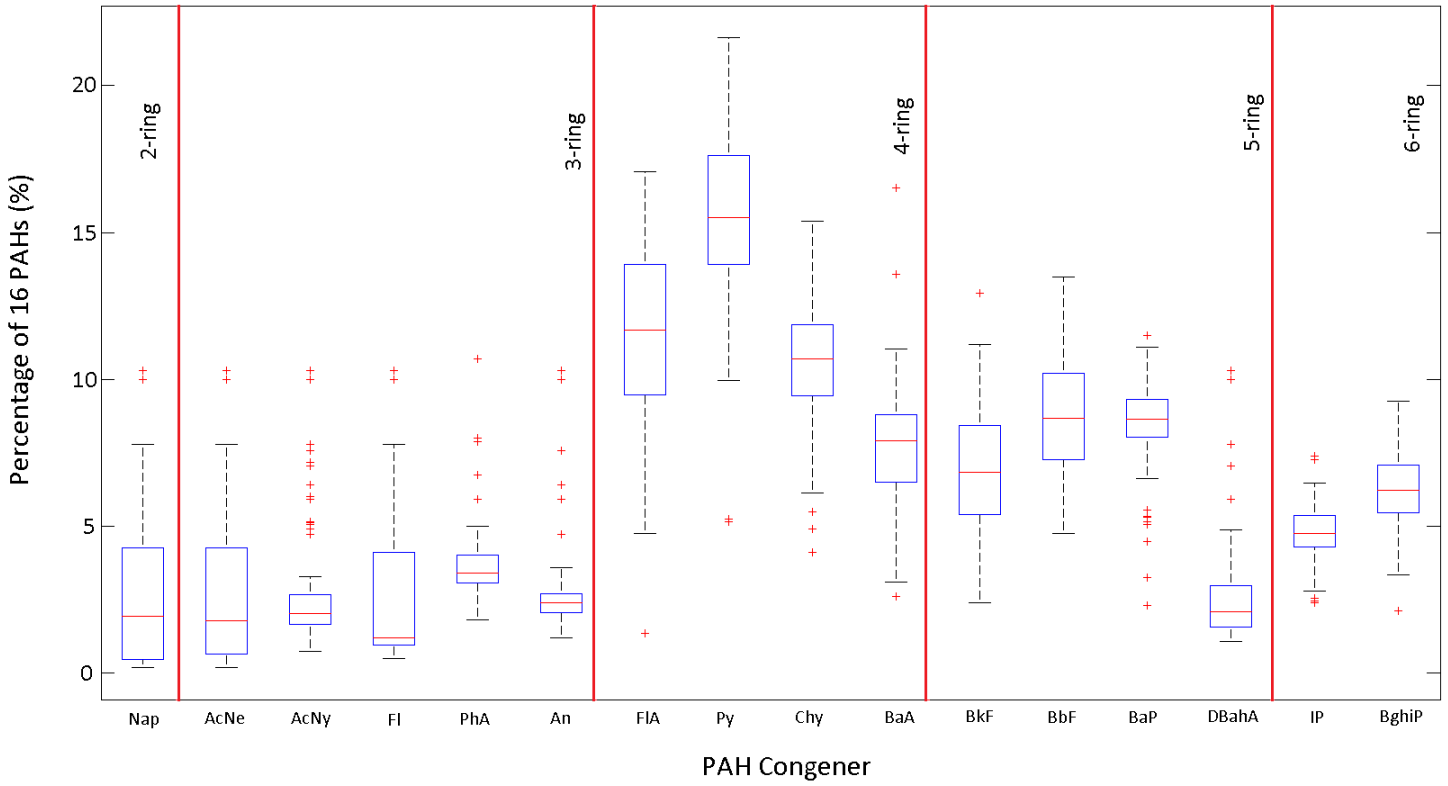

Figure 2.3. Boxplot of overall PAH composition by percentage (%) in the selected 65 sediment cores. The box shows 25 (lower bound, $Q_{25\%}$) and 75 (upper bound, $Q_{75\%}$) percentiles of the data. Red line in the box indicates the median. Dashed tails are whiskers, which are calculated by $Q_{75\%}+1.5(Q_{75\%}-Q_{25\%})$, and $Q_{25\%}-1.5(Q_{75\%}-Q_{25\%})$ respectively. "+" represents outliers.

Examining the consistency of the PAH profiles in the Peoria Pool sediments involves comparing each individual sample's profile to the profiles of the other 64 samples selected for PAH analysis. A cosine φ value (cosφ) (Soonthornnonda et al., 2011) was used to quantitatively estimate the similarity of the paired PAH profiles. When calculating the cosφ, the individual PAH profile is treated as a vector and is projected onto other profiles, so the cosφ value is calculated as

$$cos\varphi = \frac{V_i \cdot V_j}{|V_i||V_j|} \quad (1)$$

where V_i and V_j are the PAH profiles for samples *i* and *j* respectively; the numerator is the dot product of the two vectors; and the denominator is the product of the norms. The cosφ value is between 0 and 1. A value of zero means that the two PAH profiles are not similar, while a value of one means that the two profiles are identical. Generally, a cosφ value larger than 0.7 suggests the two profiles have high similarity (Soonthornnonda et al., 2011). Cosine φ values were estimated by a self-coded MATLAB program.

Relatively similar PAH compositions were exhibited in the 65 sediment cores selected for source apportionment analysis (Figure C-1). These cores exhibited higher $\sum_{16}$PAH than the 15 eliminated cores with greater than four non-detects (Figure C-1). The paired cosφ values for the 65 sediment cores ranged from 0.80 to 1.00, indicating a high degree of similarity. The PAH profiles of the 17 cores with the highest $\sum$16PAH values were further examined (Figures C-2). The pairwise cos Φ values for these cores ranged from 0.86 to 1.00. The similar ranges of the two groups of cores indicate that the PAH profiles across the Peoria Pool of Illinois River are generally consistent. Some of the similarity may have been due to mixing and redistribution of PAHs during release and transport to river sediments.

2.2.3 PAH Source Apportionment Analyses

Using diagnostic ratios (DRs) as markers of different sources is probably the most common PAH source apportionment method. The DR method uses predetermined ratios of PAHs known to be associated with specific sources for comparison with the PAH ratios of samples to determine possible sources. Two commonly-used DR plots, FlA/(FlA+Py) vs. An/(An+PhA) and IP/(IP+BghiP) vs. BaA/(BaA+Chy) (Granberg and Rockne, 2015), are shown in Figure 2.4. The FlA/(FlA+Py) vs. An/(An+PhA) plots suggest that most of the PAHs in Peoria Pool sediments were from petroleum combustion, while biomass and coal combustion had relatively small contributions. However, the IP/(IP+BghiP) vs. BaA/(BaA+Chy) plots indicated contrasting results. Petroleum combustion was suggested by IP/(IP+BghiP), while only biomass and coal combustion were indicated by BaA/(BaA+Chy) (Figure 2.4). The PAH DR method is considered questionable in apportioning PAHs sources (Galarneau, 2008; Katsoyiannis et al., 2011; Tobiszewski and Namiesnik, 2012). Therefore, conclusions should be drawn with caution from DR plots.

Principal component analysis (PCA) is another widely used source apportionment method. PCA reduces the dimensionality of a dataset by transforming a large number of interrelated variables into a new set of uncorrelated variables called principal components (Jolliffe, 2002). Principal

components are a set of orthogonal vectors (profiles) that best span the variance of data. An individual principal component can be considered as a profile of selected elements (in this case the 16 USEPA priority PAHs) generated through mathematical data matrix rotation. The PCA method suggests possible sources of the PAHs based on the PAH compounds exhibiting high positive values in the principal component. However, this inference is not evident in all cases (Mari et al., 2010; Brown and Brown, 2012; Zou et al., 2013). It is also used to evaluate data uncertainties, therefore estimating the number of factors (Brown and Brown, 2012; Zou et al., 2013). The statistical program SPSS 21 (IBM) was used to generate PCA results from the PAH data with Varimax rotation. The generated principal components are referred to as factors, which correspond to specific PAH sources. Five factors were determined (Table 2.1) based on the criterion of an eigenvalue larger than 1. The selected factors accounted for 80% of the total data variance (Table 2.1). The PCA components were distinguished by different molecular weight PAHs, e.g., component 1, 2, and 4 (Table 2.2). It was not possible to get a clear definition of PAH sources using this method with the data set. The values in each principal component reflect the pooled correlations among the 16 PAH compounds. The positive values mean these PAHs have similar contributions to the total data variance as the corresponding principal component. In contrast, the negative values indicate the PAHs have opposite contributions to the total data variance as the corresponding principal component.

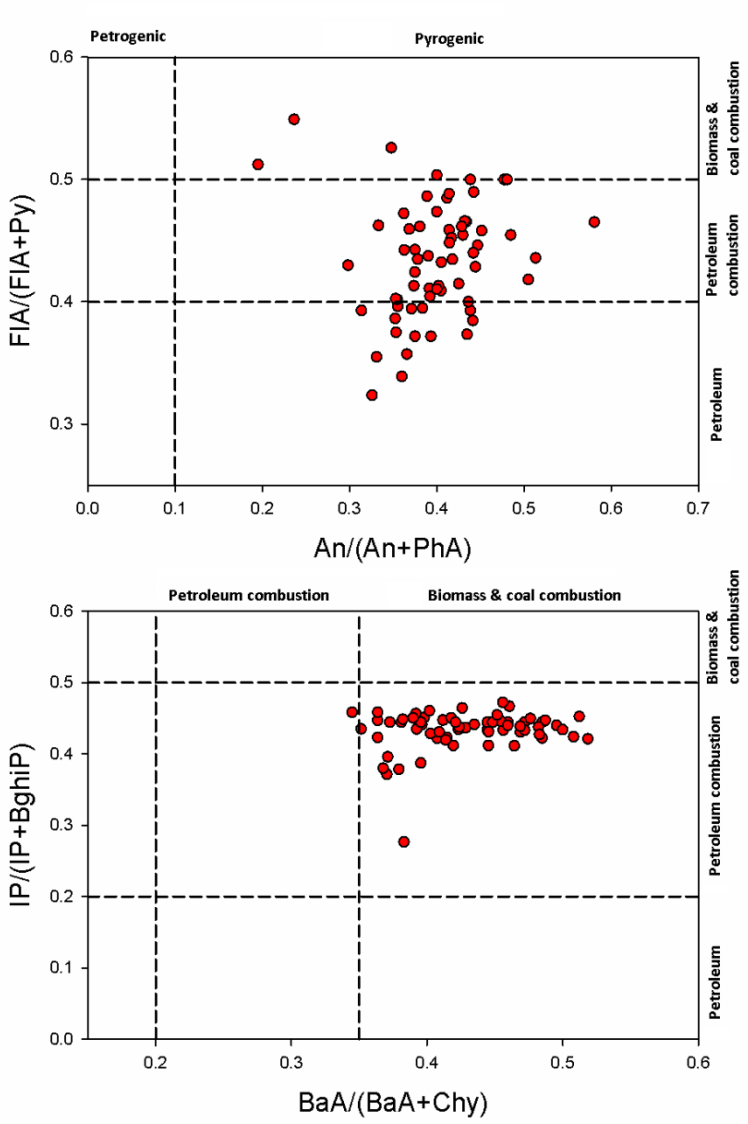

Figure 2.4. Diagnostic ratio (DR) of FlA/(FlA+Py) vs. An/(An+PhA) and IP/(IP+BghiP) vs. BaA/(BaA+Chy) plots for 65 selected sediment cores.

Table 2.1. Eigenvalues and variance explained (%) of extracted principal components from PAH data.

No. of Components	Eigenvalue	Variance explained (%)	Total variance explained (%)
1	5.26	32.90	32.90
2	3.59	22.43	55.33
3	1.59	9.93	65.26
4	1.32	8.25	73.51
5	1.05	6.57	80.09

Table 2.2. Compositions of extracted principal components from PAH data.

	Rotated Component				
PAH	1	2	3	4	5
Nap	.870	.121	-.129	-.197	-.177
AcNe	.897	.070	-.153	-.169	-.193
AcNy	.793	-.130	.096	-.327	.071
Fl	.832	-.056	-.015	-.249	-.224
PhA	-.074	-.096	.008	.795	-.114
An	-.416	-.160	-.014	.655	.177
FlA	-.241	-.646	.136	.491	-.103
Py	-.675	-.406	-.262	-.280	-.331
Chy	-.736	-.034	.140	-.126	.239
BaA	-.456	-.477	-.033	.003	.610
BkF	-.154	.518	.733	-.051	-.175
BbF	.064	.066	-.945	-.106	-.075
BaP	-.315	.223	.051	-.059	.839
DBahA	.009	.565	.537	-.224	.271
IP	.009	.904	.180	-.017	.059
BghiP	-.009	.927	.023	-.097	-.039

Using the cosφ value to compare the similarity of PAH profiles from samples to specific known sources is relatively straightforward. Source identification using 16 USEPA priority PAHs is considered superior to DRs because generally only two PAHs are used in DR comparison. There are two primary advantages of using the 16 USEPA priority PAH fingerprints. First, while some of the lower molecular weight PAH compounds (e.g., AcNe, AcNy, Fl, and Nap) are susceptible to degradation or volatilization (Atkinson and Arey, 1994; Kim et al., 2009; Dvorska et al., 2011), higher molecular weight (4-6 rings) congeners are more persistent in the environment (Kim et al., 2009; Dvorska et al., 2011). Second, the ratio of selected paired PAH compounds could be easily altered by mixing in the sediment. However, the profile based on 16 PAHs is more likely to retain its characteristics after mixing. Therefore, comparing fingerprints of 16 PAHs reduces the uncertainties of source identification.

A total of 225 PAH profiles from nine specific PAH sources were collected through a literature search (Table D-1 to D-12), including mineral coal; coal-tar; soot; asphalt; petroleum products; vehicle exhaust; particulate matter emitted from coal combustion; industry boiler and stack emissions; and emissions from wood and biomass combustion. Additionally, the PAH profiles in traffic tunnel air have also been presented because they may be more representative of real on-road PAH emissions from traffic. The PAHs in traffic tunnel air (in both particulate and gas phase) were assumed to be largely from vehicular emissions. The selection of PAH sources was based on the primary objectives of this study, i.e., understanding the contribution of mineral coal to the PAHs in the Peoria Pool of the Illinois River. In addition, we also attempted to identify the major local PAH contributors and their universally recognized sources.

The cosφ values provide a quantitative estimation of the similarity of two profiles, and therefore may help in source identification. The average cosφ values between the PAH profiles in sediment cores and the specific sources are shown in Table 2.3. Dust from lower-rank coals (lignite A and sub-bituminous) and soot from wood combustion have the most similar PAH profiles to the Peoria Pool sediments. It should be noted that there is huge variation in the PAH fingerprint of wood soot, which makes it difficult to distinguish wood soot from the other sources. Wood combustion is not considered a major energy source in Illinois. However, PAHs derived from previous wood combustion are retained. They are probably a minor portion of the total PAHs in the recently deposited sediments. On the other hand, unburned mineral coal has been shown as a significant hydrocarbon source in sediments (Tripp et al., 1981; Barrick et al., 1984; Achten and Hofmann, 2009). There are ample opportunities for mineral coal, especially fine coal dust, to enter the watershed. The mining and transportation activity of coal has been documented in previous studies; topics range from the transport of specific local coals to aquatic sediments by erosion (Barrick et al., 1984; Yang et al., 2008).

Illinois is a major coal producing state. The coals in Illinois are in the rank of bituminous (Hatch and Affolter, 2014; Hopkins and Simon, 1974), which makes it uncertain that the low-rank coals (lignite A and sub-bituminous) are the major PAHs source in the sediments. However, sub-bituminous coal from western states was increasingly used in Illinois for power generation after the 1990 Clean Air Act regulations required the reduction of sulfur emissions from flue gas. This coal supplanted much of the bituminous coal from Illinois mines which had been used previously. More importantly, trains loaded with much greater volumes of low sulfur western coal than was ever consumed within the state crossed Illinois on their way to power plants in the

eastern U.S. (Scott Elrick, Illinois State Geological Survey, personal communication). Mineral coal dust from the transport and handling of this fuel is a likely source of some of the PAH in the river sediment.

The tunnel particles from traffic emissions also exhibited high similarity to the PAH profiles in the Peoria Pool sediments. Traffic emissions have long been recognized as a major PAH source. According to the 2013 Illinois Travel Statistics, the annual vehicle miles of travel increased from 27 billion miles in 1950 to more than 108 billion miles in 2004 (IDOT, 2013). Illinois was the sixth highest fuel (gasoline + diesel) consumption state in the US in 2009 (US DOT, 2011). Therefore, it is expected that PAH emissions from motor vehicles could have contributed significantly to the PAHs in sediments.

Asphalt and coal-tar also showed relatively high similarity to the PAH sediment profile. Asphalt is widely used in road construction within the watershed and is a likely source of PAH. Coal-tar is used as a parking lot and driveway sealcoat in the eastern and central area of the US (Mahler et al., 2012). Coal-tar has been recognized as a major PAH source to urban water-body sediments (Mahler et al., 2005; Van Metre, 2010; Mahler et al., 2012). The Illinois River watershed includes the large Chicago metropolitan areas and numerous small cities and towns (Figures 1, and A-1 to A-6). Therefore, asphalt and coal-tar could be one of the PAH contributors to Peoria Pool sediments.

Coal combustion soot has a similar PAH profile to the sediments as well (Table 2.3). Coal combustion has been recognized as a major PAH source worldwide (Zhang and Tao, 2009; Zhang et al., 2008; Shen et al., 2013). Coal became a major household energy source replacing wood during the second half of the 19th century and the first quarter of the 20th century in the US (Kibbel, 2009). Illinois's coal production peaked in the late 1910s at 90 million tons per year (ISGS, 2014). The availability of coal was one of the driving powers for the rapid development of the manufacturing and steel industries in the Chicago region before the 1930s (Hirsch, 2004). Coal is currently the second largest energy source in Illinois (US EIA, 2012). Therefore, coal combustion is likely a large source of PAHs in the sediments.

Table 2.3. The similarity (cosφ values) of PAH profiles between sediments and specific sources.

Source Category	Specific source	cosφ	
		mean	**std**
Coal	Lignite A	**0.87**[a]	0.034
	Sub-bituminous	**0.82**	0.078
	Bituminous	0.33	0.15
	Anthracites	0.37	0.14
Biomass combustion	Wood (particle)	**0.89**	0.35
	Wood (gas)	0.23	0.11
	Biomass (gas + particle)	0.22	0.10
Traffic emissions	Diesel Engine (gas+particle)	0.21	0.18
	Gasoline engine (gas+particle)	0.44	0.30
	Tunnel (particle)	**0.80**	0.055
	Tunnel (gas)	0.30	0.21
Road Pavement/Sealcoat	Asphalt	**0.74**	0.023
	coal-tar	**0.70**	0.10
Coal combustion emissions	Residential (particle)	**0.71**	0.092
	Industrial (particle)	0.63	0.13
Petroleum products	Gasoline	0.089	0.058
	Diesel	0.18	0.14
	Motor/Lubricant	0.52	0.11
Industrial stack/boiler emissions	Non-coal fuel (gas+particle)	0.21	0.19

[a] cos$\varphi \geq 0.7$ were bolded, indicating high similarity of PAH profiles in sediment cores to corresponding source

One of the concerns is whether liquid petroleum products (specifically, used crank oil) was a significant PAH contributor to the sediments, considering that it was historically common for used crank oil to be disposed of improperly (John Marlin, Illinois Sustainable Technology Center, personal communication). The cosφ values indicate that unburned petroleum products, e.g., gasoline, diesel, motor oil, and lubricant oil contributed minimally to the PAHs in Peoria Pool sediments (Table 2.3). It should be noted that PAHs associated with particle emissions from combustion appeared to be well documented in sediments, while PAHs associated with gas emissions were less prevalent, probably due to volatilization (Table 2.3). Also, it is noteworthy that there was a common feature in the PAH fingerprints for liquid petroleum products and the gas phase of combustion emissions; that is, both had a high fraction of lower molecular weight PAHs, especially Nap, AcNe, and AcNy (Tables D-5 to D-12). Therefore, the low cosφ values also indicated that the gas phase of combustion emission had a minor contribution to PAHs in the sediments.

A MATLAB version of the PMF program in Bzdusek (2005) was used to analyze PMF in this study. Three to six factors were tested during the PMF analysis. To understand the PMF results, one should begin by examining the 3-factor solutions. The PMF method produced robust results for three factors. There was almost no variation in the fingerprints of the three factors. This is indicated by the extremely small standard deviations acquired from ten sequential PMF analyses using random seeds (see error bars in Figure E-1). The small variation in ten sequential PMF analyses suggests that the three factors extracted by PMF were definite and distinct. Factor PMF 3-1 is dominated by 4-ring PAHs, with a moderate fraction of 5-ring PAHs. High levels of 4-ring PAHs are normally indicative of dust from low-rank coals (Lignite A and sub-bituminous) (Stout and Emsbo-Mattingly, 2008). High levels of 4- and 5-ring PAHs are generally found in particulate matter from low temperature combustion of coals, wood, and other biomass fuels (Levendis et al., 1998; Larsen and Baker, 2003; Zhang et al., 2011). Therefore, PMF 3-1 probably indicates coal-originated inputs including coal dust; coal-derived products (e.g., coal-tar); and products of coal and wood combustion. Factor PMF 3-2 exhibits high fractions of 5- and 6-ring PAHs. High concentrations of 5- and 6-ring PAHs have been found in gasoline engine emissions (Miguel et al., 1998; Marr et al., 1999; Marr et al., 2006). Specifically, 6-ring PAHs were dominant in particle emissions from light-duty vehicles (Marr et al., 1999; Marr et al., 2006). Therefore, PMF 3-2 is likely derived from traffic-related PAH emissions. Factor PMF 3-3 shows a large fraction of 2- and 3-ring PAHs and likely represents the gas phase of combustion emissions and/or liquid petroleum products (see Appendix D).

When the number of factors was increased to four, PMF introduced a new factor (PMF 4-3, Figure E-2). The previously-determined three factors were preserved in the PMF 4-factor solutions, with slight changes to their fingerprints. Again, the uncertainties (indicated by error bars on Figures E2) of the 4-factor fingerprints remained small. The new factor (PMF 4-3) had a high fraction of 3-ring (AcNe, AcNy, Fl) and 4-ring (FlA, Py, Chy) PAHs, which is similar to the PAH profiles found in wood combustion and dust from low-rank coals; however, as previously stated, wood combustion soot and dust from low-rank coals have similar PAH fingerprints. It should be noted that this PAH profile is also very similar to urban air samples (gas + particles) collected in winter (Harrison et al., 1996). Overall, this factor is similar to wood combustion, which may be related to household heating.

The results are less definitive when the number of factors was raised to five, as indicated by the increased size of the error bars (Figure 2.5). At this point, the model may have reached the limit of data signal and noise. Recall that five factors were suggested by PCA. Although both five and six factors (Figure E-3) produce reasonable results, it is preferable to choose the smallest number of factors that sufficiently reproduce the original data matrix (Zou et al., 2013); five, in this case. The fingerprints of 5-factor solutions are given in Figure 2.5. The cosφ values were again used to provide quantitative estimation of the similarities of PMF-determined fingerprints to the PAH profiles from specific sources (Table 2.4).

The PAH profile of factor PMF 5-1 is quite similar to PAH fingerprints from low-rank coal dust (e.g., lignite A and sub-bituminous). The cosφ values between factor PMF 5-1 and low-rank coal dust are much higher than for other PAH sources (Table 2.4), which strongly suggests that PMF 5-1 is related to coal dust. It is noted that PMF 5-1 also showed high similarity to other sources,

e.g., wood combustion, particles from engine emissions, tunnel air (particle), asphalt, and coal-tar (Table 2.4). All of these sources may have contributed, as they combine during PAH transport in natural environments and homogenization of sediment samples during sample preparation. Further research may use scanning electron microscopy to differentiate these particles and determine whether they originate from oil, wood, or coal combustion, or from mineral coal particles and coal dust (Kralovec et al., 2002; Obst et al., 2011).

Two factors may have caused these sources to be clumped together in PMF 5-1. First, these PAH sources (e.g., low rank mineral coal, wood combustion soot, particle phase of traffic emissions, asphalt, and coal-tar) have similar fingerprints, which can be difficult to discern. Second, the methodology of PMF (and analogous source apportionment models, e.g., PCA) operates by aligning the most significant data feature to the most important factor (i.e., principal component) (Robinson et al., 2006). Due to the similar fingerprints of these sources, a similar central feature is likely. For these reasons, it is very likely that PMF 5-1 encompasses these aggregated sources. The contribution of each factor can be estimated simultaneously through least square regressions (Paatero, 1997; Bzdusek, 2005). Factor PMF 5-1 accounts for about 47 ± 7% of the total PAHs in Peoria Pool sediments.

Factor PMF 5-2 is similar to coal combustion, especially industrial coal combustion emissions (particle phase) (Table 2.4). The cosφ value suggests it is also similar to dust from low-rank coals (Table 2.4). However, other coal dust-related factors can be ruled out because it has a higher fraction of 5- and 6-ring PAHs than is normally found in coal dust (Figure 2.5). It is not surprising that coal combustion was identified as the second most important PAH contributor. It accounts for 28 ± 4% of the total PAH in the sediment.

The cosφ values indicate that the most probable sources represented by factor 3 (PMF 5-3) are wood combustion and traffic emissions (tunnel air particle) (Table 2.4). However, the results are not very convincing because the cosφ values are low (Table 2.4). Wood combustion is considered a minor PAH contributor because it has long been phased out as a major source of fuel for home heating. There is a lower fraction of 4-ring PAHs but higher fractions of 5- and 6-ring PAHs in PMF 5-3 (Figure 2.5), which is a characteristic that distinguishes it from coal and wood combustion. Recall that higher 5-ring and, particularly, 6-ring PAH fraction are indicators of engine emissions. Therefore, this factor likely represents PAH inputs from the particle phase of traffic emissions. This factor contributes about 15 ± 3% of the total PAHs. This estimation is very close to previous published results. For example, Shen et al. (2013) estimated that motor vehicles contribute 17.6% of total PAH emissions in the US. Simcik et al. (1999) reported a similar estimate of 15% of total PAH emission from traffic in the Chicago area.

Factor 4 (PMF 5-4) is highly similar to the gas phase of coal combustion as well as biomass combustion emissions (gas + particles), gas emissions from engines, and industrial stack/boiler emissions (gas + particles) (Table 2.4). The high fraction of Nap and AcNe are indicators of gas phase emissions from combustion. Therefore, this factor might indicate gas phase PAH emissions from different combustion processes. The gas phase emissions contribute about 5% of the total PAHs in the sediments.

Factor 5 (PMF 5-5) was not close to any of the sources in Table 2.4, according to the average cosφ values (Table 2.4). As discussed before, factor 5 (PMF 5-5) is similar to wood soot, dust from low-rank coals, and urban air in winter. It might be a factor that represents PAH emissions from wood combustion, e.g., household heating or cooking. It contributes another 5% of the total PAHs in the sediments.

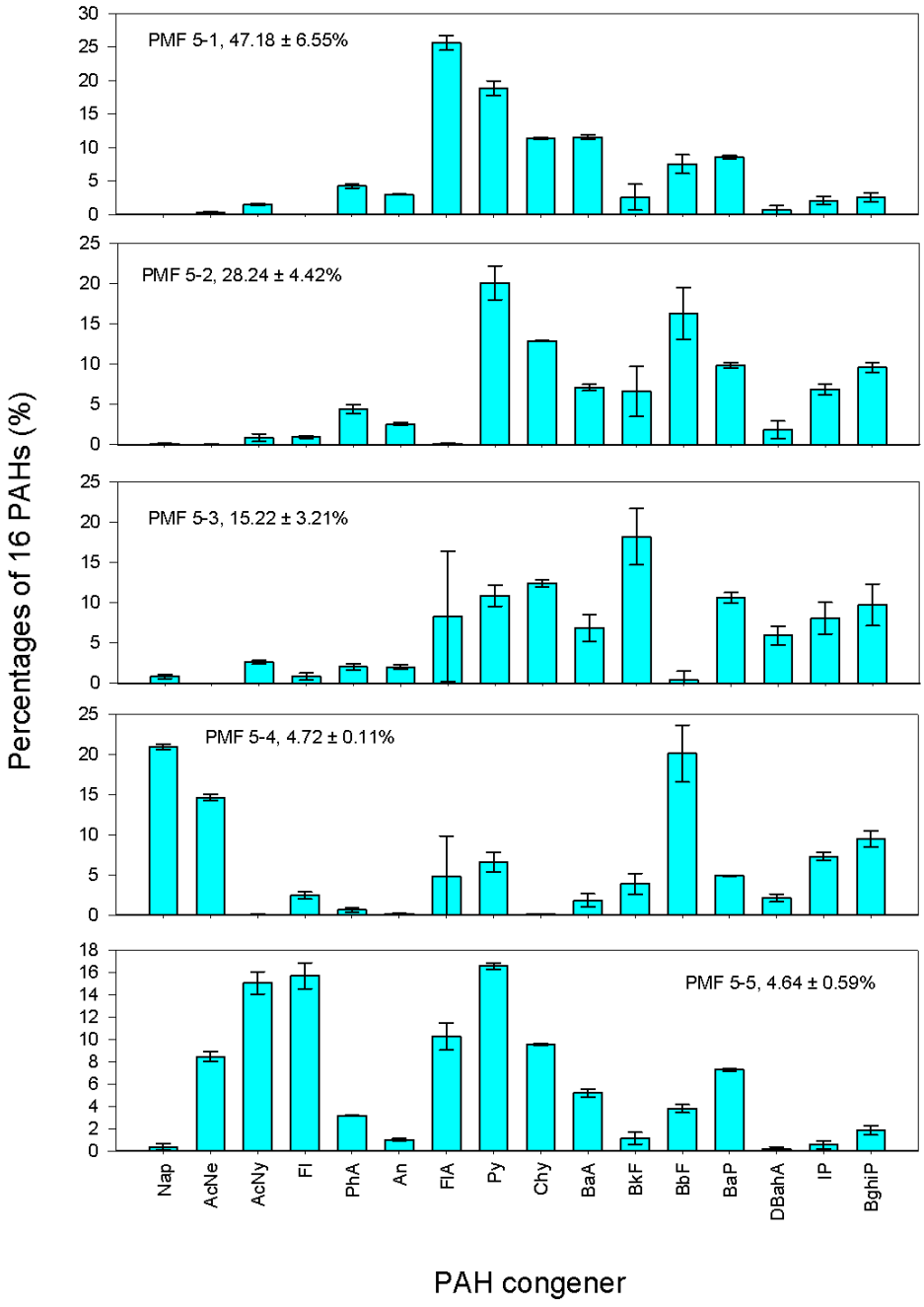

Figure 2.5. PAH 5-factor fingerprints generated by PMF analysis.

Table 2.4. The average cosφ values and corresponding standard deviations between the PMF 5-factor fingerprints and PAH sources.

Source Category	Specific source	cos*φ*				
		PMF 5-1	**PMF 5-2**	**PMF 5-3**	**PMF 5-4**	**PMF 5-5**
Coal	Lignite A	**0.91±0.026**[a]	**0.71±0.12**	0.63±0.040	0.50±0.025	0.65±0.027
	Sub-bituminous	**0.87±0.044**	0.67±0.13	0.59±0.096	0.44±0.10	0.68±0.047
	Bituminous	0.28±0.18	0.26±0.12	0.23±0.11	0.52±0.084	0.33±0.17
	Anthracites	0.28±0.12	0.37±0.21	0.24±0.11	0.51±0.10	0.33±0.17
Biomass combustion	Wood (particle)	**0.76±0.31**	0.65±0.27	0.66±0.24	0.39±0.14	0.61±0.069
	Wood (gas)	0.17±0.15	0.10±0.086	0.13±0.083	0.47±0.28	0.38±0.26
	Biomass (gas + particle)	0.20±0.17	0.19±0.18	0.17±0.12	0.63±0.010	0.23±0.17
Traffic emissions	Diesel Engine (gas)	0.14±0.041	0.15±0.037	0.15±0.025	0.62±0.036	0.22±0.058
	Diesel Engine (particle)	**0.77±0.061**	0.57±0.069	0.48±0.038	0.27±0.023	0.56±0.040
	Gasoline engine (gas)	0.049±0.065	0.040±0.038	0.060±0.034	0.60±0.018	0.076±0.055
	Gasoline engine (particle)	**0.75±0.11**	0.55±0.095	0.50±0.11	0.28±0.093	0.53±0.068
	Tunnel (particle)	**0.79±0.12**	0.69±0.11	0.63±0.10	0.43±0.14	0.59±0.089
	Tunnel (gas)	0.36±0.023	0.28±0.16	0.23±0.13	0.33±0.19	0.47±0.27
Road Pavement/Sealcoat	Asphalt	**0.70±0.12**	0.66±0.096	0.59±0.091	0.51±0.095	0.56±0.069
	Coal-tar	**0.76±0.035**	0.56±0.019	0.56±0.034	0.49±0.065	0.60±0.020
Coal combustion emissions	Residential (particle)	0.66±0.15	0.68±0.14	0.55±0.12	0.42±0.14	0.53±0.11
	Industrial (particle)	0.51±0.11	**0.76±0.056**	0.55±0.070	**0.70±0.0066**	0.44±0.0094
	Gas phase emission	0.092±0.039	0.080±0.031	0.10±0.023	0.69±0.010	0.34±0.027
Petroleum products	Gasoline	0.028±0.057	0.033±0.062	0.046±0.035	0.57±0.049	0.072±0.11
	Diesel	0.11±0.14	0.12±0.17	0.11±0.087	0.55±0.086	0.35±0.22
	Motor/Lubricant	0.50±0.13	0.48±0.093	0.39±0.085	0.40±0.15	0.46±0.073

[a] cos*φ* greater than 0.7 was bolded, indicating high similarity

One important factor that interferes with PAH source apportionment analysis is the altering of PAH profiles during transport from emission sources to receiving sites. Heterogeneous reactions such as photo degradation might be responsible for the rapid dissipation of the low molecular weight PAHs such as Nap, Fl, AcNe, and AcNy (Marr et al., 2006; Kim et al., 2009). These low molecular weight congeners are more prevalent in the gas phase. Compared to the low molecular weight PAHs, the compounds with high molecular weight are more likely sorbed to particulate matter. The condensation of the secondary aerosols will further wrap up the particulate-sorbed PAHs, which would reduce their photo-reactivity during airborne transport (Marr et al., 2006; Kim et al., 2009). In addition, these sorbed PAHs are likely inert to microbial degradation once they are trapped in sediments (Schneider et al., 2001; Thuens et al., 2013). The recalcitrance of the high molecular weight PAHs in the environment may prevent dramatic alteration of PAH profiles. Therefore, the PMF analysis in conjunction with cosφ comparison provides a useful PAH source apportionment analysis.

Another factor that may impede source recognition is that all possible sources have not been categorized. For example, coke ovens were found to be a major PAH source to the sediment of Lake Calumet, Chicago (Li et al., 2003; Bzdusek et al., 2004). However, coke ovens were not included in Table 2.4. A comparison of the coke oven profile (from Li et al., 2003) to the PMF five factor fingerprints shows a high cosφ for PMF 5-1 (0.81) and PMF 5-2 (0.88). Therefore, coke oven deposits are possibly an important PAH contributor to the sediments in the Peoria Pool of the Illinois River. Natural gas was identified as a major PAH contributor in the Chicago area (Simcik et al., 1999), likely due to its increasing use for energy production in Illinois (U.S. Energy Information Administration, http://www.eia.gov/state/?sid=IL#tabs-1). However, natural gas fingerprints are not available in the literature, so natural gas was not included in Table 2.4.

3. METALS

Excessive exposure to heavy metals has negative effects on human health (Jarup, 2003). Additionally, some heavy metals bioaccumulate through ecosystem food chains. For example, up to 100,000 times more methyl mercury was found in fish than in the surrounding water medium (Hammerschmidt and Fitzgerald, 2006). Due to their potential environmental risks, heavy metals in the environment are a major concern. Industrial facility waste, waste incineration, and fossil fuel burning are the main anthropogenic sources of heavy metal emissions (Zereini et al., 2005; Zhang et al., 2009; Rigaud et al., 2011). Motor vehicle traffic is another major source by which heavy metals can be released, through fuel combustion, tire abrasion, brake lining wear, and exhaust catalysts (Zereini et al., 2005; Loganathan et al., 2013). Additional sources include fuel spills, tailing water from mines, and improper disposal of electronics (Zhang et al., 2009; Lee et al., 2013). It is also important to note that the main sources of heavy metal emissions are changing. For example, gold mining was the major source of mercury release in the early 1900s, but coal-burning power plants are now the dominant source (Tewalt, 2001).

Heavy metals from anthropogenic sources enter sediments through different pathways. Suspended particles carried by stormwater runoff are widely recognized as an important source of heavy metals to river sediments (Taylor and Owens, 2009; Loganathan et al., 2013; Rossi et al., 2013). Industrial and domestic wastewater discharge and improper solid waste disposal are additional sources (Zhang et al., 2009). Atmospheric deposition is also a widely recognized major input of heavy metals into terrestrial and aquatic ecosystems (Zereini et al., 2005; Duan and Tan, 2013; Gratz et al., 2013). Heavy metals deposited in sediments undergo dynamic transformation, as evidenced by physicochemical changes of the sediments, including redox potential and pH (Calmano, 2004; Equeenuddin et al., 2013; Percival and Outridge, 2013; Ye et al., 2013). Acidity is the most serious long-term threat from metal-bearing sediments, due to the potential oxidization of sulfide to sulfate, which, when accompanied by a decrease in pH, can lead to the release of heavy metals such as copper and lead (Calmano, 2004). Microbial activity may also change the form of metals; that is, inorganic mercury can be transformed to organic mercury (methyl mercury) by a complex bacterial conversion (Tewalt, 2001; Ullrich et al., 2001). Methyl mercury is a highly toxic compound that bioaccumulates in fish and birds (Williams, 1953). Generally, leaching of heavy metals from metal-bearing sediments poses risks to ecosystems and human health.

Unlike anthropogenic organic contaminants, heavy metals can also be introduced by natural geological processes (Taylor and Mclennan, 1995; Wimpenny et al., 2010; Sandler et al., 2012). Therefore, the background concentrations of heavy metals have to be taken into account when evaluating pollution levels. Several indexes have been introduced; for example, the geo-accumulation index and the enrichment factor. Understanding the sources of heavy metals to receiving aquatic environments is important in contaminant mitigation and pollution control. Source apportionment analysis of heavy metals in sediments has been intensively studied (Lu et al., 2012; Chen et al., 2013; Lee et al., 2013; Peng et al., 2013; Sun et al., 2013).

Investigation of heavy metal contamination comprised the second part of our analysis. In this study, we sought to acquire a deeper understanding of the sources of metals present in the Illinois River Basin.

3.1 MATERIALS AND METHODS FOR METAL ANALYSIS

The metals in the collected Illinois River sediment cores were measured by TestAmerica Chicago. First, the collected samples were digested according to USEPA Method 3050B "Acid Digestion of Sediments, Sludges, and Soils." Metals analysis, with the exception of mercury, was performed by inductively coupled plasma (ICP) based on USEPA Method 6010B. Mercury analysis was performed by USEPA Method 7471 "Mercury in Solid or Semisolid Waste (Manual Cold-Vapor Technique)." Quality control measures associated with metal analysis included continuing calibration blanks/verifications (ICB-CCB/ICV-CCV), preparation/method blanks, laboratory control samples (LCS), matrix spikes, and sample duplicates.

A total of 25 inorganic elements were analyzed. Sediment cores with more than 25% non-detections were excluded from further analysis. Several elements that have naturally high background concentrations in the environment were discarded, e.g., Ca, K, and Na. These are not good indicators of anthropogenic sources of contaminants, even though substantial quantities of Na can be derived from road salt (deicing salt). However, the three highly enriched elements Al, Fe, and Mg were retained to act as indicators of earth crustal background input. Seventeen metals were selected for further data analysis after screening: Al, As, Ba, Be, Cd, Cr, Co, Cu, Fe, Pb, Mg, Mn, Hg, Mo, Ni, V, and Zn. For source apportionment analysis, 80 samples were selected (n = 1,360 [17 × 80]). The RL was used for those entities with non-detect "U" values.

3.2 METALS RESULTS AND DISCUSSION

3.2.1 Metal Concentrations in Sediments

The concentrations of metals in sediments ranged from parts per billion (µg/kg, Hg) to parts per hundred (K, Mg, Al, Ca, and Fe), but most metals were present in the parts per million (mg/kg) range. The concentrations of six metals (As, Cd, Cu, Pb, Hg, and Zn) which are considered to be introduced mainly by anthropogenic activities are shown in Figure 3.1. The six metals showed roughly similar spatial variations to $\sum_{16}$PAH in Illinois River sediments. This spatial distribution pattern indicated that the discharge of anthropogenic metal pollution was generally accompanied by the discharge of PAHs.

3.2.2 Source Apportionment Analysis of Metals

The PCA method was performed on metals data by SPSS 21.0 (IBM, 2012) using Varimax rotation in a manner similar to PAH analysis. PCA results are given in Tables 3.1 and 3.2. Three factors were suggested, accounting for 80% of the total data variance. Component 1 contained high fractions of As, Cd, Cr, Cu, Pb, Hg, and Zn. A literature search suggested these elements were likely introduced via anthropogenic means in the sediments. Arsenic, Cr, Cu, Pb, Hg, and Zn are suggested to originate from steel industry waste, smelting furnace burning (Chow et al., 2004; Querol et al., 2006; Li et al., 2012), coal, and coal combustion (Chow et al., 2004; Tian et al., 2010). Therefore, component 1 likely represents industrial inputs.

Component 2 was dominated by Al, Ba, Be, Co, Fe, and V. Component 3's high fraction of Mg, Mn, and Mo could be another crustal input factor representing different clay minerals in sediments. Magnesium and Mn were found to be highly associated in soils with both high and low organic matter content, suggesting that they were contained in the background soil materials (Niu et al., 2013). Liu et al. (2009) suggested bulk sediments showed higher Mg (MgO) and Mn (MnO) contents than the clay fraction of river sediments (Luzon, Philippines), while the clay fraction showed high contents of Al (Al_2O_3) and Fe (Fe_2O_3). The difference in mineral compositions was due to the sequential processes of clay mineral formation (Liu et al., 2009). Therefore, both component 2 and component 3 represented metals from crustal material weathering, but from different mineral components.

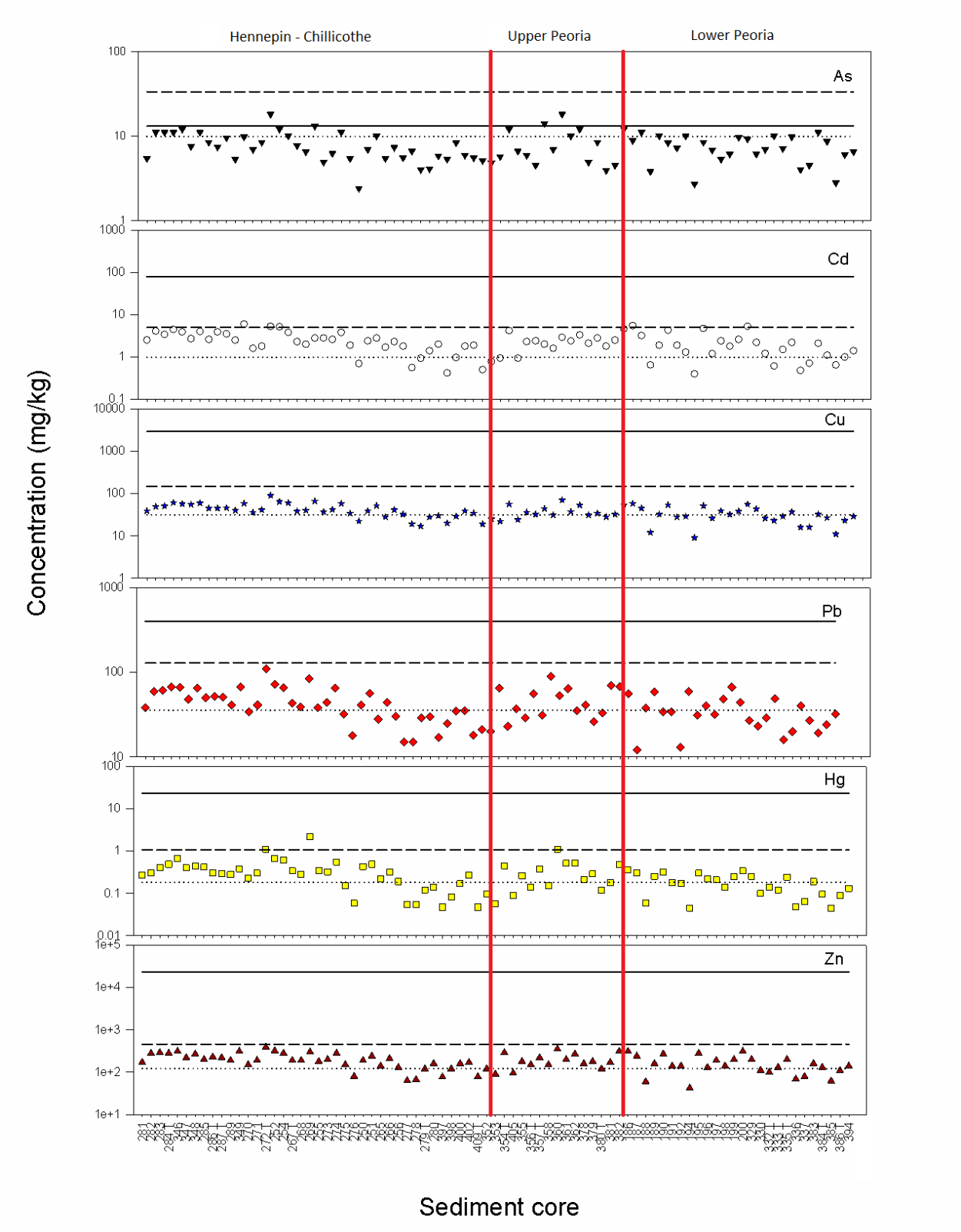

Figure 3.1 Metal concentrations (As, Cd, Cu, Pb, Hg, Zn) in selected sediment cores. Dotted line indicates the TEC value, dashed line the PEC value, and solid line the TACO Tier 1 objective.

Table 3.1. Eigenvalues and data variance explained by corresponding principal components.

Component	Eigenvalue	Variance Explained (%)	Total variance explained (%)
1	**9.66**	56.84	56.84
2	**2.66**	15.64	72.48
3	**1.17**	6.85	79.33
4	0.88	5.16	84.50
5	0.82	4.82	89.31

PMF analyses were also carried out on metals data. Three-factor PMF fingerprints are given in Figure F-1. Highly consistent with PCA results, factor 1, with a high fraction of As, Cd, Cr, Cu, Pb, Hg, and Zn, represents anthropogenic inputs; factor 2, with a high fraction of Al, Ba, Be, Co, Fe, Ni, and V, indicates crustal weathering; and factor 3, dominated by Mg and Mn, with moderate Mo and As, suggests another crustal input factor.

Notice that in the PCA results, the eigenvalues of components 4 and 5 were very similar (Table 3.1) and five factors spanned 89% of the data variance. Therefore, in order to validate the model output, four and five factors were tested in the PMF analysis. The fingerprints of PMF 4- and 5-factor solutions are given in Figures 3.2 and F-2. Increased uncertainties were associated with 4- and 5-factor fingerprints (as indicated by the error bars). Again, this suggests that the limit of the data signal and noise was reached. The newly-introduced factor 4 (PMF 4-4) was enriched with Cd, Cr, Cu, Pb, Ni, Zn, and a high fraction – as well as a high uncertainty – of Mn. Cadmium was suggested to be derived from rubber tire wear (Hjortenkrans et al., 2007) and lubricating oil (Aucelio et al., 2007). Nickel is known to be released from petroleum combustion (Tian et al., 2012). Zinc has been widely recognized to be partially from vehicle emissions and tire wear (Chow et al., 2004). Manganese can be released from lubricating oil (Aucelio et al., 2007), tire wear (Hjortenkrans et al., 2007), corrosion and wearing of auto parts (Duan and Tan, 2013); it was also used as a gasoline antiknock additive (Loranger and Zayed, 1995). Therefore, this newly introduced factor very likely represents traffic emissions. Notice that this factor was also suggested by the PMF 5-factor solution (PMF 5-2, Figure F-2). Factor 5 is dominated by the single metal Mo and small amounts of all other metals in the PMF 5-factor fingerprints (PMF 5-5, Figure F-2), which probably represents data uncertainty. Generally, the 4-factor PMF results represent a clear and meaningful interpretation of the sources of metals in the Peoria Pool sediments.

Table 3.2. Rotated principal component profiles of metal data. Vales are loadings for individual factors on each principal component; high loadings (those shown in bold) indicate the principal components with which the factors are most strongly correlated.

	Rotated principal component		
	1	**2**	**3**
Al	.297	**.899**	.103
As	**.811**	.159	.253
Ba	.303	**.802**	.064
Be	.294	**.768**	.235
Cd	**.828**	.348	.095
Cr	**.850**	.474	.088
Co	.175	**.902**	.186
Cu	**.921**	.341	.039
Fe	.267	**.871**	.231
Pb	**.964**	.233	.071
Mg	.003	-.626	**.451**
Mn	.098	.301	**.667**
Hg	**.832**	-.016	-.043
Mo	.077	.067	**.678**
Ni	.530	**.649**	.183
V	.231	**.895**	.064
Zn	**.916**	.358	.098

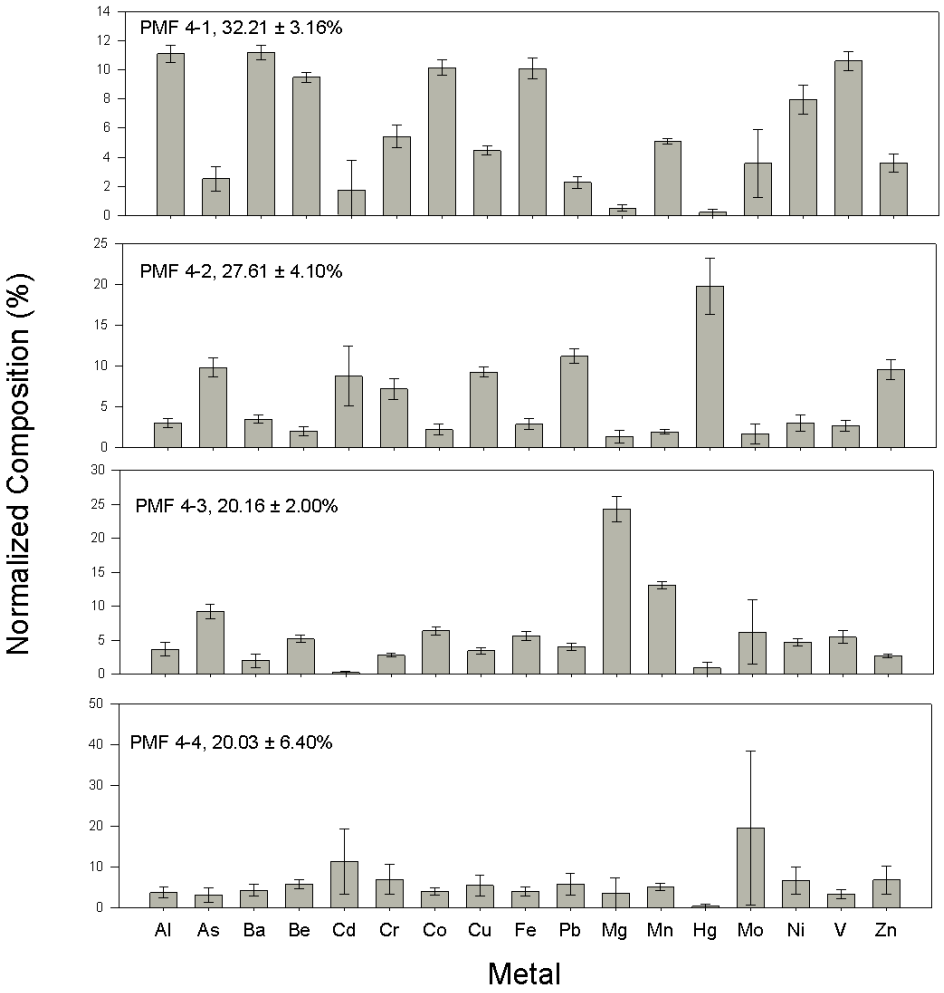

Figure 3.2. Metal 4-factor fingerprints generated by PMF analysis of metal data.

4. CONCLUSIONS

PAHs and metals detected in Illinois River sediments were analyzed to provide information on the possible sources of contaminants to the Peoria Pool. The following conclusions could be drawn from this study:

(1) Both PAH and metal concentrations showed some spatial variation within the Peoria Pool of the Illinois River. Some of the high-concentration samples were taken in locations close to the main river channel. The sediment cores taken downstream of Spring Bay in Upper Peoria Lake and in Lower Peoria Lake generally showed lower concentrations. Concentrations showed considerable variation in cores collected above Spring Bay and in the backwater lakes above Chillicothe.

(2) Concentrations of 4- and 5-ring PAHs were dominant in Peoria Pool sediments; 6-ring PAHs were moderately abundant; and 2- and 3-ring PAHs were generally rare. The comparison of PAH profiles in Peoria Pool sediments with PAH fingerprints from specific sources ($\cos\varphi$) suggested that low-rank coals (lignite and sub-bituminous), coal-tar sealcoats, coal and wood combustion soot, and traffic soot were the most probable sources of PAHs in Illinois River sediments.

(3) Positive matrix factorization (PMF) analysis suggested five factors, and when combined with $\cos\varphi$, indicated multiple potential PAH sources for several of those factors. Further evaluation led to selection of dominant sources for each factor. Coal dust was the most likely PAH source in the first factor (PMF 5-1), but PMF 5-1 may also have represented aggregated PAH sources. In total, PMF 5-1 represented 47 ± 7% of the total PAHs in sediments within the Peoria Pool of the Illinois River. Coal combustion soot was likely the dominant source of factor 2 (PMF 5-2), which accounted for 28 ± 4% of the PAHs. Another possible source associated with factor 2 (PMF 5-2) is coke oven emissions. Traffic soot, represented by factor 3 (PMF 5-3), contributed another 15 ± 3% of the total PAHs. Combining the PMF deductions and our prior knowledge, wood combustion soot was identified as a minor PAH contributor (factor 5, PMF 5-5), making up about 5% of the total PAHs. In addition, the gas phase of PAH emissions from combustion and engine exhaust (factor 4, PMF 5-4) accounted for the remaining portion (about 5%) of the total PAHs in the sediments.

(4) The analysis indicated that metals in the Peoria Pool sediments were mainly derived from weathering of Earth crustal materials. The two different fractions of the crustal-based materials, the Al/Fe-based fraction (clay materials) and Mn/Mg- based fraction (bulk sediments) contributed 32% and 20% of the metals in the sediments, respectively. The industrial-associated metal emissions composed slightly less than 28% of the total metals, while traffic emissions accounted for about 20% of the total metals.

5. REFERENCES

Alkurdi, F., Karabet, F., and Dimashki, M. 2013. Characterization, concentrations and emission rates of polycyclic aromatic hydrocarbons in the exhaust emissions from in-service vehicles in Damascus. Atmos Res 120: 68-77.

Agency for Toxic Substances and Disease Registry (ATSDR). 1995. Toxicological profile for polycyclic aromatic hydrocarbons. Agency for Toxic Substances and Disease Registry, Division of Toxicology/Toxicology Information Branch, U.S. Department of Health and Human Services, Atlanta, GA.

Atkinson, R. and Arey, J. 1994. Atmospheric chemistry of gas-phase polycyclic aromatic hydrocarbons: formation of atmospheric mutagens. Environ Health Perspect 102: 117-126.

Aucelio, R.Q., Souza, R.M., de Campos, R.C., Miekeley, N., and da Silveira, C.L.P. 2007. The determination of trace metals in lubricating oils by atomic spectrometry. Spectrochim Acta B 62: 952-961.

Barrick, R.C., Furlong, E.T., and Carpenter, R. 1984. Hydrocarbon and azaarene markers of coal transport to aquatic sediments. Environ. Sci. Technol. 18(11): 846-854.

Belis, C.A., Karagulian, F., Larsen, B.R., and Hopke, P.K. 2013. Critical review and meta-analysis of ambient particulate matter source apportionment using receptor models in Europe. Atmos Environ 69: 94-108.

Bellrose, F. C., Havera, S. P., Paveglio, F. L. Jr., and Steffeck, D. W. 1983. The fate of lakes in the Illinois River Valley. Biological Notes No. 119. Illinois Natural History Survey, Champaign, Illinois. 37 pp.

Bhowmik, N. G., Demissie, M., Marlin, J. C., and Mick, J. 2001. Integrated management of the Illinois River with an emphasis on the ecosystem. International Symposium on Integrated Water Resources Management 272: 365-372.

Brown, A.S. and Brown, R.J.C. 2012. Correlations in polycyclic aromatic hydrocarbon (PAH) concentrations in UK ambient air and implications for source apportionment. J Environ Monitor 14: 2072-2082.

Bzdusek, P.A. 2005. PCB or PAH sources and degradation in aquatic sediments determined by positive matrix factorization. Civil Engineering and Mechanics. University of Wisconsin - Milwaukee, Milwaukee, WI.

Bzdusek, P.A., Christensen, E.R., Li, A., and Zou, Q.M. 2004. Source apportionment of sediment PAHs in Lake Calumet, Chicago: Application of factor analysis with nonnegative constraints. Environmental Science & Technology 38: 97-103.

Cahill, R.A. 2001. Final report assessment of sediment quality in Peoria Lake: Results from the chemical analysis of sediment core samples collected in 1998, 1999, and 2000. Illinois State Geological Survey Open File Series 2001-4.

Cahill, R.A., Salmon, G.L., and Slowikowski, J.A. 2008. Investigation of metal and organic contaminant distributions and sedimentation rates in backwater lakes along the Illinois River. Illinois State Geological Survey, Illinois State Water Survey, Champaign, IL.

Calmano, W. and Forstner U. 2004. III.5 Dredged material. In: Solid Waste: Assessment, Monitoring and Remediation. Twardowska, A., Allen, H.E., Kettrup, A.F., and Lacy, W.J. (Eds.). Pergamon Press, Oxford UK. pp: 297-318.

Chen, F., Taylor, W.D., Anderson, W.B., and Huck, P.M. 2013. Application of fingerprint-based multivariate statistical analyses in source characterization and tracking of contaminated sediment migration in surface water. Environ Pollut 179: 224-231.

Chow, J.C., Watson, J.G., Kuhns, H., Etyemezian, V., Lowenthal, D.H., Crow, D., Kohl, S.D., Engelbrecht, J.P., and Green, M.C. 2004. Source profiles for industrial, mobile, and area sources in the Big Bend Regional Aerosol Visibility and Observational study. Chemosphere 54: 185-208.

Christensen, E.R. and Bzdusek, P.A. 2005. PAHs in sediments of the Black River and the Ashtabula River, Ohio: Source apportionment by factor analysis. Water Res 39(4): 511-524.

Demissie, M.B. and Bhowmik, N.G. 1986. Peoria Lake sediment investigation. Illinois State Water Survey, University of Illinois at Urbana-Champaign, Champaign, IL, p. 88.

Demissie, M., Keefer, L., and Xia, R. 1992. Erosion and sedimentation in the Illinois River Basin. Illinois State Water Survey, Univeristy of Illinois at Urbana-Champaign, Springfield, IL.

Demissie, M. 1997. Patterns of erosion and sedimentation in the Illinois River Basin. Proceedings of the 1997 Governor's Conference on the Management of the Illinois River System, Oct. 7–9, 1997. Special Report No. 23. Water Resources Center, University of Illinois. Urbana, IL.

Demissie, M. and Keefer, L. 2013. Sediment budget and trends in sediment delivery for the last 30 years in the Illinois River Basin. Proceedings of the 2013 Governor's Conference on the Management of the Illinois River System. Water Resources Center, University of Illinois. Urbana, IL.

Darmody, R.G. and Marlin, J.C. 2002. Sediments and sediment-derived soils in Illinois: Pedological and agronomic assessment. Environmental Monitoring and Assessment 77: 209-227.

Duan, J.C. and Tan, J.H. 2013. Atmospheric heavy metals and arsenic in China: Situation, sources and control policies. Atmos Environ 74: 93-101.

Dvorska, A., Lammel, G., and Klanova, J. 2011. Use of diagnostic ratios for studying source apportionment and reactivity of ambient polycyclic aromatic hydrocarbons over Central Europe. Atmos Environ 45: 420-427.

Equeenuddin, S.M., Tripathy, S., Sahoo, P.K., and Panigrahi, M.K. 2013. Metal behavior in sediment associated with acid mine drainage stream: Role of pH. J Geochem Explor 124: 230-237.

Galarneau, E. 2008. Source specificity and atmospheric processing of airborne PAHs: Implications for source apportionment. Atmos Environ 42: 8139-8149.

Granberg, K.J. and Rockne, K.J. 2015. Source apportionment of polycyclic aromatic hydrocarbons in Illinois River Sediment. University of Illinois at Chicago. ISTC Reports TR-058.

Gratz, L.E., Keeler, G.J., Morishita, M., Barres, J.A., and Dvonch, J.T. 2013. Assessing the emission sources of atmospheric mercury in wet deposition across Illinois. Sci Total Environ 448: 120-131.

Hammerschmidt, C.R. and Fitzgerald, W.F. 2006. Bioaccumulation and trophic transfer of methylmercury in Long Island Sound. Arch Environ Con Tox 51: 416-424.

Harrison, R.M., Smith, D.J.T., and Luhana, L. 1996. Source apportionment of atmospheric polycyclic aromatic hydrocarbons collected from an urban location in Birmingham, UK. Environ Sci Technol 30: 825-832.

Hatch, J.R. and Affolter, R.H. 2014. Resource assessment of the Springfield, Herrin, Danville, and Baker Coals in the Illinois Basin, Chapter A Executive Summary. United States Geological Survey.

Henry, R.C. 2003. Multivariate receptor modeling by N-dimensional edge detection. Chemometr Intell Lab 65: 179-189.

Hirsch, S.E. 2004. Economic geography in the encyclopedia of Chicago. The Newberry Library. http://www.encyclopedia.chicagohistory.org/pages/409.html. Accessed on July 17, 2014.

Hjortenkrans, D.S.T., Bergback, B.G., and Haggerud, A.V. 2007. Metal emissions from brake linings and tires: Case studies of Stockholm, Sweden 1995/1998 and 2005. Environ Sci Technol 41: 5224-5230.

Hopkins, M.E. and Simon, J.A. 1974. Coal resources of Illinois. In: Illinois Mineral Notes. Frye, F.C. (Ed.). Illinois State Geological Survey, Urbana, IL, p. 26.

Illinois Department of Transportation (IDOT). 2013. Illinois travel statistics, 2013. http://www.dot.state.il.us/travelstats/2013_ITS.pdf. Accessed on July 17, 2014.

Illinois Environmental Protection Agency (IEPA). 2013. Tiered approach to corrective action objectives, Ill. Admin. Code tit.35, pt. 742. http://www.epa.state.il.us/land/taco/second-notice. Accessed on July 17, 2014.

Illinois State Geological Survey (ISGS). Illinois energy production and consumption. http://www.isgs.uiuc.edu/outreach/geology-resources/illinois-energy-production-and-consumption. Accessed on July 17, 2014.

Jarup. L. 2003. Hazards of heavy metal contamination. Br Med Bull 68: 167-182.

Jolliffe, I.T. 2002. Principal Component Analysis, 2nd ed. Springer, New York, NY.

Katsoyiannis, A., Sweetman, A.J., and Jones, K.C. 2011. PAH molecular diagnostic ratios applied to atmospheric sources: A critical evaluation using two decades of source inventory and air concentration data from the UK. Environ Sci Technol 45: 8897-8906.

Kibbel, W. 2009 The history of coal heating. http://www.oldhouseweb.com/blog/the-history-of-coal-heating/. Accessed on July 17, 2014.

Kim, D., Kumfer, B.M., Anastasio, C., Kennedy, I.M., and Young, T.M. 2009. Environmental aging of polycyclic aromatic hydrocarbons on soot and its effect on source identification. Chemosphere 76: 1075-1081.

Kralovec, A., Christensen, E.R., and Van Camp, R.P. 2002. Fossil fuel and wood combustion as recorded by carbon particles in Lake Erie sediments 1850-1998. Environmental Science and Technology 36 (7): 1405-1413.

Larsen, R.K. and Baker, J.E. 2003. Source apportionment of polycyclic aromatic hydrocarbons in the urban atmosphere: A comparison of three methods. Environ Sci Technol 37: 1873-1881.

Lee, P.K., Youm, S.J., and Jo, H.Y. 2013. Heavy metal concentrations and contamination levels from Asian dust and identification of sources: A case-study. Chemosphere 91: 1018-1025.

Levendis, Y.A., Atal, A., and Carlson, J.B. 1998. On the correlation of CO and PAH emissions from the combustion of pulverized coal and waste tires. Environ Sci Technol 32: 3767-3777.

Li, A., Jang, J-K., and Scheff, P.A. 2003. Application of EPA CMB8.2 model for source apportionment of sediment PAHs in Lake Calumet, Chicago. Environ Sci Technol 37: 2958-2965.

Li, Q., Cheng, H.G., Zhou, T., Lin, C.Y., and Guo, S. 2012. The estimated atmospheric lead emissions in China, 1990-2009. Atmos Environ 60: 1-8.

Liu, Y., Beckingham, B., Ruegner, H., Li, Z., Ma, L.M., Schwientek, M., Xie, H., Zhao, J.F., and Grathwohl, P. 2013. Comparison of sedimentary PAHs in the rivers of Ammer

(Germany) and Liangtan (China): Differences between early- and newly-industrialized countries. Environ Sci Technol 47: 701-709.

Liu, Z.F., Zhao, Y.L., Colin, C., Siringan, F.P., and Wu, Q. 2009. Chemical weathering in Luzon, Philippines from clay mineralogy and major-element geochemistry of river sediments. Appl Geochem 24: 2195-2205.

Loganathan, P., Vigneswaran, S., and Kandasamy, J. 2013. Road-deposited sediment pollutants: A critical review of their characteristics, source apportionment, and management. Crit Rev Env Sci Tec 43: 1315-1348.

Loranger, S., and Zayed, J. 1995. Contribution of methylcyclopentadienyl manganese tricarbonyl (MMT) to atmospheric Mn concentration near expressway: Dispersion modeling estimations. Atmos Environ 29: 591-599.

Lu, A.X., Wang, J.H., Qin, X.Y., Wang, K.Y., Han, P., and Zhang, S.Z. 2012. Multivariate and geostatistical analyses of the spatial distribution and origin of heavy metals in the agricultural soils in Shunyi, Beijing, China. Sci Total Environ 425: 66-74.

MacDonald, D.D., Ingersoll, C.G., and Berger, T.A. 2000. Development and evaluation of consensus-based sediment quality guidelines for freshwater ecosystems. Arch Environ Con Tox 39: 20-31.

Mahler, B.J., Van Metre, P.C., Bashara, T.J., Wilson, J.T., and Johns, D.A. 2005. Parking lot sealcoat: An unrecognized source of urban polycyclic aromatic hydrocarbons. Environ Sci Technol 39: 5560-5566.

Mahler, B.J., Van Metre, P.C., Crane, J.L., Watts, A.W., Scoggins, M., and Williams, E.S. 2012. Coal-tar-based pavement sealcoat and PAHs: Implications for the environment, human health, and stormwater management. Environ Sci Technol 46: 3039-3045.

Malinowski, E.R. 1991. Factor Analysis in Chemistry, 2nd ed. John Wiley & Sons, Inc, New York, NY.

Mari, M., Harrison, R.M., Schuhmacher, M., Domingo, J.L., and Pongpiachan, S. 2010. Inferences over the sources and processes affecting polycyclic aromatic hydrocarbons in the atmosphere derived from measured data. Sci Total Environ 408: 2387-2393.

Marlin, J.C. 2002. Evaluation of sediment removal options and beneficial use of dredged material for Illinois River restoration: Preliminary report. In: Proceedings of the Western Dredging Association Twenty-Second Technical Conference and Thirty-Fourth Texas A&M Dredging Seminar. Randall, R.E. (Ed.). Center for Dredging Studies Ocean Engineering Department, Texas A&M University, Denver, CO, pp. 131-146.

Marr, L.C., Dzepina, K., Jimenez, J.L., Reisen, F., Bethel, H.L., Arey, J., Gaffney, J.S., Marley, N.A., Molina, L.T., and Molina, M.J. 2006. Sources and transformations of particle-bound polycyclic aromatic hydrocarbons in Mexico City. Atmos Chem Phys 6: 1733-1745.

Marr, L.C., Kirchstetter, T.W., Harley, R.A., Miguel, A.H., Hering, S.V., and Hammond, S.K. 1999. Characterization of polycyclic aromatic hydrocarbons in motor vehicle fuels and exhaust emissions. Environ Sci Technol 33: 3091-3099.

Meyer, W., Seiler, T-B., Reininghaus, M., Schwarzbauer, J., Puttmann, W., Hollert, H., and Achten,C. 2013. Limited waterborne acute toxicity of native polycyclic aromatic compounds from coals of different types compared to their total hazard potential. Environ Sci Technol 47: 11766-11775.

Mi, H.H., Lee, W.J., Chen, C.B., Yang, H.H., and Wu, S.J. 2000. Effect of fuel aromatic content on PAH emission from a heavy-duty diesel engine. Chemosphere 41: 1783-1790.

Miguel, A.H., Kirchstetter, T.W., Harley, R.A., and Hering, S.V. 1998. On-road emissions of particulate polycyclic aromatic hydrocarbons and black carbon from gasoline and diesel vehicles. Environ Sci Technol 32: 450-455.

Niu, L.L., Yang, F.X., Xu, C., Yang, H.Y., and Liu, W.P. 2013. Status of metal accumulation in farmland soils across China: From distribution to risk assessment. Environ Pollut 176: 55-62.

Oanh, N.T.K., Reutergardh, L.B., and Dung, N.T. 1999. Emission of polycyclic aromatic hydrocarbons and particulate matter from domestic combustion of selected fuels. Environ Sci Technol 33: 2703-2709.

Obst, M., Grathwohl, P., Kappler, A., Eibl, O., Peranio, N., and Gocht, T. 2011. Quantitative high-resolution mapping of phenanthrene sorption to black carbon particles. Environmental Science & Technology 45: 7314-7322.

Paatero, P. 1997. Least squares formulation of robust non-negative factor analysis. Chemometr Intell Lab 37: 23-35.

Page, D.S., Boehm, P.D., Douglas, G.S., Bence, A.E., Burns, W.A., and Mankiewicz, P.J. 1999. Pyrogenic polycyclic aromatic hydrocarbons in sediments record past human activity: A case study in Prince William Sound, Alaska. Mar Pollut Bull 38: 247-260.

Peng, C., Ouyang, Z.Y., Wang, M.E., Chen, W.P., Li, X.M., and Crittenden, J.C. 2013. Assessing the combined risks of PAHs and metals in urban soils by urbanization indicators. Environ Pollut 178: 426-432.

Percival, J.B. and Outridge, P.M. 2013. A test of the stability of Cd, Cu, Hg, Pb and Zn profiles over two decades in lake sediments near the Flin Flon Smelter, Manitoba, Canada. Sci Total Environ 454: 307-318.

Querol, X., Zhuang, X.G., Alastuey, A., Viana, M., Lv, W.W., Wang, Y.X., Lopez, A., Zhu, Z.C., Wei, H.M., and Xu, S.Q. 2006. Speciation and sources of atmospheric aerosols in a highly industrialised emerging mega-city in Central China. J Environ Monitor 8: 1049-1059.

Rachdawong, P. and Christensen, E.R. 1997. Determination of PCB sources by a principal component method with nonnegative constraints. Environ Sci Technol 31: 2686-2691.

Ravindra, K., Sokhi, R., and Van Grieken, R. 2008. Atmospheric polycyclic aromatic hydrocarbons: Source attribution, emission factors and regulation. Atmos Environ 42: 2895-2921.

Rigaud, S., Radakovitch, O., Nerini, D., Picon, P., and Garnier, J.M. 2011. Reconstructing historical trends of Berre Lagoon contamination from surface sediment datasets: Influences of industrial regulations and anthropogenic silt inputs. J Environ Manage 92: 2201-2210.

Robinson, A.L., Subramanian, R., Donahue, N.M., Bernardo-Bricker, A., and Rogge, W.F. 2006. Source apportionment of molecular markers and organic aerosol -- 1. Polycyclic aromatic hydrocarbons and methodology for data visualization. Environ Sci Technol 40: 7803-7810.

Rossi, L., Chevre, N., Fankhauser, R., Margot, J., Curdy, R., Babut, M., and Barry, D.A. 2013. Sediment contamination assessment in urban areas based on total suspended solids. Water Res 47: 339-350.

Sandler, A., Teutsch, N., and Avigad, D. 2012. Sub-Cambrian pedogenesis recorded in weathering profiles of the Arabian-Nubian Shield. Sedimentology 59: 1305-1320.

Schauer, J.J., Kleeman, M.J., Cass, G.R., and Simoneit, B.R.T. 1999. Measurement of emissions from air pollution sources. 2. C1 through C30 organic compounds from medium duty diesel trucks. Environ Sci Technol 33: 1578-1587.

Schauer, J.J., Kleeman, M.J., Cass, G.R., and Simoneit, B.R.T. 2001. Measurement of emissions from air pollution sources. 3. C-1-C-29 organic compounds from fireplace combustion of wood. Environ Sci Technol 35: 1716-1728.

Schauer, J.J., Kleeman, M.J., Cass, G.R., and Simoneit, B.R.T. 2002. Measurement of emissions from air pollution sources. 5. C-1-C-32 organic compounds from gasoline-powered motor vehicles. Environ Sci Technol 36: 1169-1180.

Schneider, A.R., Stapleton, H.M., Cornwell, J., and Baker, J.E. 2001. Recent declines in PAH, PCB, and toxaphene levels in the northern Great Lakes as determined from high resolution sediment cores. Environ Sci Technol 35(19): 3809-3815.

Shah, S.D., Ogunyoku, T.A., Miller, J.W., and Cocker, D.R. 2005. On-road emission rates of PAH and n-alkane compounds from heavy-duty diesel vehicles. Environ Sci Technol 39: 5276-5284.

Shen, H.Z., Huang, Y., Wang, R., Zhu, D., Li, W., Shen, G.F., Wang, B., Zhang, Y.Y., Chen, Y.C., Lu, Y., Chen, H., Li, T.C., Sun, K., Li, B.G., Liu, W.X., Liu, J.F., and Tao, S. 2013. Global atmospheric emissions of polycyclic aromatic hydrocarbons from 1960 to 2008 and future predictions. Environ Sci Technol 47: 6415-6424.

Simcik, M.F., Eisenreich, S.J., and Lioy, P.J. 1999. Source apportionment and source/sink relationships of PAHs in the coastal atmosphere of Chicago and Lake Michigan. Atmos Environ 33(30): 5071-5079.

Simon, V.M., L., Romdhana, M.H., Sablayrolles, C., Montrejaud-Vignoles, M., and Lecomte, D. 2012. Emissions of polycyclic aromatic hydrocarbon particulates from combustion of different fuels. Fresenius Environmental Bulletin 21: 946-955.

Slowikowski, J.A.L., B.D., and Russell, A.M. 2008. Database development to support sediment characterization of the middle Illinois River. Illinois State Water Survey, Institute of Natural Resource Sustainability, University of Illinois at Urbana-Champaign, Champaign, pp. 1-15.

Soonthornnonda, P., Zou, Y.H., Christensen, E.R., and Li, A. 2011. PCBs in Great Lakes sediments, determined by positive matrix factorization. J Great Lakes Res 37: 54-63.

Stout, S.A., and Emsbo-Mattingly, S.D. 2008. Concentration and character of PAHs and other hydrocarbons in coals of varying rank: Implications for environmental studies of soils and sediments containing particulate coal. Org Geochem 39: 801-819.

Stout, S.A. and Wang, Z. 2007. Chemical fingerprinting of spilled and discharged petroleum-methods and factors affecting petroleum fingerprints in the environment. In: Oil Spill Environmental Forensics: Fingerprinting And Source Identification. Wang, Z.-D.S. and Stout, S.A (Eds.). Academic Press. Waltham, MA.

Sun, C.Y., Liu, J.S., Wang, Y., Sun, L.Q., and Yu, H.W. 2013. Multivariate and geostatistical analyses of the spatial distribution and sources of heavy metals in agricultural soil in Dehui, Northeast China. Chemosphere 92: 517-523.

Taylor, K.G. and Owens, P.N. 2009. Sediments in urban river basins: A review of sediment-contaminant dynamics in an environmental system conditioned by human activities. J Soil Sediment 9: 281-303.

Taylor, S.R. and Mclennan, S.M. 1995. The geochemical evolution of the continental-crust. Rev Geophys 33: 241-265.

Tewalt, S.J.B., Bragg, L.J., and Finkelman, R.B. 2001. Mercury in U.S. coal-abundance, distribution, and modes of occurrence. USGS Fact Sheet 095-01. US Geological Survey, Washington D.C.

Thuens S., Blodau, C., and Radke, M. 2013. How suitable are peat cores to study historical deposition of PAHs? Sci Total Environ 450-451: 271-279.

Tian, H.Z., Lu, L., Cheng, K., Hao, J.M., Zhao, D., Wang, Y., Jia, W.X., and Qiu, P.P. 2012. Anthropogenic atmospheric nickel emissions and its distribution characteristics in China. Sci Total Environ 417: 148-157.

Tian, H.Z., Wang, Y., Xue, Z.G., Cheng, K., Qu, Y.P., Chai, F.H., and Hao, J.M. 2010. Trend and characteristics of atmospheric emissions of Hg, As, and Se from coal combustion in China, 1980-2007. Atmos Chem Phys 10: 11905-11919.

Tobiszewski, M. and Namiesnik, J. 2012. PAH diagnostic ratios for the identification of pollution emission sources. Environ Pollut 162: 110-119.

Tripp, B.W., Farrington, J.W., and Teal, J.M. 1981. Unburned coal as a source of hydrocarbons in surface sediments. Marine Pollution Bulletin 12(4): 122-126.

Ullrich, S.M., Tanton, T.W., and Abdrashitova, S.A. 2001. Mercury in the aquatic environment: A review of factors affecting methylation. Crit Rev Env Sci Tec 31: 241-293.

US Army Corp of Engineers (USACE) and Illinois Department of Natural Resources (IDNR). 2007. Illinois River basin restoration comprehensive plan with integrated environmental assessment. Rock Island District, Dept. of the Army, Rock Island, Il. http://www.mvr.usace.army.mil/Portals/48/docs/Environmental/ILRBR/CompPlan/MAIN%20REPORT%20and%20APPENDICES%20-%20CD.pdf. Accessed on July 22, 2014.

US Environmental Protection Agency (USEPA). 1996a. Method 8270C. Semivolatile organic compounds by gas chromatography/mass spectrometry (GC/MS). USEPA, Washington D.C.

US Environmental Protection Agency (USEPA). 1996b. Method 3540. Soxhlet extraction. USEPA, Washington D.C.

US Environmental Protection Agency (USEPA). 1996c. Method 3050B. Acid digestion of sediments, sludges and soils. USEPA, Washington D.C.

US Environmental Protection Agency (USEPA). 1998. Method 6010B. Inductively coupled plasma atomic emission spectometry. USEPA, Washington D.C.

US Environmental Protection Agency (USEPA). 2001. Method 7471. Mercury in sediments by manual cold vapor atomic absorption (CVAA). USEPA, Washington D.C.

Van Metre, P.C.M. and Mahler, B.J. 2010. Contribution of PAHs from coal-tar pavement sealcoat and other sources to 40 U.S. lakes. Sci Total Environ 409: 334-344.

Williams, R.J.P. 1953. Metal ions in biological systems. Biological Reviews 28 (4): 381-412.

Wimpenny, J., James, R.H., Burton, K.W., Gannoun, A., Mokadem, F., and Gislason, S.R. 2010. Glacial effects on weathering processes: New insights from the elemental and lithium isotopic composition of West Greenland rivers. Earth Planet Sc Lett 290: 427-437.

Woermann, J.W., 1905. Maps of Illinois and Des Plaines Rivers from Lockport, Illinois to the mouth of the Illinois River. Washington, D.C. U.S. Army Corps of Engineers.

World Health Organization (WHO). 2000. Air quality guidelines for Europe. WHO Regional Publications, European Series, Copenhagen, Denmark.

Yang, Y., Ligouis, B., Pies, C., Gruthwohl, P., and Hofmann, T. 2008. Occurrence of coal and coal-derived particle-bound polycyclic aromatic hydrocarbons (PAHs) in a river floodplain soil. Environ Pollut 151(1): 121-129.

Ye, S.Y., Laws, E.A., and Gambrell, R. 2013. Trace element remobilization following the resuspension of sediments under controlled redox conditions: City Park Lake, Baton Rouge, LA. Appl Geochem 28: 91-99.

Yunker, M.B., Macdonald, R.W., Vingarzan, R., Mitchell, R.H., Goyette, D., and Sylvestre, S. 2002. PAHs in the Fraser River basin: A critical appraisal of PAH ratios as indicators of PAH source and composition. Org Geochem 33: 489-515.

Zereini, F., Alt, F., Messerschmidt, J., Wiseman, C., Feldmann, I., Von Bohlen, A., Muller, J., Liebl, K., and Puttmann, W. 2005. Concentration and distribution of heavy metals in urban airborne particulate matter in Frankfurt am main, Germany. Environ Sci Technol 39: 2983-2989.

Zhang, J. and Liu, C.L. 2002. Riverine composition and estuarine geochemistry of particulate metals in China: Weathering features, anthropogenic impact and chemical fluxes. Estuar Coast Shelf S 54: 1051-1070.

Zhang, K., Wang, J.Z., Liang, B., and Zeng, E.Y. 2011. Occurrence of polycyclic aromatic hydrocarbons in surface sediments of a highly urbanized river system with special reference to energy consumption patterns. Environ Pollut 159: 1510-1515.

Zhang, W.G., Feng, H., Chang, J.N., Qu, J.G., Xie, H.X., and Yu, L.Z. 2009. Heavy metal contamination in surface sediments of Yangtze River intertidal zone: An assessment from different indexes. Environ Pollut 157: 1533-1543.

Zhang, Y.X., Schauer, J.J., Zhang, Y.H., Zeng, L.M., Wei, Y.J., Liu, Y., and Shao, M. 2008. Characteristics of particulate carbon emissions from real-world Chinese coal combustion. Environ Sci Technol 42: 5068-5073.

Zhang, Y.X. and Tao, S. 2009. Global atmospheric emission inventory of polycyclic aromatic hydrocarbons (PAHs) for 2004. Atmos Environ 43: 812-819.

Zou, Y.H., Christensen, E.R., and Li, A. 2013. Characteristic pattern analysis of polybromodiphenyl ethers in Great Lakes sediments: A combination of eigenspace projection and positive matrix factorization analysis. Environmetrics 24: 41-50.

APPENDIX A: Sediment Core Locations in Illinois River

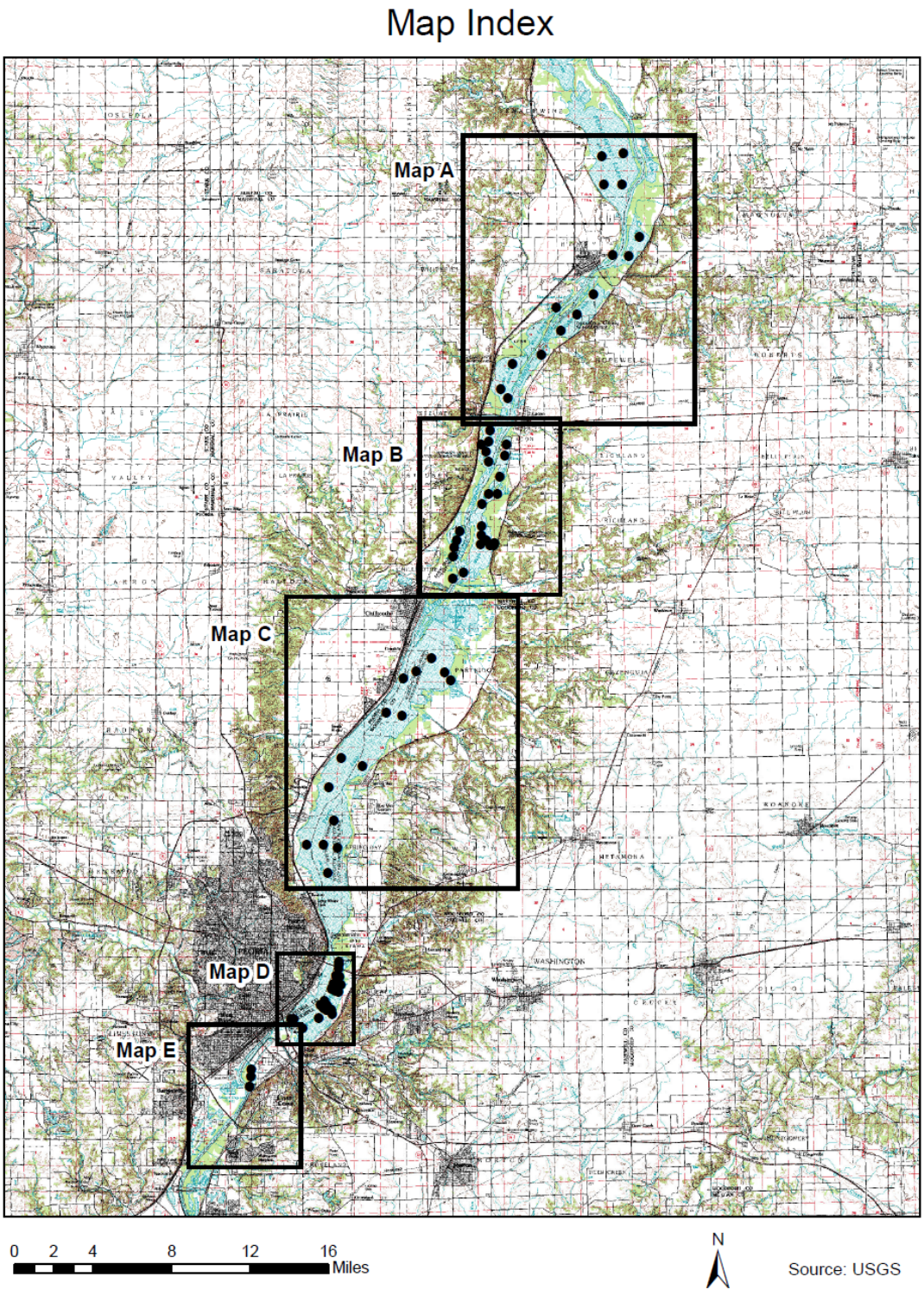

Figure A-1. Map index for sampling sites in Peoria Pool of Illinois River.

Map A

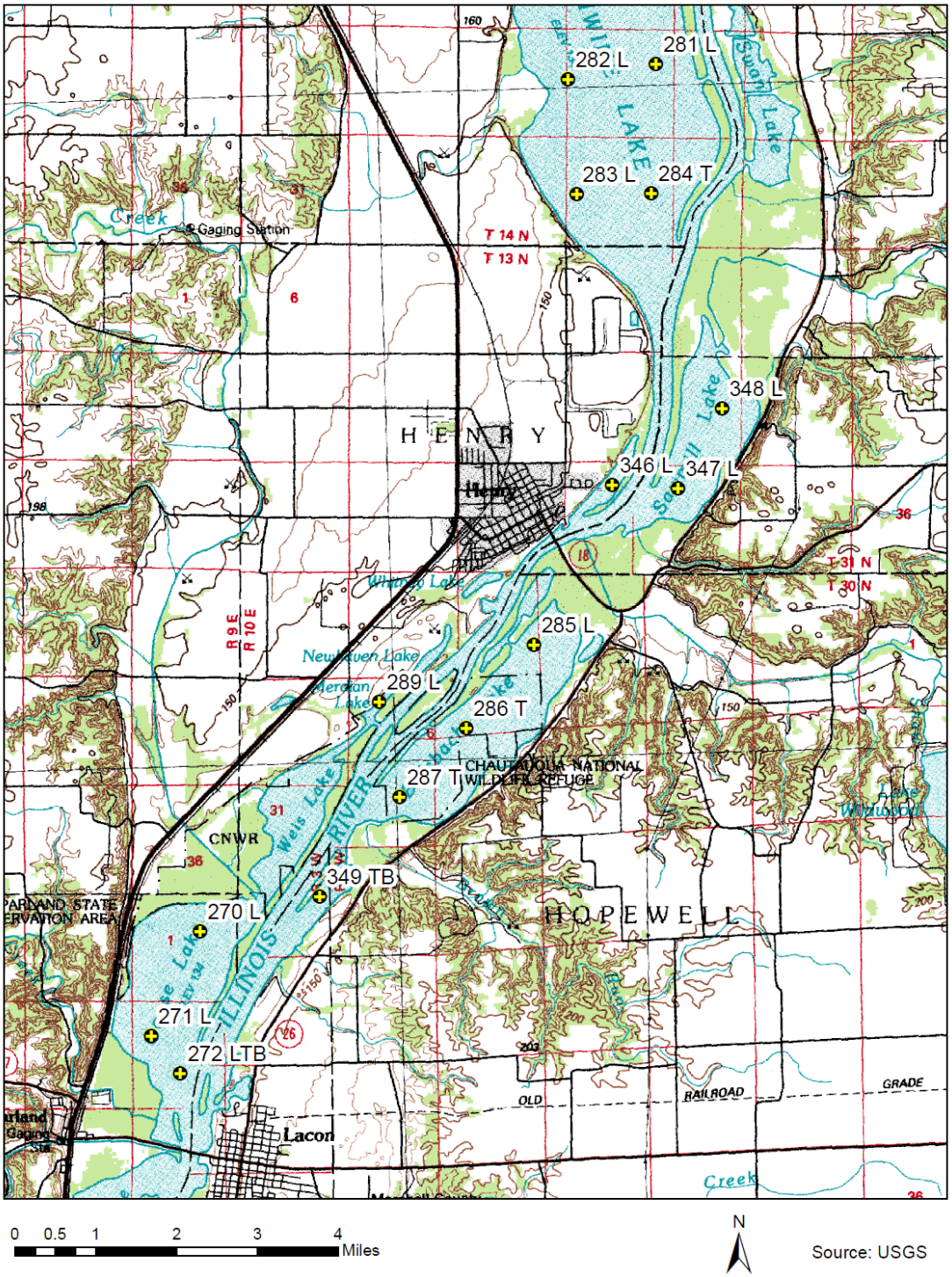

Figure A-2. Locations of sediment cores taken in backwater lakes Senachwine, Sawmill, Billsbach, Weis, and Goose (at Marshall). L indicates sediment sample was generated by long core composite; T, top segment composite; B, bottom segment composite.

Map B

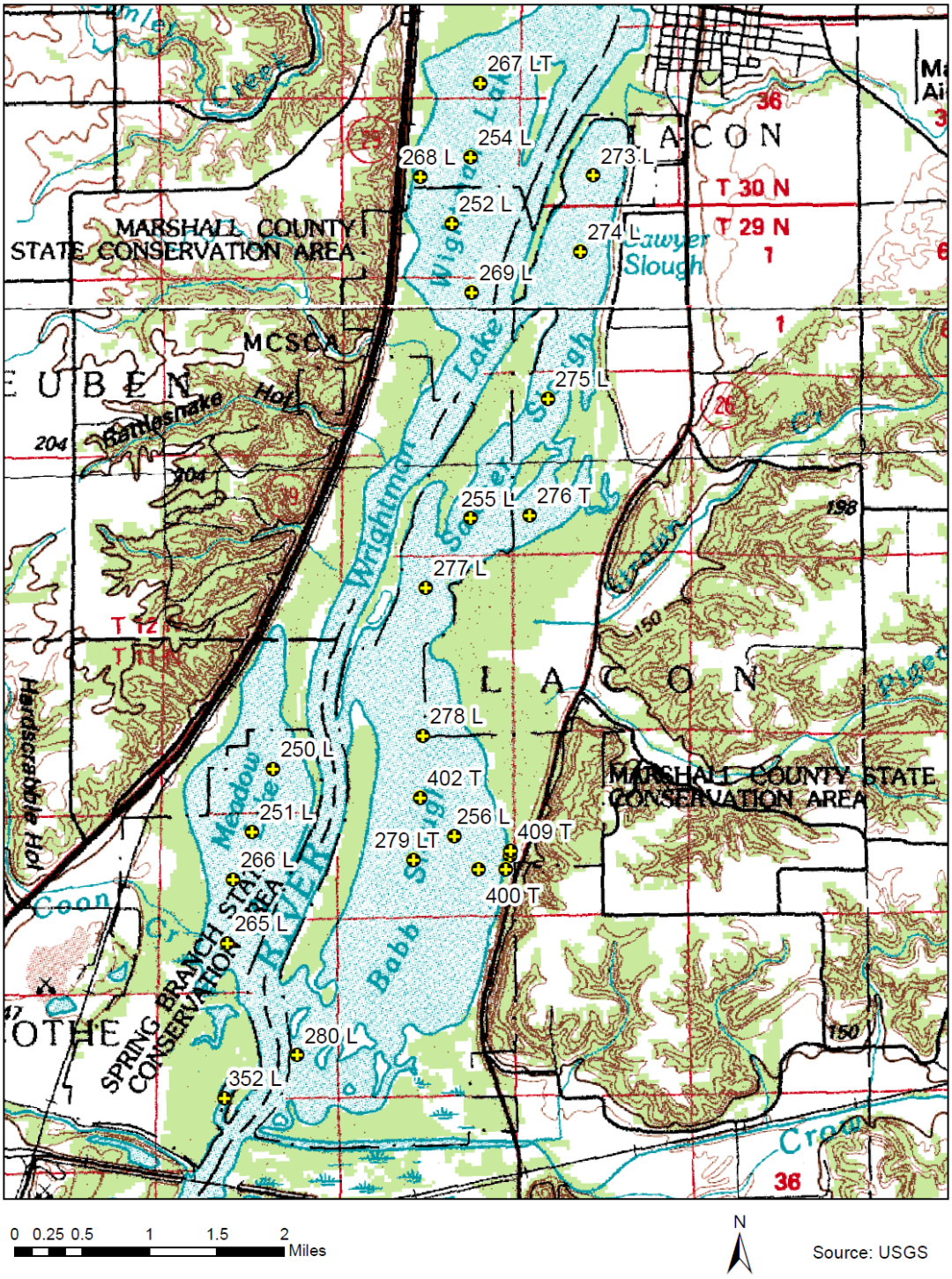

Figure A-3. Locations of sediment cores taken in backwater lakes Wrightman, Sawyer Slough, Meadow, and Babb Slough. L indicates sediment sample was generated by long core composite; T, top segment composite; B, bottom segment composite.

Map C

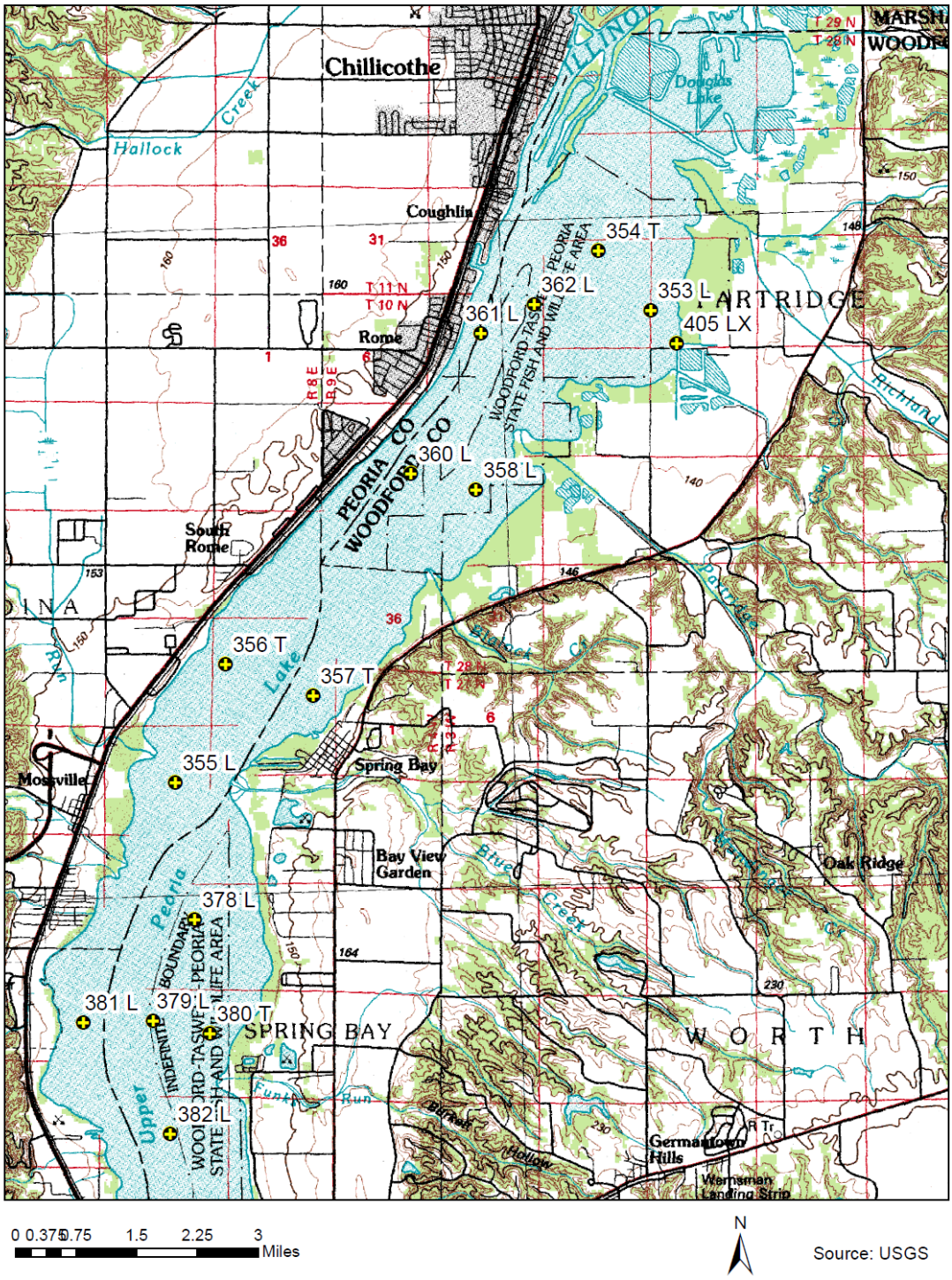

Figure A-4. Locations of sediment cores taken in Upper Peoria Lake. L indicates sediment sample was generated by long core composite; T, top segment composite; B, bottom segment composite.

Map D

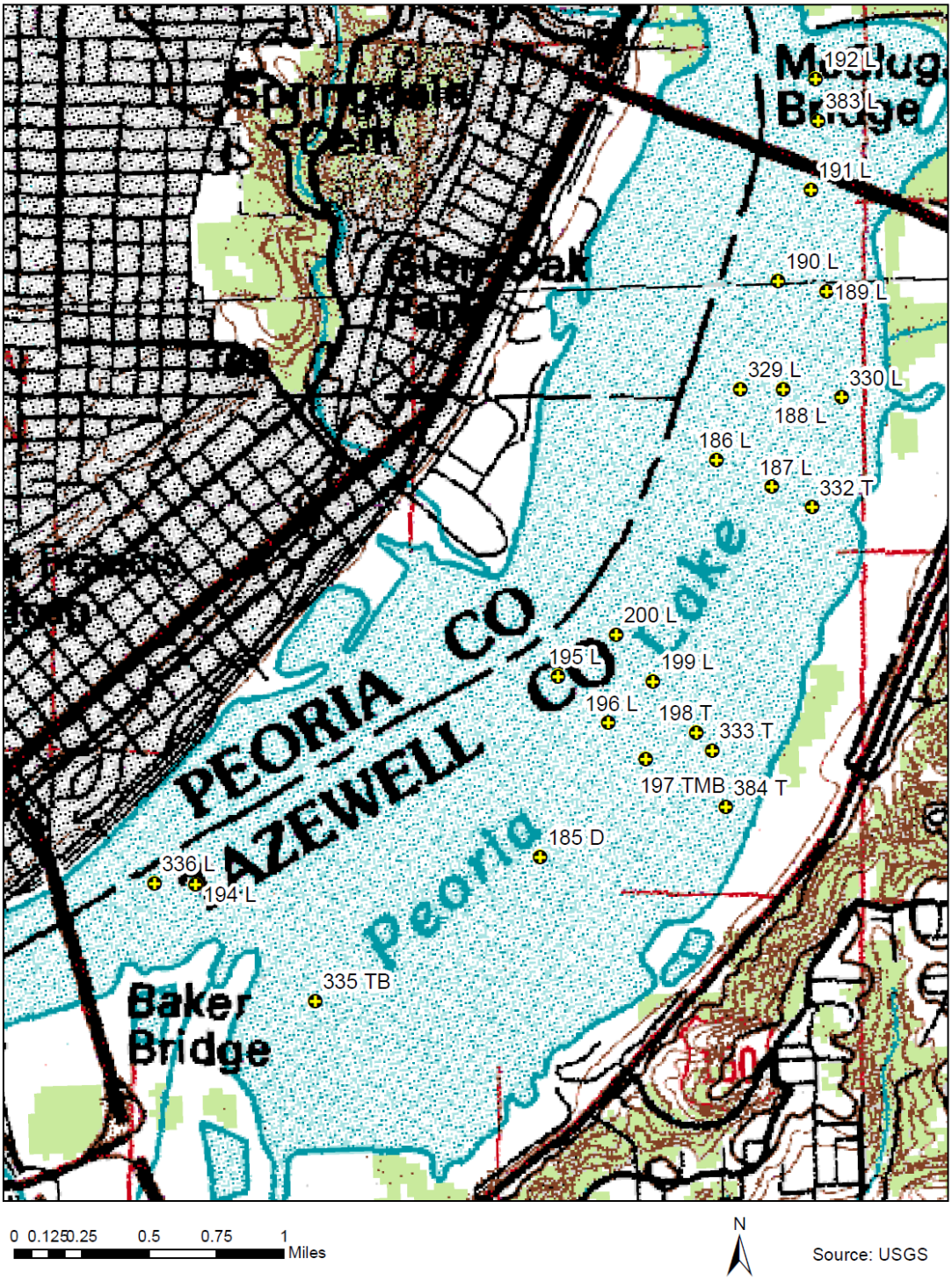

Figure A-5. Locations of sediment cores taken in Lower Peoria Lake. L indicates sediment sample was generated by long core composite; T, top segment composite; B, bottom segment composite.

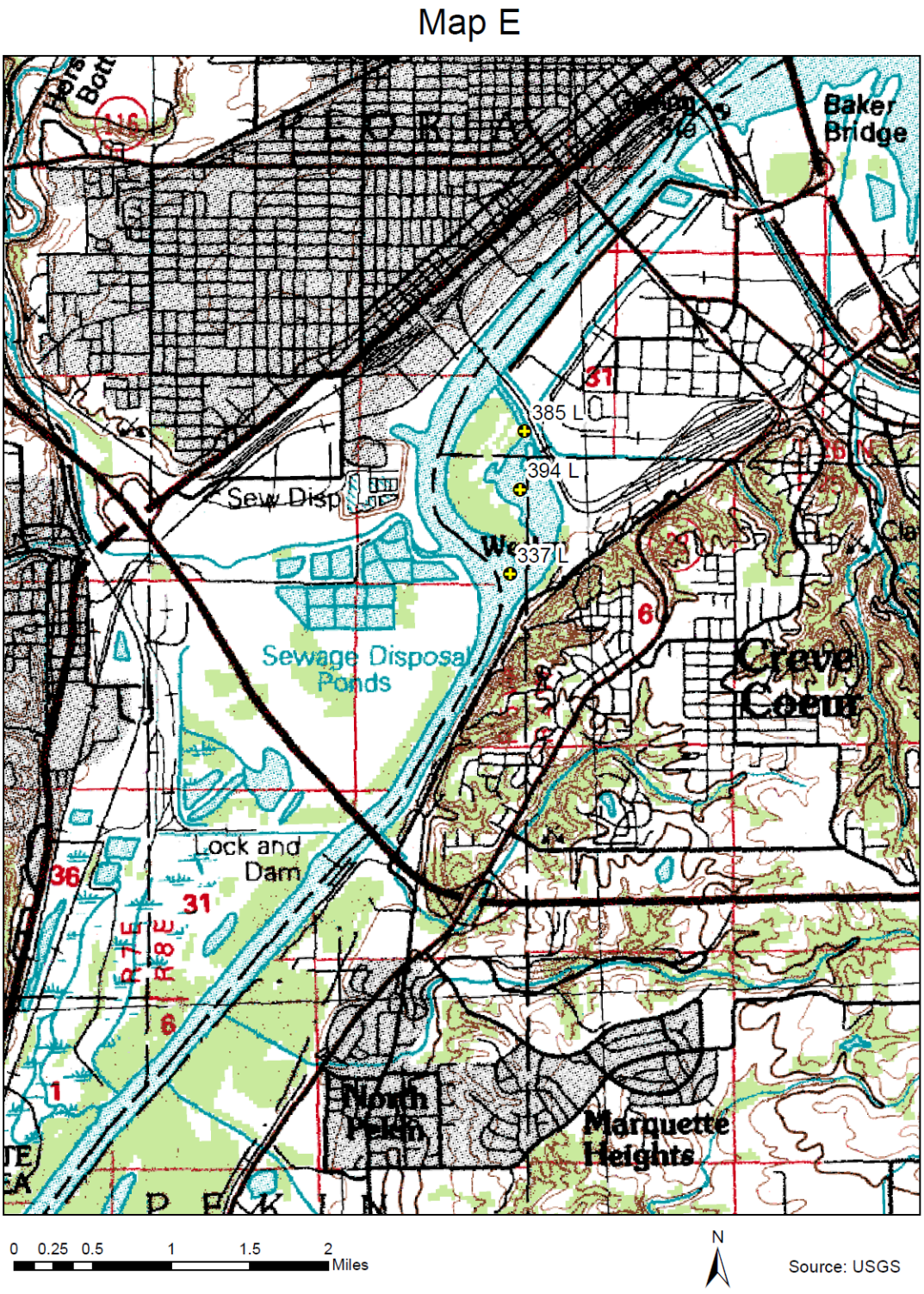

Figure A-6. Locations of sediment cores taken in Wesley Lake. L indicates sediment sample was generated by long core composite; T, top segment composite; B, bottom segment composite.

APPENDIX B: Detailed Information About Selected Sediment Cores

Table B-1. Core ID, locations, and sampling date of the selected sediment cores.

core #	latitude	longitude	date
185	40.69134605	-89.55825967	7-Oct-2004
186	40.70748007	-89.54881642	7-Oct-2004
187	40.7063746	-89.54585069	7-Oct-2004
189	40.71431163	-89.54292152	7-Oct-2004
190	40.71473175	-89.54551814	7-Oct-2004
191	40.7184454	-89.54376554	7-Oct-2004
192	40.72293695	-89.54349859	7-Oct-2004
194	40.69023257	-89.57672442	17-Nov-2004
195	40.69868109	-89.55730962	17-Nov-2004
196	40.6967953	-89.55461019	17-Nov-2004
197	40.69533527	-89.55261357	17-Nov-2004
198	40.69640443	-89.54988513	17-Nov-2004
199	40.69846969	-89.55221255	17-Nov-2004
200	40.70036277	-89.55417848	17-Nov-2004
250	40.9627	-89.45424	23-Mar-2006
251	40.95761	-89.45648	23-Mar-2006
252	41.0069	-89.4351	23-Mar-2006
254	41.01226	-89.43306	23-Mar-2006
255	40.98302	-89.43306	23-Mar-2006
256	40.95726	-89.43479	23-Mar-2006
265	40.94858333	-89.45913889	8-May-2006
266	40.95375	-89.45852778	8-May-2006
267	41.01827778	-89.43202778	8-May-2006
268	41.01066667	-89.43844444	8-May-2006
269	41.00130556	-89.43291667	8-May-2006
270	41.05563889	-89.4155	8-May-2006
271	41.04152778	-89.42430556	8-May-2006
272	41.03638889	-89.41908333	8-May-2006
273	41.01077778	-89.41991667	8-May-2006
274	41.00461111	-89.42130556	8-May-2006
275	40.99269444	-89.42477778	9-May-2006
276	40.98325	-89.42675	9-May-2006
277	40.97738889	-89.43786111	9-May-2006
278	40.96538889	-89.43819444	9-May-2006
279	40.95536111	-89.43916667	9-May-2006
280	40.93952778	-89.45166667	9-May-2006
281	41.1725	-89.33397222	17-May-2006
282	41.17044444	-89.34969444	17-May-2006
283	41.15494444	-89.34811111	17-May-2006
284	41.15505556	-89.33483333	17-May-2006

Table B-1 (continued).

core #	latitude	longitude	date
285	41.09427778	-89.35580556	17-May-2006
286	41.08305556	-89.36791667	17-May-2006
287	41.07375	-89.37983333	17-May-2006
289	41.08655556	-89.3835	17-May-2006
329	40.71035	-89.54754	25-Oct-2006
330	40.71001	-89.54211	25-Oct-2006
332	40.70555	-89.54369	25-Oct-2006
333	40.69566	-89.54906	25-Oct-2006
335	40.68549	-89.57031	25-Oct-2006
336	40.69027	-89.57893	25-Oct-2006
337	40.65269	-89.60925	25-Oct-2006
346	41.11574	-89.34181	11-Apr-2007
347	41.11529	-89.33	11-Apr-2007
348	41.1261	-89.32214	11-Apr-2007
349	41.0603	-89.39419	11-Apr-2007
352	40.93602	-89.45947	11-Apr-2007
353	40.88385	-89.46573	11-Apr-2007
354	40.89196	-89.47507	11-Apr-2007
355	40.82007	-89.5507	23-May-2007
356	40.83606	-89.54172	23-May-2007
357	40.8318	-89.52606	23-May-2007
358	40.85965	-89.49696	23-May-2007
360	40.86183	-89.50861	23-May-2007
361	40.88076	-89.49605	23-May-2007
362	40.8847	-89.4866	23-May-2007
378	40.80153	-89.54725	9-Aug-2007
379	40.78779	-89.55466	9-Aug-2007
380	40.78608	-89.54455	9-Aug-2007
381	40.78756	-89.56714	9-Aug-2007
382	40.77251	-89.5516	9-Aug-2007
383	40.72123	-89.54338	9-Aug-2007
384	40.69337	-89.54832	9-Aug-2007
385	40.66267	-89.6079	9-Aug-2007
394	40.65858	-89.60832	2-Mar-2009
397	40.9557	-89.42882	22-Mar-2010
398	40.95459	-89.42928	22-Mar-2010
400	40.95459	-89.43221	22-Mar-2010
402	40.96038	-89.43848	22-Mar-2010
405	40.87942	-89.46111	27-May-2010
409	40.95607	-89.4288	27-May-2010

APPENDIX C: PAH Profiles in Sediment Samples

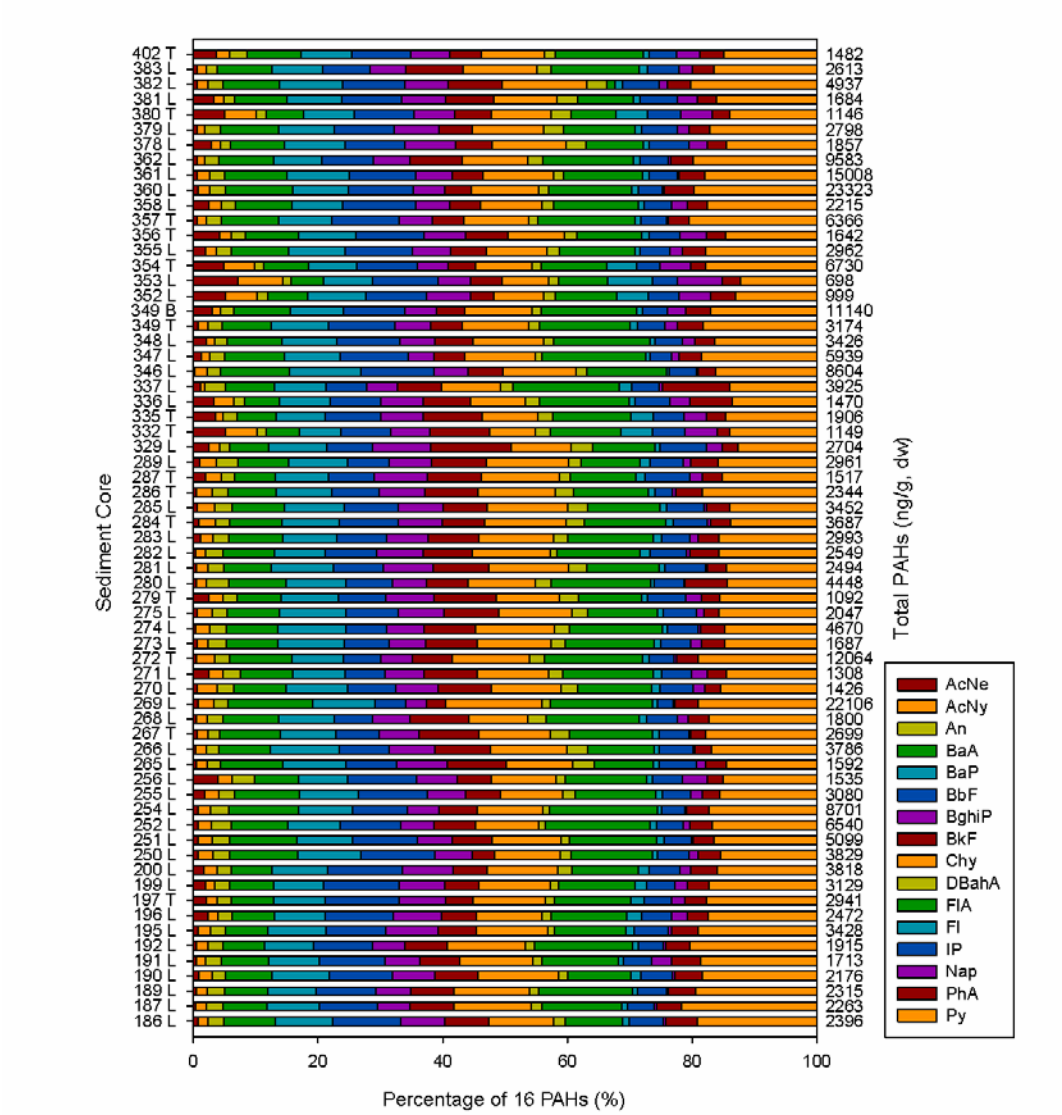

Figure C-1. PAH profiles of selected 65 sediment cores (for source apportionment analysis).

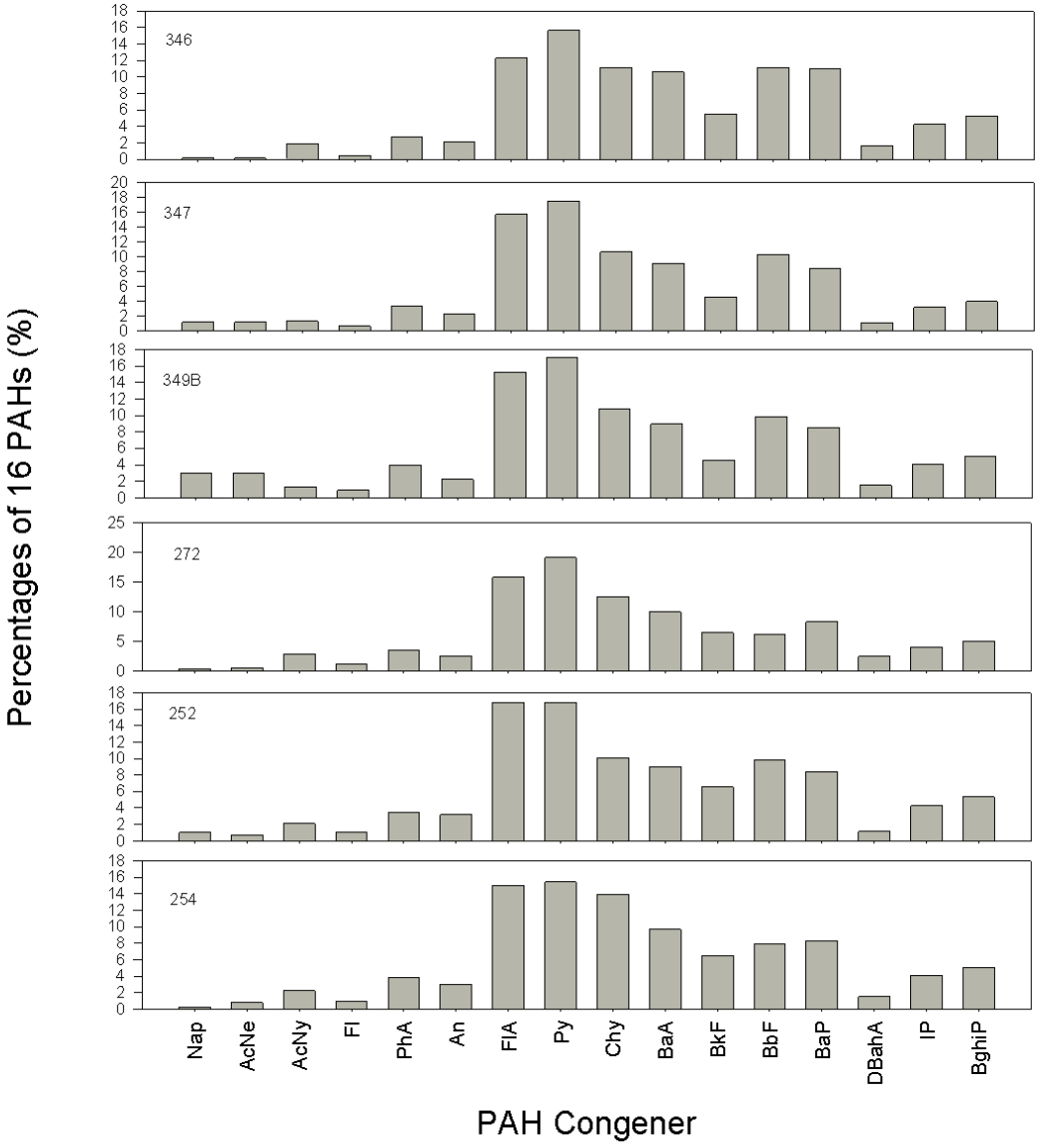

Figure C-2. PAH profiles in sediment cores whose total PAH concentration is higher than mean concentration (part 1).

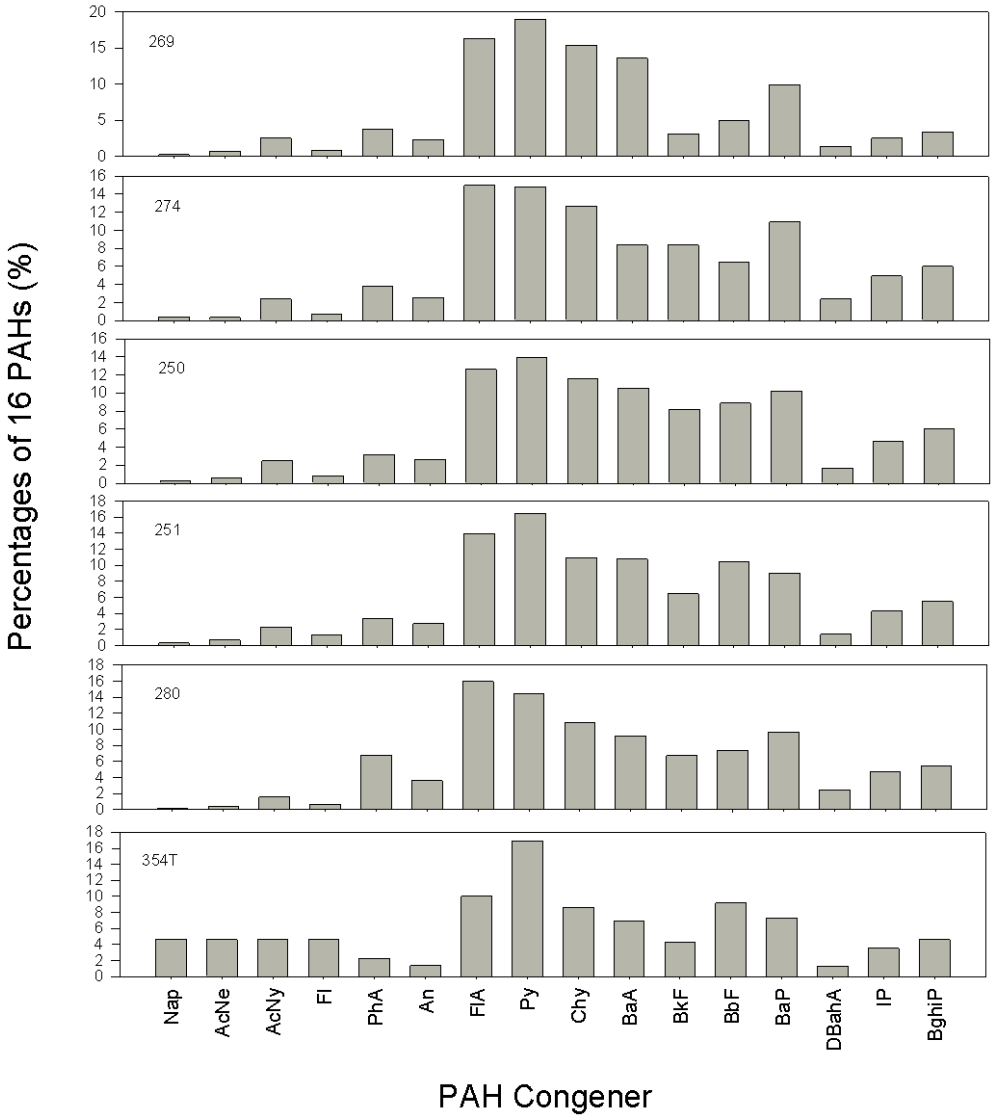

Figure C-2 (continued). PAH profiles in sediment cores whose total PAH concentration higher than mean concentration (part 2).

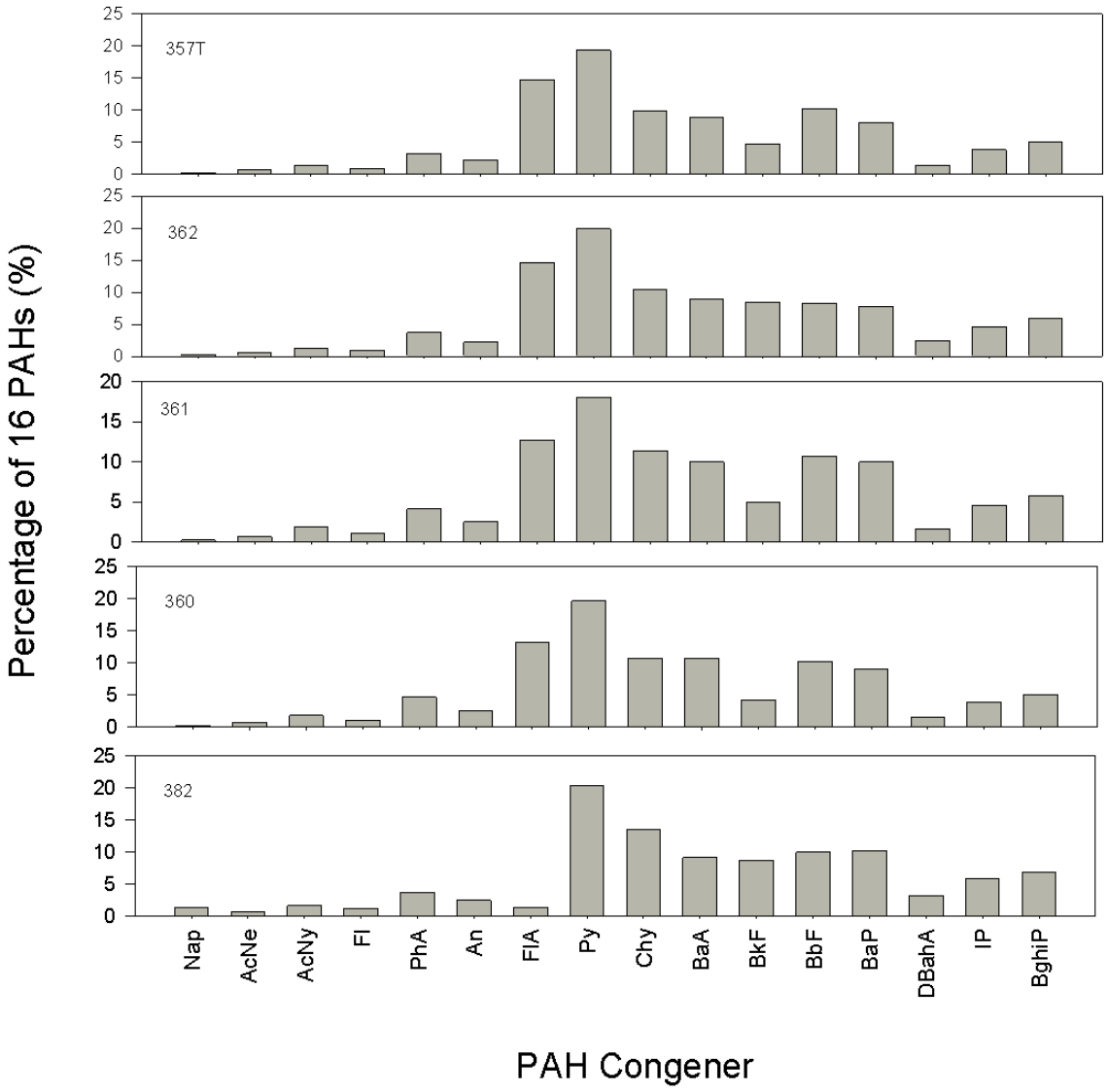

Figure C-2 (continued). PAH profiles in sediment cores whose total PAH concentration higher than mean concentration (part 3).

APPENDIX D: PAH Profiles in Specific Sources

Table D-1. PAH profiles in coals. List of abbreviations: Lig – Lignite, Sub – Sub-bituminous, HVC – high volatile C, HVB – high volatile B, HVA – high volatile A, MV – medium volatile, LV – low volatile, ANTH – Anthracite.

	1	2	3	4	5	6	7	8	9	10	11	12	13	14	15	16	17	18	19
									COAL										
	Lignite A			Sub-bituminous					Bituminous							Anthracites			charcoal
PAH	Lig A	Lig A	Lignite A	Sub C	Sub C	Sub B	Sub B	Sub A	HVC	HVB	HVA	HVA	MV	LV	HVA	SEMI-ANTH	ANTH	ANTH	charcoal
AcNe	2.70	0.52	2.24	12.60	0.56	2.61	9.47	0.46	3.24	7.88	3.53	1.36	1.44	0.53	1.85	0.20	2.53	5.10	19.29
AcNy	0.00	0.00	0.00	0.00	0.00	0.00	0.00	0.19	0.57	0.36	0.61	0.96	0.53	0.04	1.39	0.00	0.00	1.28	2.21
An	1.38	0.89	1.35	1.10	0.00	1.40	1.25	0.64	6.18	5.39	14.47	0.43	1.01	0.46	0.74	0.11	0.00	1.53	0.22
BaA	4.44	9.60	5.23	5.28	4.47	7.02	4.89	6.88	3.68	3.99	5.38	2.25	1.97	1.64	2.31	1.05	0.00	0.77	0.28
BaP	2.34	2.73	3.74	1.97	4.47	1.80	2.17	6.88	1.25	2.99	1.86	1.20	0.58	0.70	1.39	1.57	0.00	0.00	0.00
BbF	15.58	14.03	14.95	4.73	9.87	3.31	3.36	20.65	2.21	1.80	2.41	0.63	1.73	3.37	0.92	20.97	0.00	1.02	0.00
BghiP	1.14	0.81	1.49	0.57	2.54	0.45	0.52	3.07	0.44	1.20	0.95	0.59	0.53	1.54	0.46	4.81	0.00	2.04	0.00
BkF	5.99	6.94	5.98	2.28	4.70	1.70	1.92	9.53	1.19	1.30	1.50	0.68	0.25	0.24	0.74	0.96	0.00	0.00	0.00
Chy	6.59	9.60	7.47	5.99	14.10	5.21	5.19	7.41	4.41	3.59	7.24	2.41	9.60	8.67	2.77	19.66	0.00	2.04	0.00
DBahA	0.50	0.25	0.75	0.42	0.44	0.32	0.37	1.01	0.40	0.27	0.19	0.18	0.30	0.87	0.18	2.66	0.00	0.00	0.00
FlA	29.37	14.03	26.16	20.48	19.74	22.05	25.96	16.94	11.47	3.39	9.09	1.44	2.30	0.87	1.85	1.79	0.00	2.04	1.93
Fl	1.98	0.81	1.49	2.60	0.47	7.62	3.67	0.35	12.06	9.98	8.91	3.85	7.68	13.73	4.62	8.30	16.02	15.31	2.76
IP	4.32	3.62	6.35	1.34	4.70	1.10	1.19	6.88	0.40	0.77	0.83	0.19	0.10	0.58	0.46	2.88	0.00	0.00	0.00
Nap	1.08	0.74	0.75	1.81	1.03	1.30	2.47	0.58	22.06	17.96	18.18	60.16	25.45	38.53	59.10	2.05	40.73	35.71	68.91
PhA	5.81	8.12	5.61	3.39	9.40	22.05	12.83	0.53	19.12	31.94	17.81	20.86	43.70	26.49	18.47	29.70	27.15	20.41	4.13
Py	16.78	27.32	16.44	35.45	23.50	22.05	24.74	18.00	11.33	7.19	7.05	2.81	2.83	1.76	2.77	3.28	13.58	12.76	0.28
Total PAH	1668.3	1354.4	8508	1269.5	2127.3	997.7	327.4	1888.9	6799	10020	5390	12467	2082.6	4152.5	76258	2289.2	36.83	177	8258
Unit	ng/g	ng/g	µg/g	ng/g	ng/g	ng/g	ng/g	ng/g	ng/g	ng/g	ng/g	ng/g	ng/g	ng/g	µg/g	ng/g	ng/g	µg/g	µg/g
Reference	**1**	**1**	**2**	**1**	**1**	**1**	**1**	**1**	**1**	**1**	**1**	**1**	**1**	**1**	**2**	**1**	**1**	**2**	**2**

Table D-2. PAH profiles in coal soot. List of abbreviations: Comb – combustion, Ind – industrial, Res – residential, Bitu – bituminous, Briq – briquette.

	21	22	23	24	25	26	27	28	29	30	31	32	33
	COAL COMBUSTION												
	Industrial Coal Comb		Residential Coal Comb					coal briquette			charcoal		
PAH	Ind Brown	Ind Mixed	Res Anthracite	Res sub-bitu	Res Bitu	Res Coal Briq (Lab)	Res Coal Briq (field)	total	vapor	particle	total	vapor	particle
AcNe	0.00	0.00	0.04	0.13	0.05	0.00	0.00	30.07	30.07	0.00	37.78	39.19	1.06
AcNy	0.00	0.00	0.02	0.12	0.08	0.04	0.00	14.39	14.40	0.00	7.01	7.28	0.00
An	0.97	0.64	8.64	14.61	3.77	1.41	0.04	1.27	1.27	5.26	2.46	2.53	0.64
BaA	6.37	3.53	7.40	5.34	10.67	6.55	7.20	0.11	0.11	5.26	0.24	0.24	0.42
BaP	11.97	14.58	3.74	3.70	11.73	6.41	9.18	0.30	0.30	5.26	0.67	0.70	0.00
BbF	22.11	21.07	8.87	7.30	17.40	19.64	26.28	0.57	0.57	0.00	0.07	0.00	1.80
BghiP	15.03	15.35	1.67	1.83	6.58	9.99	13.61	0.00	0.00	0.00	0.01	0.00	0.30
BkF	3.46	4.24	1.89	1.80	4.03	2.31	3.25	1.66	1.66	0.00	3.38	0.04	90.49
Chy	5.96	3.02	4.98	4.14	11.46	15.47	22.75	0.59	0.59	0.00	0.41	0.42	0.11
DBahA	1.17	2.63	0.65	0.55	3.82	5.08	7.63	0.00	0.00	0.00	0.00	0.00	0.00
FlA	7.54	1.93	12.72	10.12	5.47	5.03	0.51	0.99	0.99	26.32	2.37	2.37	2.54
Fl	1.73	12.97	15.32	9.27	1.91	0.81	0.34	3.01	3.01	0.00	1.93	2.00	0.11
IP	13.14	10.60	1.77	2.44	10.36	5.20	7.86	0.00	0.00	0.00	0.00	0.00	0.00
Nap	1.83	4.17	0.07	0.03	0.06	0.08	0.00	43.87	43.88	0.00	29.31	30.44	0.00
PhA	2.90	3.53	22.39	28.50	6.90	18.24	0.47	1.03	1.03	5.26	9.44	9.78	0.42
Py	5.81	1.73	9.82	10.13	5.72	3.75	0.88	2.15	2.14	52.63	4.90	5.01	2.12
Total PAH	196.3	155.7	14948.9	26944.6	12506.8	5401	6210.5	101.436	101.417	0.019	25.5168	24.573	0.9438
Unit								mg/kg	mg/kg	mg/kg	mg/kg	mg/kg	mg/kg
Reference	**3**	**3**	**3**	**3**	**3**	**3**	**3**	**4**	**4**	**4**	**4**	**4**	**4**

Table D-3. PAH profiles in coal-tar products. List of abbreviations: SRM – standard reference material.

	35	36	37	38	39	40	41	42	43	44	45	46	47	48	49	50	51	52	53
	COAL TAR																		
PAH	Product 2	Product 3	Product 4	Product 5	Product 6	Product 7	Product 8	Product 9	Product 10	Product 11	Product 12	SRM 1597a	SRM 1597	CTp1	CTp2	CTp3	CTp4	CTp5	CTp6
AcNe	3.53	3.40	4.74	3.46	3.24	3.21	3.98	4.10	3.99	3.88	3.52	0.25	0.00	4.05	4.16	3.98	4.07	3.59	3.65
AcNy	0.27	0.40	0.11	0.65	0.03	0.56	0.98	0.75	0.54	1.11	1.44	8.59	7.91	0.00	0.00	0.00	0.00	0.00	0.00
An	8.52	6.54	6.19	5.07	4.94	5.13	5.10	5.16	5.06	4.95	5.23	3.50	3.20	5.22	5.24	5.09	5.17	5.34	5.43
BaA	5.80	5.30	6.33	5.89	6.02	6.10	4.17	4.02	4.26	4.28	4.99	3.21	3.12	4.21	4.08	4.29	4.37	5.13	5.14
BaP	4.66	4.91	4.69	6.04	6.38	6.00	4.58	4.56	4.76	4.82	5.16	3.05	3.03	4.66	4.63	4.78	4.71	5.39	5.26
BbF	3.96	4.73	4.44	6.26	6.32	6.09	4.06	3.83	3.97	4.22	4.40	2.16	2.09	4.11	3.89	3.99	4.22	4.90	4.23
BghiP	2.36	1.29	2.17	4.02	4.51	4.07	3.18	3.08	3.28	3.26	3.11	1.65	1.70	3.23	3.13	3.30	3.27	3.21	3.21
BkF	3.34	4.34	3.45	4.46	5.20	4.79	2.76	2.81	2.95	2.74	3.46	1.35	1.36	2.80	2.86	2.97	2.86	3.47	3.63
Chy	5.77	5.87	5.86	6.82	7.12	7.13	4.17	4.05	4.33	4.37	5.13	2.16	2.27	4.21	4.11	4.35	4.37	5.32	5.26
DBahA	0.27	0.81	1.03	1.65	1.93	1.81	0.98	0.75	0.29	1.11	1.44	0.23	0.00	0.00	0.00	0.29	0.00	0.00	0.00
FlA	18.23	17.51	16.95	16.80	16.33	16.76	17.30	17.46	17.70	17.38	14.47	10.68	10.19	17.72	17.72	17.80	17.47	14.84	14.96
Fl	3.48	4.39	5.17	2.89	3.25	2.92	3.31	3.41	3.37	3.27	3.45	5.03	4.43	3.35	3.46	3.39	3.43	3.52	3.58
IP	2.68	2.61	2.15	4.00	4.28	4.15	2.47	2.42	2.54	2.55	2.51	1.81	1.91	2.50	2.45	2.55	2.56	2.61	2.56
Nap	5.86	5.58	4.29	2.06	1.37	1.32	8.27	8.23	7.93	7.63	13.17	33.65	36.72	8.39	8.36	7.97	8.57	13.36	13.72
PhA	18.50	20.80	20.19	22.17	21.68	22.18	21.07	21.80	21.25	21.16	17.24	14.83	14.62	21.47	22.14	21.38	21.53	17.69	17.81
Py	12.76	11.50	12.23	7.75	7.38	7.77	13.61	13.57	13.80	13.25	11.25	7.84	7.44	14.08	13.78	13.88	13.40	11.61	11.57
Total PAH	9323	20959	22359.5	70823	58111.8	79364	70304	131181	233390	89781	65538	3060.66	3159	98740	129200	232030	39100	57090	70190
Unit	mg/kg	mg/kg	mg/kg	mg/kg	mg/kg	mg/kg	mg/kg	mg/kg	mg/kg	mg/kg	mg/kg	mg/kg	mg/kg	mg/kg	mg/kg	mg/kg	mg/kg	mg/kg	mg/kg
Reference	**5**	**5**	**5**	**5**	**5**	**5**	**5**	**5**	**5**	**5**	**5**	**6**	**6**	**7**	**7**	**7**	**7**	**7**	**7**

Table D-4. PAH profiles in other combustion soot and asphalts. List of abbreviations: SRM – standard reference material, Asp – asphalt product.

	54	55	56	57	58	59	60	61	62	63	64	65	66	67	68
PAH	**SOOT**									**ASPHALT**					
								VEHICLE SOOT							
	Traffic soot	Oil soot	Wood soot	Coal soot	coal	charcoal	Diesel soot SRM 1650	Gasoline eigine	Diesel engine	ASp1	ASp2	ASp3	Brazilian asphalt binder	Asphalt	road asphalt
AcNe	0.00	0.00	0.00	0.00	0.00	0.00	0.32	0.00	0.00	3.58	2.97	3.71	0.00	0.00	0.00
AcNy	0.00	0.00	0.00	0.00	0.00	0.00	0.32	0.00	0.00	0.07	0.00	0.00	0.00	0.00	0.00
An	5.59	1.97	1.22	0.64	0.55	4.23	1.60	1.36	3.92	5.03	4.86	4.40	4.46	3.64	0.00
BaA	4.05	3.22	6.78	9.48	3.10	6.62	3.84	5.46	4.51	6.30	5.64	4.69	6.93	3.47	10.34
BaP	5.10	0.21	14.48	1.60	1.24	7.14	0.32	10.78	4.51	4.80	4.64	4.85	7.21	8.32	0.00
BbF	5.43	18.07	13.34	14.33	3.69	5.95	3.20	12.69	6.83	10.42	4.20	4.97	8.70	12.48	10.34
BghiP	18.04	1.48	13.25	3.91	2.41	3.63	0.77	31.79	4.80	0.00	1.87	2.70	14.64	11.96	13.79
BkF	2.22	2.84	5.83	5.23	1.15	2.84	1.92	0.00	0.00	0.00	3.97	3.00	5.94	0.00	5.17
Chy	3.87	17.81	8.32	21.61	9.36	6.76	11.51	5.18	11.05	6.57	5.70	4.93	1.77	9.01	17.24
DBahA	0.62	0.74	1.29	2.08	0.83	1.03	0.32	0.00	0.00	0.00	0.00	0.00	11.24	0.00	0.00
FlA	13.26	31.18	8.45	21.17	5.64	12.15	23.02	5.46	11.77	14.92	20.17	17.78	5.02	10.23	3.45
Fl	0.00	0.00	0.00	0.00	0.00	0.00	1.28	0.00	0.00	3.85	3.55	3.40	7.07	0.00	3.45
IP	8.07	1.78	12.62	5.06	1.67	2.78	0.64	15.14	2.76	0.00	1.80	2.43	11.67	5.37	5.17
Nap	0.00	0.00	0.00	0.00	0.00	0.00	0.45	0.00	0.00	11.81	3.22	6.76	3.47	0.00	10.34
PhA	16.40	12.10	4.10	2.97	50.74	33.50	27.49	3.55	29.65	17.97	22.71	22.60	5.66	22.01	13.79
Py	17.36	8.60	10.32	11.93	19.61	13.36	23.02	8.59	20.20	14.68	14.70	13.78	6.22	13.52	6.90
Total PAH	128.26	58.01	118.62	785.63	71.23	44.68	882000	73.3	68.8	337.83	7485	1451.3	141.4	57.7	29
Unit	mg/kg	mg/kg	mg/kg	mg/kg	mg/kg	mg/kg	µg/g	µg/g	µg/g	mg/kg	mg/kg	mg/kg	mg/kg	µg/g	µg/g
Reference	**8**	**8**	**8**	**8**	**8**	**8**	**2**	**9**	**9**	**7**	**7**	**7**	**10**	**9**	**2**

Table D-5. PAH profiles in gasoline. Notes: A, B, C, D, E refer to gas stations where gasoline samples were taken. LFG – lead-free gasoline, PLG – premium leaded gasoline.

	69	70	71	72	73	74	75	76	77	78	79	80	81	82	83	84
	PETROLEUM (Products)															
	Gasoline															
PAH	Straight-run	light cracked distillate		A1	A2	B1	B2	C1	C2	D1	D2	E1	E2	95-LFG	92-LFG	PLG
AcNe	6.67	10.26	0.00	0.40	0.29	0.37	0.29	0.44	0.51	0.38	0.23	0.21	0.27	1.19	1.79	1.62
AcNy	0.00	0.00	0.00	0.03	0.01	0.01	0.01	0.03	0.02	0.01	0.01	0.10	0.14	4.12	5.62	4.79
An	0.00	3.42	0.41	1.56	0.93	1.24	1.01	1.70	2.01	0.51	0.68	0.19	0.66	1.26	1.91	1.42
BaA	0.00	0.85	0.00	0.05	0.06	0.09	0.08	0.05	0.04	0.06	0.08	0.00	0.04	0.28	0.12	0.34
BaP	0.00	0.00	0.00	0.02	0.02	0.05	0.03	0.04	0.05	0.02	0.03	0.00	0.04	0.07	0.06	0.05
BbF	0.00	0.00	0.00	0.01	0.01	0.02	0.01	0.01	0.02	0.01	0.02	0.00	0.01	0.03	0.01	0.01
BghiP	0.00	0.00	0.00	0.02	0.03	0.04	0.03	0.02	0.04	0.04	0.03	0.00	0.03	1.05	0.84	0.94
BkF	0.00	0.00	0.03	0.00	0.01	0.01	0.01	0.01	0.01	0.01	0.01	0.00	0.01	0.21	0.06	0.02
Chy	0.00	1.71	0.00	0.02	0.04	0.04	0.05	0.02	0.03	0.05	0.06	0.00	0.02	0.07	0.12	0.20
DBahA	0.00	0.00	0.00	0.00	0.00	0.00	0.00	0.00	0.00	0.00	0.00	0.00	0.00	0.14	0.24	0.27
FlA	0.00	1.71	0.11	0.11	0.12	0.13	0.13	0.12	0.18	0.13	0.13	0.02	0.09	0.42	0.72	0.54
Fl	20.00	13.68	0.00	0.61	0.36	0.39	0.32	0.53	0.78	0.40	0.23	0.62	0.87	6.15	7.42	5.73
IP	0.00	0.00	0.00	0.00	0.00	0.01	0.01	0.01	0.01	0.00	0.01	0.00	0.01	2.59	1.85	1.69
Nap	26.67	29.06	98.26	96.17	97.32	96.68	97.20	95.90	95.05	97.40	97.78	98.42	96.98	79.70	76.73	77.59
PhA	40.00	32.48	0.87	0.87	0.65	0.75	0.65	0.97	1.03	0.72	0.56	0.42	0.73	2.66	2.15	4.52
Py	6.67	6.84	0.32	0.13	0.14	0.18	0.16	0.15	0.20	0.25	0.15	0.02	0.10	0.07	0.36	0.27
Total PAH	24100	75700	1058.4	831.878	2157.874	1861.81	2469.16	823.801	946.88	1950.696	2659.06	121.922	71.1473	14.304	16.722	14.822
Unit	µg/g	µg/g	µg/g	mg/L	mg/L	mg/L	mg/L	mg/L	mg/L	mg/L	mg/L	mg/L	mg/L	mg/l	mg/l	mg/l
Reference	**2**	**2**	**11**	**12**	**12**	**12**	**12**	**12**	**12**	**12**	**12**	**12**	**12**	**13**	**13**	**13**

Table D-6. PAH profiles in diesel and motor/lubricant oil. Note: number of kilometers refers to the distance of the vehicle has been driven.

	85	86	87	88	89	90	91	92	93	94	95	96	97	98	99	100	101	102
	PETROLEUM (Products)																	
	Diesel fuel										Motor Oil/Lubracant Oil							
PAH		Diesel 1	Diesel 2	Diesel 3	Diesel 4	Diesel 5	min	max	mean	Oil Shale	0 km	473 km	2130 km	3144 km	3635 km	Used crankcase oil	used motor oil	used hydraulic oil
AcNe	0.00	2.82	14.58	6.16	0.85	17.37	18.99	18.88	18.81	5.38	0.00	1.58	0.97	1.03	0.96	0.00	0.71	0.00
AcNy	0.00	0.07	0.29	0.32	0.09	2.29	26.38	27.64	28.53	1.77	0.00	0.45	0.35	0.27	0.36	0.00	0.71	0.00
An	0.64	0.00	0.00	0.00	0.00	0.00	3.32	3.26	3.61	15.29	0.00	12.09	14.26	14.36	14.05	9.65	3.55	13.51
BaA	0.00	0.00	0.00	0.00	0.00	0.00	0.10	0.22	0.22	2.48	0.00	4.55	5.27	5.74	5.71	5.95	7.80	0.00
BaP	0.00	0.00	0.00	0.00	0.00	0.00	0.66	0.61	0.62	3.66	0.00	6.00	6.18	6.48	6.66	5.13	2.13	0.00
BbF	0.00	0.00	0.00	0.00	0.00	0.00	0.40	0.30	0.34	10.90	0.00	3.06	2.99	3.20	3.18	4.11	0.35	0.00
BghiP	0.00	0.12	0.00	0.00	0.00	0.58	0.13	0.17	0.14	0.23	0.00	4.38	4.46	4.57	4.64	3.90	4.26	0.00
BkF	0.00	0.00	0.00	0.00	0.00	0.00	0.06	0.05	0.06	3.91	0.00	0.68	0.33	0.55	0.66	0.00	3.55	0.00
Chy	0.00	0.00	0.00	0.47	0.00	0.00	0.16	0.22	0.15	3.58	0.00	2.35	2.58	2.81	2.74	5.13	5.32	0.00
DBahA	0.00	0.00	0.00	0.00	0.00	0.00	0.35	0.42	0.34	0.39	0.00	0.02	0.19	0.23	0.23	0.00	0.00	0.00
FlA	0.00	0.17	0.07	0.17	0.01	0.00	1.54	1.86	1.92	13.52	0.00	5.99	6.73	7.05	6.91	13.14	6.03	0.00
Fl	6.68	7.16	31.23	20.52	1.83	0.00	11.55	13.82	12.39	0.96	0.00	9.25	7.01	5.90	5.37	0.00	2.48	13.51
IP	0.00	0.00	0.00	0.00	0.00	0.00	0.29	0.23	0.24	0.39	0.00	4.09	3.98	4.09	4.09	2.67	0.71	0.00
Nap	77.12	76.36	31.23	52.23	94.97	4.09	33.30	27.45	28.46	4.20	12.00	14.02	9.08	8.71	10.30	0.00	40.43	5.41
PhA	7.33	11.45	15.62	17.35	1.43	22.33	2.63	4.53	3.86	20.30	52.00	22.53	25.93	24.72	24.16	29.16	11.35	43.24
Py	8.23	1.86	6.98	2.80	0.82	53.34	0.15	0.35	0.29	13.04	36.00	8.98	9.69	10.28	9.98	21.15	10.64	24.32
Total PAH	778	2095.4	96.051	536.1	600.219	161.23	209.6	361.78	284.93	355.1	2.5	621.4	910	1027.4	1050.6	48.7	81570	630000
Unit	µg/km	mg/L	mg/L	mg/L	mg/L	mg/L	µg/m^3	µg/m^3	µg/m^3		µg/g	µg/g	µg/g	µg/g	µg/g	µg/g	µg/g	µg/g
Reference	**14**	**12**	**12**	**12**	**12**	**12**	**15**	**15**	**15**	**16**	**17**	**17**	**17**	**17**	**17**	**9**	**2**	**2**

Table D-7. PAH profiles in oil spill and industrial boiler/stack emissions. List of abbreviations: HO – heavy oil, NG – natural gas, COG – coke oven gas, BFG – blast furnace gas, BOF – biomass oil fuel, EAF – electric arc furnace.

	103	104	105	106	107	108	109	110	111	112	113	114	115	116	117	118	119	120	121
	Oil Spill						Industrial boiler/stack												
PAH	Sample 1460	Sample 1461	Sample 1462	Sample 1463	Sea water	sediment	Heavy oil	Diesel	HO+NG	COG+BFG	cooking oil	Blast furnace	BOF	Coke Oven	EAF	Heavy oil plant	Power plant	Cement 1	Cement 2
AcNe	11.36	12.34	10.05	8.07	0.72	1.08	0.51	1.65	0.81	0.05	0.87	0.90	1.40	1.31	1.50	1.72	1.80	16.74	21.43
AcNy	4.08	3.90	3.90	3.48	0.00	0.70	0.50	0.75	0.36	0.02	1.16	0.88	0.82	1.76	5.89	2.32	2.55	9.05	1.44
An	2.03	2.63	2.10	2.09	12.85	3.08	0.80	1.08	0.34	1.01	3.35	0.06	0.07	0.34	0.26	0.41	0.20	0.15	0.54
BaA	0.11	0.15	0.11	0.32	0.47	8.79	0.24	0.28	0.13	0.00	0.73	0.33	0.13	0.47	0.05	0.13	0.15	0.14	0.16
BaP	0.04	0.05	0.03	0.16	0.31	7.03	0.82	0.91	0.59	0.74	1.15	2.98	0.60	6.66	2.52	8.13	1.54	1.50	1.79
BbF	0.00	0.06	0.00	0.00	0.29	20.22	0.48	0.66	0.09	0.07	3.05	0.44	0.19	0.74	0.74	1.09	1.08	0.84	0.54
BghiP	0.00	0.00	0.00	0.00	0.56	4.83	0.95	0.26	0.00	0.00	3.00	0.06	0.03	0.06	0.16	0.16	0.26	0.18	0.11
BkF	0.04	0.00	0.00	0.22	0.17	1.98	0.27	1.69	0.18	0.29	5.73	0.19	0.10	0.21	0.39	0.30	0.36	0.25	0.29
Chy	0.20	0.26	0.17	0.38	1.03	5.05	0.21	0.18	0.42	0.02	1.50	0.04	0.05	0.24	0.16	0.25	0.28	0.13	0.11
DBahA	0.00	0.00	0.00	0.00	0.00	2.42	2.84	0.39	0.03	0.26	0.06	0.22	0.14	0.27	1.69	1.12	2.20	0.45	0.29
FlA	1.11	1.10	0.93	1.53	2.41	11.43	2.79	38.97	4.54	76.28	6.61	0.26	0.27	0.55	0.52	0.70	0.69	0.56	0.44
Fl	27.80	27.17	23.84	19.10	11.60	2.20	2.49	2.39	2.57	0.75	2.08	0.58	0.52	1.44	2.31	1.56	0.79	2.04	4.05
IP	0.00	0.00	0.00	0.00	0.60	6.37	2.18	0.10	0.00	0.12	1.59	0.07	0.02	0.01	0.28	0.09	0.12	0.06	0.20
Nap	1.37	2.74	15.97	24.82	59.57	4.61	79.92	44.15	65.06	18.01	50.54	91.37	93.59	81.65	79.90	77.19	83.90	64.81	62.63
PhA	42.21	40.22	34.73	31.79	4.70	10.99	2.36	2.75	21.80	0.11	12.45	0.77	1.04	2.52	2.10	2.56	1.46	1.10	4.61
Py	9.64	9.39	8.18	8.04	4.70	9.23	2.62	3.78	3.08	2.26	6.13	0.85	1.02	1.76	1.54	2.27	2.61	1.99	1.37
Total PAH	492.76	474.83	486.62	298.5	31.897	455.1	13638.6	2860.84	2820.66	207.12	45465	75.629	512.88	232.709	160.2	3506.98	560.168	124.82	174.025
Unit	mg/g	mg/g	mg/g	mg/g	ng/L	ng/g dw	µg/kg	µg/kg	µg/kg	µg/kg		µg/N m^3	µg/N m^3	µg/N m^3	µg/N m^3	µg/N m^3	µg/N m^3	µg/N m^3	µg/N m^3
Reference	**18**	**18**	**18**	**18**	**19**	**19**	**20**	**20**	**20**	**20**	**16**	**21**	**21**	**21**	**21**	**21**	**21**	**21**	**21**

Table D-8. PAH profiles in diesel engine emissions. Note: creep, transient, and cruise refer to the operation mode. Mazda, King Long, and MAN are the manufacturers' names, but here they refer to specific engine models from corresponding manufacturers. D – diesel engine.

	122	123	124	125	126	127	128	129	130	131	132	133	134	135	136	137	138	139	140
	Engine Emissions																		
	Diesel Engine																		
PAH	Creep	Transient	Cruise	Diesel Engines	Mean (mg/k	gas	particle	Mazda min	King Long (c	MAN (non-c	model 1	model 2	model 3	model 4	model 5	Light-duty D	Heavy-duty	ave D	ave D
AcNe	3.15	2.37	2.28	12.93	2.48	1.97	0.00	9.83	13.28	4.47	2.91	4.13	4.08	2.82	2.51	0.00	0.00	0.00	0.00
AcNy	1.45	1.61	1.15	10.60	4.44	7.17	0.00	0.00	0.00	0.00	3.19	6.54	6.54	2.27	4.30	5.88	2.30	0.00	0.00
An	1.19	0.89	0.54	5.74	1.02	1.28	1.30	5.55	12.19	4.93	1.96	1.79	2.37	3.80	5.79	0.00	0.00	18.57	30.53
BaA	1.57	1.06	1.16	5.69	0.47	0.30	0.93	1.17	0.64	0.41	0.11	0.11	0.09	0.04	0.16	0.30	2.49	2.54	2.24
BaP	1.66	0.90	1.08	6.90	0.23	0.00	0.00	2.51	2.12	1.24	0.20	0.12	0.13	0.13	0.43	0.00	0.00	1.30	1.47
BbF	1.72	1.31	0.94	3.13	0.26	0.00	0.00	4.49	2.34	0.86	0.29	0.11	0.14	0.48	0.14	0.84	0.19	3.80	6.28
BghiP	6.54	3.51	3.71	2.47	0.35	0.00	0.00	1.84	1.02	0.40	0.32	0.19	0.17	0.14	0.75	0.30	0.56	2.74	2.05
BkF	1.42	1.27	1.14	2.23	0.26	0.00	0.00	0.10	0.50	0.22	0.13	0.14	0.15	0.12	0.24	0.00	0.00	0.00	0.00
Chy	1.41	1.05	1.13	3.27	0.38	0.34	1.87	0.65	0.30	1.30	0.17	0.22	0.24	0.13	0.31	0.42	0.44	5.06	3.23
DBahA	5.06	3.53	3.30	3.88	0.00	0.00	0.00	0.79	0.41	0.15	0.22	0.20	0.15	0.12	0.93	0.00	0.00	0.13	0.20
FlA	6.57	5.77	8.68	1.84	0.79	5.42	6.77	0.76	0.91	1.24	0.25	0.36	0.82	0.44	1.33	3.30	1.37	29.60	24.56
Fl	6.65	8.28	6.16	14.88	5.26	3.54	1.14	2.13	1.40	24.87	2.37	3.01	3.01	7.19	8.16	6.06	3.05	0.00	0.00
IP	4.09	3.45	2.67	5.71	0.35	0.00	0.00	2.27	0.95	0.33	0.62	0.80	0.40	0.44	0.33	0.12	0.06	1.57	1.08
Nap	24.54	29.63	25.22	8.82	76.15	63.10	71.78	58.94	60.32	51.00	86.81	81.65	80.51	79.83	72.76	79.08	87.12	0.00	0.00
PhA	16.13	18.92	16.31	10.79	6.28	9.52	5.62	6.14	2.43	7.09	0.21	0.21	0.29	1.71	0.66	0.00	0.00	0.00	0.00
Py	16.83	16.42	24.52	1.12	1.26	7.35	10.59	2.84	1.19	1.49	0.24	0.42	0.92	0.35	1.21	3.72	2.43	34.70	28.36
Total PAH	99.82	99.882	99.918	4.3762	3421	977.83	235.86	671.36	508.58	2169.41	1497.47	505.81	561.39	1119.83	316.09	0.01668	0.001607	3.0266	0.73692
Unit	µg/mi	µg/mi	µg/mi		mg/kg	µg/km	µg/km	µg/m^3	µg/m^3	µg/m^3	µg/m^3	µg/m^3	µg/m^3	µg/m^3	µg/m^3	mg/kg	mg/kg.		
Reference	**22**	**22**	**22**	**23**	**24**	**14**	**14**	**13**	**13**	**13**	**15**	**15**	**15**	**15**	**15**	**25**	**25**	**26**	**26**

Table D-9. PAH profiles in gasoline engine emissions. Note: L, ML, M, H, and S are measurements of engine emission rates. L –low emitter, ML – medium low emitter, M – medium emitter, H – high emitter, and S – gasoline engine.

	141	142	143	144	145	146	147	148	149	150	151	152	153	154	155	156	157	158	159
	Gasoline Engine																		
	summer				winter														
PAH	ave L	ave M	ave H	ave S	ave L	ave ML	ave m	ave H	ave S	Phase 1	Phase 2	Smoker	catalyst-equipped, gas	catalyst-equipped, particle	noncatalyst-equipped, gas	noncatalyst-equipped, particle	Hyundai Avanta (catalytic) (ug/m3)	Hyundai Elantra (non-catalytic)	DACIA Super Nova (catalytic)
AcNe	0.00	0.00	0.00	0.00	0.00	0.00	0.00	0.00	0.00	0.00	0.00	0.00	0.60	0.00	0.33	0.00	2.80	1.92	2.69
AcNy	0.00	0.00	0.00	0.00	0.00	0.00	0.00	0.00	0.00	5.91	5.05	7.81	3.40	0.00	4.05	0.00	0.00	0.00	0.00
An	16.83	28.51	20.52	16.77	20.56	16.45	21.39	15.54	26.27	0.00	0.00	0.00	0.34	0.00	0.27	8.69	2.57	1.18	18.48
BaA	1.22	2.25	2.95	3.27	0.25	0.56	0.39	0.98	1.53	0.05	0.11	0.08	0.02	14.56	0.01	4.26	0.71	0.26	0.24
BaP	0.40	1.46	3.84	4.76	0.12	0.40	0.27	1.86	1.96	0.00	0.00	0.00	0.00	3.15	0.00	3.36	1.59	0.84	1.22
BbF	0.05	1.74	4.49	4.03	0.00	0.94	0.73	3.06	3.84	0.14	0.10	0.17	0.00	0.00	0.00	3.06	2.57	0.91	0.87
BghiP	0.68	3.43	6.57	10.48	0.03	0.70	0.64	5.10	5.39	0.17	0.07	0.20	0.02	9.46	0.02	3.84	1.14	0.43	0.37
BkF	0.00	0.00	0.00	0.00	0.00	0.00	0.00	0.00	0.00	0.00	0.00	0.00	0.00	12.46	0.00	2.68	0.81	0.20	0.20
Chy	0.96	2.22	3.05	3.74	0.25	0.62	0.43	1.08	1.38	0.05	0.11	0.06	0.04	30.93	0.01	4.27	0.46	0.41	0.12
DBahA	0.05	0.20	0.31	0.18	0.00	0.01	0.01	0.08	0.15	0.00	0.00	0.00	0.00	0.00	0.00	0.00	0.46	0.17	0.15
FlA	37.02	28.10	25.30	20.07	36.15	34.32	33.24	29.14	25.32	1.77	10.74	1.80	0.39	10.36	0.30	12.47	0.91	0.67	0.19
Fl	0.00	0.00	0.00	0.00	0.00	0.00	0.00	0.00	0.00	1.88	2.50	2.39	0.89	0.00	0.67	1.65	5.18	2.63	0.82
IP	0.25	1.21	2.84	2.37	0.00	0.24	0.20	1.26	1.67	0.05	0.02	0.06	0.00	7.51	0.00	2.34	1.07	1.10	1.07
Nap	0.00	0.00	0.00	0.00	0.00	0.00	0.00	0.00	0.00	87.75	67.28	85.27	91.90	0.00	92.89	0.00	77.08	81.06	72.92
PhA	0.00	0.00	0.00	0.00	0.00	0.00	0.00	0.00	0.00	0.00	0.00	0.00	1.99	0.00	1.16	35.59	0.92	7.48	0.13
Py	42.53	30.88	30.14	34.33	42.62	45.76	42.71	41.91	32.48	2.25	14.02	2.16	0.39	11.56	0.30	17.80	1.73	0.73	0.53
Total PAH	0.13073	0.1687	0.27869	0.87678	0.602992	0.77802	1.30874	3.49361	2.31823	0.19032	0.19694	0.06516	1088.089	0.666	53825.57	1219.4	69.28	361.06	133.12
Unit	mg/mi	mg/mi	mg/mi	mg/mi	mg/mi	mg/mi	mg/mi	mg/mi	mg/mi				µg/km	µg/km	µg/km	µg/km	$\mu g/m^3$	$\mu g/m^3$	$\mu g/m^3$
Reference	**26**	**26**	**26**	**26**	**26**	**26**	**26**	**26**	**26**	**25**	**25**	**25**	**11**	**11**	**11**	**11**	**13**	**13**	**13**

Table D-10. PAH profiles in wood combustion emissions.

	160	161	162	163	164	165	166	167	168	169	170	171	172	173	174	175	176	177	178
	Wood Combustion																		
PAH	Oak gas+particle	Beech gas+particle	Pine, gas	Pine, particle	Pine, gas+particle	Oak, gas	Oak, particle	Oak, gas+particle	Eucalyptus gas	Eucalyptus particle	Eucalyptus gas+particle	Wood combustion	wood, gas+particle	wood, gas	wood, particle	softwood	hardwood	woodstove	synthetic log
AcNe	5.04	7.08	0.73	0.00	0.70	3.47	0.00	3.03	2.99	0.00	2.67	1.47	32.35	33.95	0.00	0.59	7.41	0.81	0.41
AcNy	2.42	3.49	6.74	0.00	6.41	32.62	0.00	28.45	33.42	0.00	29.87	52.30	10.05	10.55	0.00	10.05	7.08	8.24	13.49
An	20.86	13.22	1.25	1.61	1.26	6.43	0.47	5.67	5.89	0.17	5.28	10.00	1.67	1.73	0.39	0.00	0.00	0.00	0.00
BaA	1.49	2.03	0.00	8.64	0.42	0.00	12.97	1.66	0.08	15.02	1.66	0.53	0.74	0.39	7.92	0.07	0.04	0.04	0.00
BaP	2.85	5.52	0.00	5.04	0.25	0.00	5.05	0.65	0.00	8.48	0.90	5.80	0.63	0.15	10.34	0.51	0.25	0.27	0.62
BbF	1.70	3.88	0.00	5.60	0.27	0.00	8.24	1.05	0.00	9.21	0.98	0.67	0.49	0.19	6.65	0.00	0.00	0.00	0.00
BghiP	0.64	0.65	0.00	3.10	0.15	0.00	0.00	0.00	0.00	4.87	0.52	0.00	0.46	0.00	9.65	0.29	0.16	0.15	0.41
BkF	2.70	4.64	0.00	4.75	0.23	0.00	6.24	0.80	0.00	8.06	0.86	1.27	0.41	0.29	2.70	0.00	0.00	0.00	0.00
Chy	2.88	3.39	0.00	8.07	0.39	0.00	15.55	1.99	0.09	16.71	1.85	0.94	0.80	0.33	10.31	0.00	0.00	0.00	0.00
DBahA	0.23	0.56	0.00	0.00	0.00	0.00	0.00	0.00	0.00	0.00	0.00	0.00	0.55	0.00	11.60	0.00	0.00	0.00	0.00
FlA	7.60	9.90	1.10	27.98	2.41	10.90	24.71	12.67	12.54	14.34	12.74	2.74	4.50	3.83	18.11	11.37	11.89	15.05	6.64
Fl	9.42	11.00	1.61	0.00	1.53	11.57	0.00	10.09	8.73	0.00	7.80	3.66	4.40	4.62	0.00	0.00	0.00	0.00	0.00
IP	0.51	0.60	0.00	3.67	0.18	0.00	0.00	0.00	0.00	4.73	0.50	0.00	1.03	0.49	11.94	0.29	0.12	0.15	0.41
Nap	21.12	3.32	82.21	0.00	78.21	0.00	0.00	0.00	0.00	0.00	0.00	11.49	35.63	37.40	0.00	43.21	53.54	59.77	50.21
PhA	11.64	14.78	5.69	4.77	5.64	27.76	1.43	24.39	27.23	1.92	24.54	6.26	4.06	4.24	0.58	28.61	15.68	12.15	19.50
Py	8.89	15.94	0.68	26.77	1.95	7.25	25.33	9.56	9.03	16.48	9.82	2.86	2.22	1.85	9.82	4.99	3.83	3.37	8.30
Total PAH	610.7	463.6	276.12	14.119	290.239	33.11	4.8555	37.9655	29.893	3.5494	33.4424	3.4989	109.743	104.552	5.191	0.01363	0.0243	0.02585	0.00482
Unit			mg/kg	mg/kg	mg/kg	mg/kg	mg/kg	mg/kg	mg/kg	mg/kg	mg/kg		mg/kg	mg/kg	mg/kg				
Reference	**16**	**16**	**27**	**27**	**27**	**27**	**27**	**27**	**27**	**27**	**27**	**23**	**4**	**4**	**4**	**25**	**25**	**25**	**25**

Table D-11. PAH profiles wood/biomass combustion emissions.

	179	180	181	182	183	184	185	186	187	188	189	190	191	192	193	194	195	196	197	198
	Wood/Biomass Combustion																			
PAH	almond, flaming	almond, stoked/flaming	almond, average	walnut, flaming	walnut, stoked/flaming	walnut, average	fir, flaming	fir, stoked/flaming	fir, average	pine, flaming	pine, stoked/flaming	pine, average	barley straw 1	barley straw 2	corn straw 1	corn straw 2	rice straw 1	rice straw 2	wheat straw 1	wheat straw 2
AcNe	1.23	1.31	1.27	6.90	8.18	7.47	8.24	11.94	9.01	7.96	6.24	7.00	0.32	29.15	2.21	8.97	3.75	0.76	0.45	0.02
AcNy	19.19	18.64	18.96	4.59	4.62	4.60	8.14	10.58	8.65	5.04	5.48	5.29	10.37	2.30	0.98	7.08	4.38	10.84	1.26	3.61
An	2.80	1.58	2.27	1.92	1.24	1.62	2.87	1.51	2.59	2.11	1.20	1.61	1.87	3.29	0.19	4.50	2.10	1.97	1.76	1.50
BaA	1.52	1.52	1.52	0.21	0.32	0.26	0.89	0.90	0.89	0.61	0.29	0.43	0.52	1.86	0.67	2.48	0.79	1.22	3.14	0.56
BaP	0.24	0.15	0.20	0.05	0.00	0.03	0.14	0.07	0.13	0.16	0.00	0.07	0.35	1.33	13.84	0.09	0.28	0.74	0.91	0.27
BbF	0.37	0.22	0.31	0.00	0.00	0.00	0.23	0.08	0.20	0.31	0.00	0.14	1.09	4.04	29.73	0.26	0.78	1.21	2.69	0.55
BghiP	0.02	0.00	0.01	0.00	0.00	0.00	0.00	0.04	0.01	0.00	0.00	0.00	0.25	0.00	0.90	0.00	0.13	0.26	1.44	0.00
BkF	0.35	0.37	0.36	0.00	0.00	0.00	0.56	0.22	0.49	0.33	0.00	0.15	0.32	0.84	13.57	0.43	0.50	0.78	0.91	0.52
Chy	1.03	2.04	1.46	0.31	0.38	0.34	0.76	0.85	0.78	0.52	0.26	0.37	0.65	2.37	1.00	3.32	0.90	1.47	3.21	0.71
DBahA	0.00	0.00	0.00	0.00	0.00	0.00	0.00	0.00	0.00	0.00	0.00	0.00	0.00	0.00	0.90	0.00	0.00	0.00	0.00	0.00
FlA	3.97	3.41	3.72	5.17	6.18	5.62	6.46	5.79	6.32	5.49	4.73	5.07	1.34	2.85	2.03	13.77	3.23	3.56	9.17	2.08
Fl	0.46	0.15	0.33	4.78	3.09	4.03	3.22	2.48	3.07	2.79	2.37	2.55	1.54	3.46	0.50	1.21	4.66	1.20	0.42	0.57
IP	0.00	0.00	0.00	0.00	0.00	0.00	0.00	0.00	0.00	0.00	0.00	0.00	0.28	0.00	2.67	0.00	0.13	0.59	0.93	0.00
Nap	50.23	54.16	51.94	61.66	65.07	63.17	47.31	53.22	48.54	58.11	67.97	63.60	70.26	17.96	24.37	18.96	63.96	61.44	61.20	82.64
PhA	15.34	13.37	14.49	10.81	5.91	8.65	15.73	7.81	14.09	12.58	7.46	9.73	9.83	22.38	4.43	25.99	12.16	11.07	7.18	5.13
Py	3.24	3.09	3.18	3.60	5.00	4.22	5.45	4.52	5.26	3.99	4.01	4.00	1.00	8.18	2.00	12.94	2.24	2.91	5.34	1.84
Total PAH	15976	12168	14069	25698	20406	23053	44288	11619	27952	15368	64231	26667	212840	61531	31322	7015	15077	11928	72537	58070
Unit	µg/kg	µg/kg	µg/kg	µg/kg	µg/kg	µg/kg	µg/kg	µg/kg	µg/kg	µg/kg	µg/kg	µg/kg	µg/kg	µg/kg	µg/kg	µg/kg	µg/kg	µg/kg	µg/kg	µg/kg
Reference	**28**	**28**	**28**	**28**	**28**	**28**	**28**	**28**	**28**	**28**	**28**	**28**	**28**	**28**	**28**	**28**	**28**	**28**	**28**	**28**

Table D-12. PAH profiles in tunnel air (gas phase).

	199	200	201	202	203	204
	Tunnel air, gas					
PAH	winter	summer	Roadside air	Lundby Tunnel	gasoline exhaust	diesel exhaust
AcNe	8.79	16.19	0.00	2.03	0.00	0.00
AcNy	10.96	10.69	0.00	2.17	9.97	0.00
An	3.04	1.85	5.06	1.88	9.97	3.83
BaA	3.05	0.86	1.38	0.00	1.53	0.14
BaP	0.06	0.08	0.00	0.00	2.35	0.00
BbF	0.21	0.16	0.00	0.00	1.71	0.08
BghiP	0.04	0.00	0.00	0.00	1.96	0.00
BkF	0.07	0.08	0.00	0.00	0.00	0.00
Chy	3.32	1.64	3.07	0.00	1.43	0.81
DBahA	0.04	0.00	0.00	0.00	0.00	0.00
FlA	8.29	7.23	26.84	3.82	7.30	6.50
Fl	9.33	27.91	0.00	12.62	14.95	0.00
IP	0.01	0.00	0.00	0.00	0.57	0.00
Nap	9.30	7.11	0.00	32.87	8.19	0.00
PhA	17.07	14.76	32.98	41.09	32.39	84.88
Py	26.44	11.43	30.67	3.52	7.69	3.77
Total PAH						
Unit						
Reference	**29**	**29**	**9**	**30**	**30**	**30**

Table D-13. PAH profiles in tunnel air (particle phase) continued. Note: 41506 – 41509 are sample numbers marked by the researchers.

	208	209	210	211	212	213	214	215	216	217	218	219	220	221	222	223	224	225
	Tunnel air, particle																	
PAH	truck-influenced bore	truck-influenced bore	light-duty bore	light-duty bore	light duty	light duty	heavy duty	heavy duty	41506	41507	41508	41509	41514	Traffic site day		suburban site	suburban site	Lundby Tunnel
AcNe	0.00	0.00	0.00	0.00	0.00	0.00	0.00	0.00	0.00	0.00	0.00	0.00	0.00	0.00	0.00	0.00	0.00	0.00
AcNy	0.00	0.00	0.00	0.00	0.00	0.00	0.00	0.00	0.00	0.00	0.00	0.00	0.00	0.00	0.00	0.00	0.00	0.00
An	0.00	0.00	0.00	0.00	0.00	0.00	0.00	0.00	0.00	0.00	0.00	0.00	0.00	1.63	1.59	0.00	0.00	4.13
BaA	8.25	8.83	8.80	10.24	5.42	9.73	9.97	7.58	5.16	5.61	10.03	9.34	8.99	8.99	7.80	3.92	3.64	1.59
BaP	7.04	7.42	8.80	8.40	7.23	9.18	0.00	5.31	8.23	6.31	1.73	0.00	1.86	2.29	3.03	3.92	5.45	0.45
BbF	5.28	6.00	9.34	8.14	8.59	8.96	1.78	3.79	8.95	8.30	4.70	4.34	3.94	3.43	4.62	9.80	9.09	0.53
BghiP	0.93	2.03	22.67	21.00	20.34	22.90	0.00	0.00	20.40	20.36	2.93	3.01	2.06	3.43	4.78	7.84	7.27	0.71
BkF	2.78	3.18	3.20	2.89	2.82	3.32	0.20	2.48	3.16	2.40	1.29	0.98	0.81	1.31	1.75	3.92	3.64	0.04
Chy	7.23	7.95	8.54	9.98	7.91	9.51	4.70	5.89	8.12	7.68	6.82	6.14	6.00	4.90	5.89	5.88	5.45	1.67
DBahA	0.53	0.36	1.57	1.29	18.31	1.44	0.00	0.00	16.81	19.72	3.80	2.89	2.75	0.16	0.16	1.96	0.00	0.08
FlA	29.66	27.38	12.54	12.86	9.04	11.39	34.19	33.43	8.86	9.13	29.00	29.37	29.92	22.22	20.54	25.49	30.91	30.97
Fl	0.00	0.00	0.00	0.00	0.00	0.00	0.00	0.00	0.00	0.00	0.00	0.00	0.00	0.65	0.64	0.00	0.00	0.87
IP	0.30	0.64	8.27	7.35	10.17	8.30	0.00	0.00	11.20	9.19	1.04	1.50	1.38	1.63	2.55	7.84	7.27	0.21
Nap	0.00	0.00	0.00	0.00	0.00	0.00	0.00	0.00	0.00	0.00	0.00	0.00	0.00	2.12	2.71	3.92	1.82	0.00
PhA	0.00	0.00	0.00	0.00	0.00	0.00	0.00	0.00	0.00	0.00	0.00	0.00	0.00	10.62	11.46	11.76	12.73	20.64
Py	38.00	36.21	16.27	17.85	10.17	15.27	49.15	41.52	9.12	11.28	38.67	42.43	42.30	36.60	32.48	13.73	12.73	38.11
Total PAH																		
Unit																		
Reference	**12**	**12**	**12**	**12**	**12**	**12**	**12**	**12**	**31**	**31**	**31**	**31**	**31**	**32**	**32**	**32**	**32**	**30**

Appendix D References (see tables)

1 Stout, S.A., Emsbo-Mattingly, S.D. 2008. Concentration and character of PAHs and other hydrocarbons in coals of varying rank - Implications for environmental studies of soils and sediments containing particulate coal. Org Geochem 39, 801-819.

2 Wang, Z-D., and Stout, S.A. 2008. Chemical fingerprinting of spilled or discharged petroleum. Oil Spill Environmental Forensics Fingerprinting and Source Identification. Science Direct. ISBN: 978-0-12-369523-9

3 Zhang, Y.X., Schauer, J.J., Zhang, Y.H., Zeng, L.M., Wei, Y.J., Liu, Y., Shao, M. 2008. Characteristics of particulate carbon emissions from real-world Chinese coal combustion. Environ Sci Technol 42, 5068-5073.

4 Oanh, N.T.K., Reutergardh, L.B., Dung, N.T. 1999. Emission of polycyclic aromatic hydrocarbons and particulate matter from domestic combustion of selected fuels. Environ Sci Technol 33, 2703-2709.

5 Scoggins, M., Ennis, T., Parker, N., Herrington, C. 2009. A photographic method for estimating wear of coal-tar sealcoat from parking lots. Environ Sci Technol 43 4909-4914.

6 Wise, S. A., Poster, D. L., Leigh, S. D., Rimmer, C. A., Mössner, S., Schubert, P., Sander, L. C., Schantz, M. M. 2010. Polycyclic aromatic hydrocarbons (PAHs) in a coal-tar standard reference material - SRM 1597a updated. Anal Bioanal Chem 398, 717-728.

7 Mahler, B.J., Van Metre, P.C., Bashara, T.J., Wilson, J.T., Johns, D.A. 2005. Parking lot sealcoat: an unrecognized source of urban polycyclic aromatic hydrocarbons. Environ Sci Technol 39, 5560-5566.

8 Jonker, M.T.O., Hawthorne, S.B., Koelmans, A.A. 2005. Extremely slowly desorbing polycyclic aromatic hydrocarbons from soot and soot-like materials: Evidence by supercritical fluid extraction. Environ Sci Technol 39, 7889-7895.

9 Boonyatumanond, R., Murakami, M., Wattayakorn, G., Togo, A., Takada, H. 2007. Sources of polycyclic aromatic hydrocarbons (PAHs) in street dust in a tropical Asian mega-city, Bangkok, Thailand. Sci Total Environ 384, 420-432.

10 Fernandes, P.R.N., Soares, S.A., Nascimento, R.F., Soares, J.B., Cavalcante, R.M. 2009. Evaluation of polycyclic aromatic hydrocarbons in asphalt binder using matrix solid-phase dispersion and gas chromatography. J Chrom Sci 47 789-793.

11 Schauer, J.J., Kleeman, M.J., Cass, G.R., Simoneit, B.R.T. 2002. Measurement of emissions from air pollution sources. 5. C-1-C-32 organic compounds from gasoline-powered motor vehicles. Environ Sci Technol 36, 1169-1180.

12 Marr, L.C., Kirchstetter, T.W., Harley, R.A., Miguel, A.H., Hering, S.V., Hammond, S.K. 1999. Characterization of polycyclic aromatic hydrocarbons in motor vehicle fuels and exhaust emissions. Environ Sci Technol 33, 3091-3099.

13 Alkurdi, F., Karabet, F., Dimashki, M. 2013. Characterization, concentrations and emission rates of polycyclic aromatic hydrocarbons in the exhaust emissions from in-service vehicles in Damascus. Atmos Res 120, 68-77.

14 Schauer, J.J., Kleeman, M.J., Cass, G.R., Simoneit, B.R.T. 1999. Measurement of Emissions from Air Pollution Sources. 2. C1 through C30 Organic Compounds from Medium Duty Diesel Trucks. Environ Sci Technol 33, 1578-1587.

15 Mi, H.H., Lee, W.J., Chen, C.B., Yang, H.H., Wu, S.J. 2000. Effect of fuel aromatic content on PAH emission from a heavy-duty diesel engine. Chemosphere 41, 1783-1790.

16 Simon, V.M., L., Romdhana, M.H., Sablayrolles, C., Montrejaud-Vignoles, M., Lecomte, D. 2012. Emissions of polycyclic aromatic hydrocarbon particulates from combustion of different fuels. Fresenius Environmental Bulletin 21, 946-955.

17 Wang., J., Jia, C.R., Wong, C.K., Wong, P.K. 2000. Characterization of Polycyclic Aromatic Hydrocarbons Created in Lubricating Oils. Water, Air, and Soil Pollution 120 381-396.

18 Wang, Z.D., Yang C,. Yang, Z., Sun, J., Hollebone, B., Landriault, M. 2011. Forensic fingerprinting and source identification of the 2009 Sarnia (Ontario) oil spill. J Environ Monit 13: 3004-3017.

19 Liu X., Jia, H., Wang, L., Hong, Q., Ma, W., Hong, W., Guo, J., Yang, M., Sun, Y., Li, Y-F. 2013. Ecotoxicology and Environmental Safety 90 151-156.

20 Li, C.T., Mi, H.H., Li, W.J., Wang, Y.F. 1999. PAH emission from the industrial boilers. J Hazad Mater 69, 1-11.

21 Yang,H-H., Lee, W-J., Chen, S-J., Lai, S-O. 1998. PAH emission from various industrial stacks. J Hazardous Materials 60 159-174.

22 Shah, S.D., Ogunyoku, T.A., Miller, J.W., Cocker, D.R. 2005. On-road emission rates of PAH and n-alkane compounds from heavy-duty diesel vehicles. Environ Sci Technol 39, 5276-5284.

23 Khalili, N.R., Scheff, P.A., Holsen, T.M. 1995. PAH Source Fingerprints for Coke Ovens, Diesel and Gasoline-Engines, Highway Tunnels, and Wood Combustion Emissions. Atmos Environ 29, 533-542.

24 Nelson, P.F., Tibbett, A.R., Day, S.J. 2008. Effects of vehicle type and fuel quality on real world toxic emissions from diesel vehicles. Atmospheric Environment 42 5291-5303.

25 Watson, J.G., Fujita, E., Chow, J.C., Zielinska, B., Richards, L.W., Neff, W., Dietrich, D. 1998. Northern Front Range Air Quality Study. Available through: https://www.dri.edu/images/stories/editors/eafeditor/Watsonetal1998NFRAQSFinal.pdf.

26 Cadle, S.H., Mulawa, P.A., Hunsanger, E.C., Nelson, K., Ragazzi, R.A., Barrett, R., Gallagher, G.L., Lawson, D.R., Knapp, K.T., Snow, R. 1999. Composition of light-duty motor vehicle exhaust particulate matter in the Denver, Colorado Area. Environ Sci Technol 33, 2328-2339.

27 Schauer, J.J., Kleeman, M.J., Cass, G.R., Simoneit, B.R.T. 2001. Measurement of emissions from air pollution sources. 3. C-1-C-29 organic compounds from fireplace combustion of wood. Environ Sci Technol 35, 1716-1728.

28 Jenkins, B.M., Jones, A.D., Turn, S.Q., Williams, R.B. 1996. Emission factors for polycyclic aromatic hydrocarbons from biomass burning. Environ Sci Technol 30, 2462-2469.

29 Harrison, R.M., Smith, D.J.T., Luhana, L. 1996. Source apportionment of atmospheric polycyclic aromatic hydrocarbons collected from an urban location in Birmingham, UK. Environ Sci Technol 30, 825-832.

30 Wingfors, H., Sjodin, A., Haglund, P., Brorstrom-Lunden, E. 2001. Characterisation and determination of profiles of polycyclic aromatic hydrocarbons in a traffic tunnel in Gothenburg, Sweden. Atmospheric Environment 35 6361-6369.

31 Miguel, A.H., Kirchstetter, T.W., Harley, R.A., Hering, S.V. 1998. On-road emissions of particulate polycyclic aromatic hydrocarbons and black carbon from gasoline and diesel vehicles. Environ Sci Technol 32, 450-455.

32 Ringuet, J., Albinet, A., Leoz-Garziandia, E., Budzinski, H., Villenave, E. 2012. Diurnal/nocturnal concentrations and sources of particulate-bound PAHs, OPAHs and NPAHs at traffic and suburban sites in the region of Paris (France). Science of the Total Environment 437 297-305.

APPENDIX E: PMF Extracted PAH Fingerprints

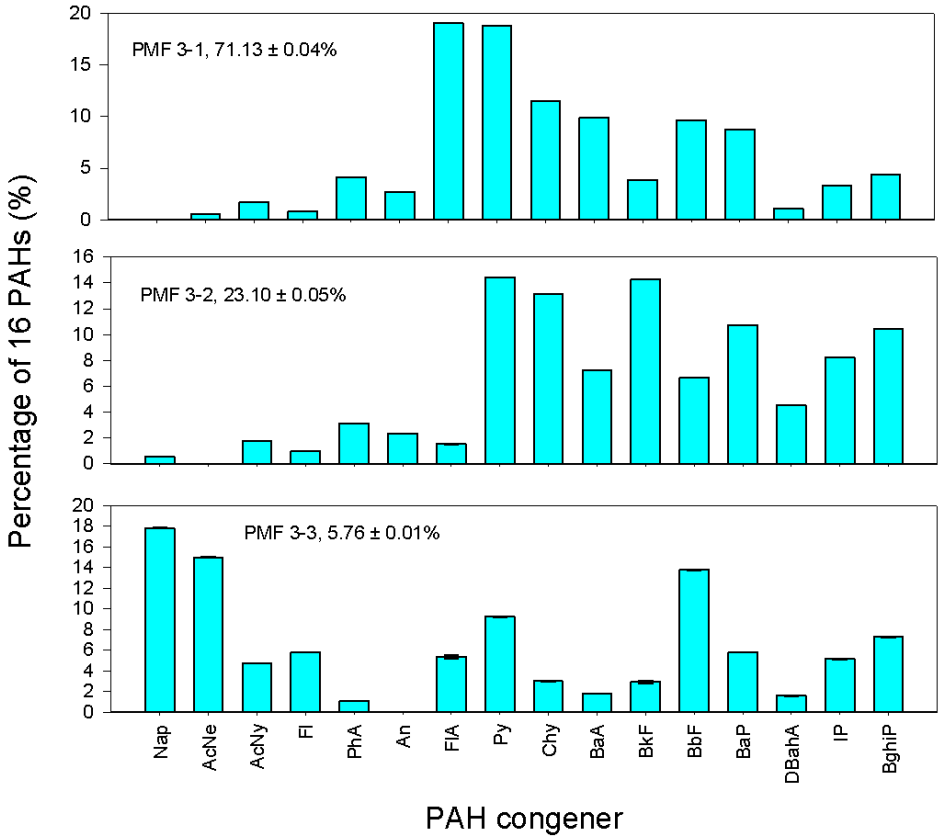

Figure E-1. PAH 3-factor fingerprints generated by PMF analysis.

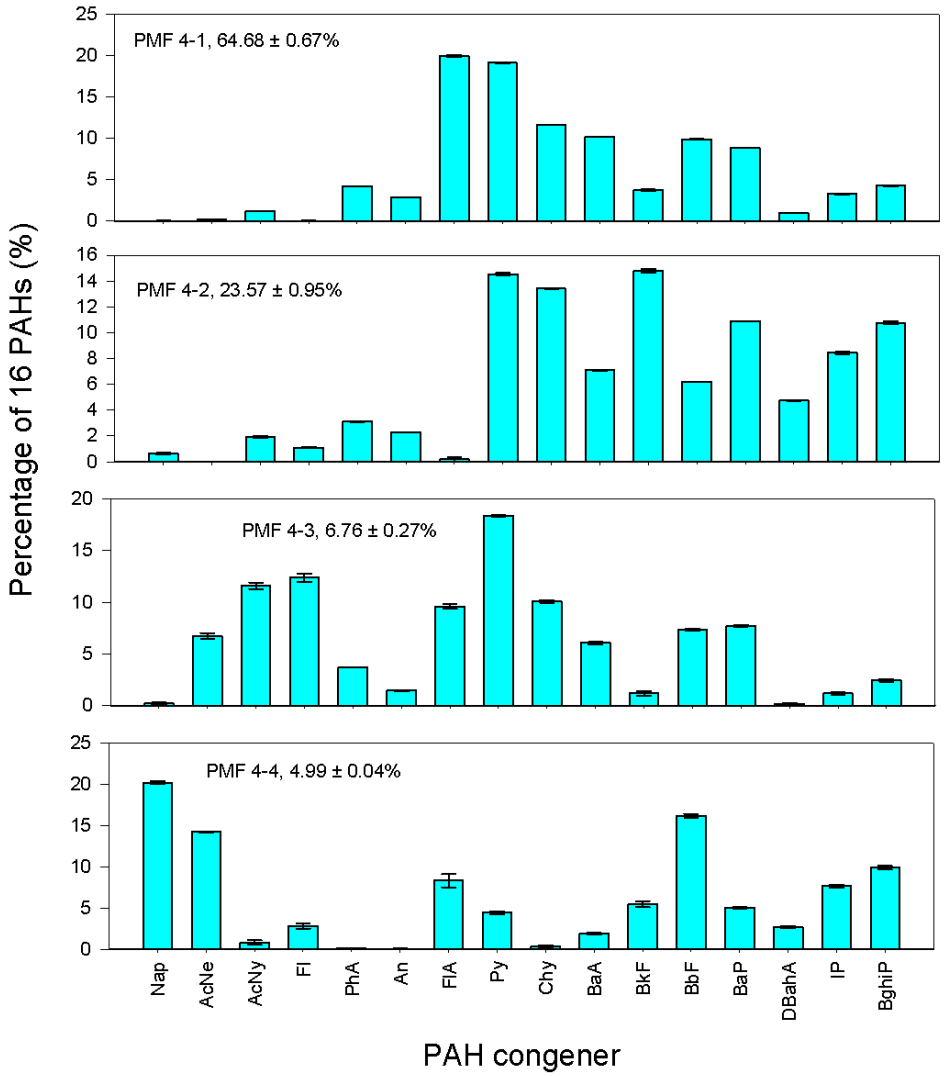

Figure E-2. PAH 4-factor fingerprints generated by PMF analysis.

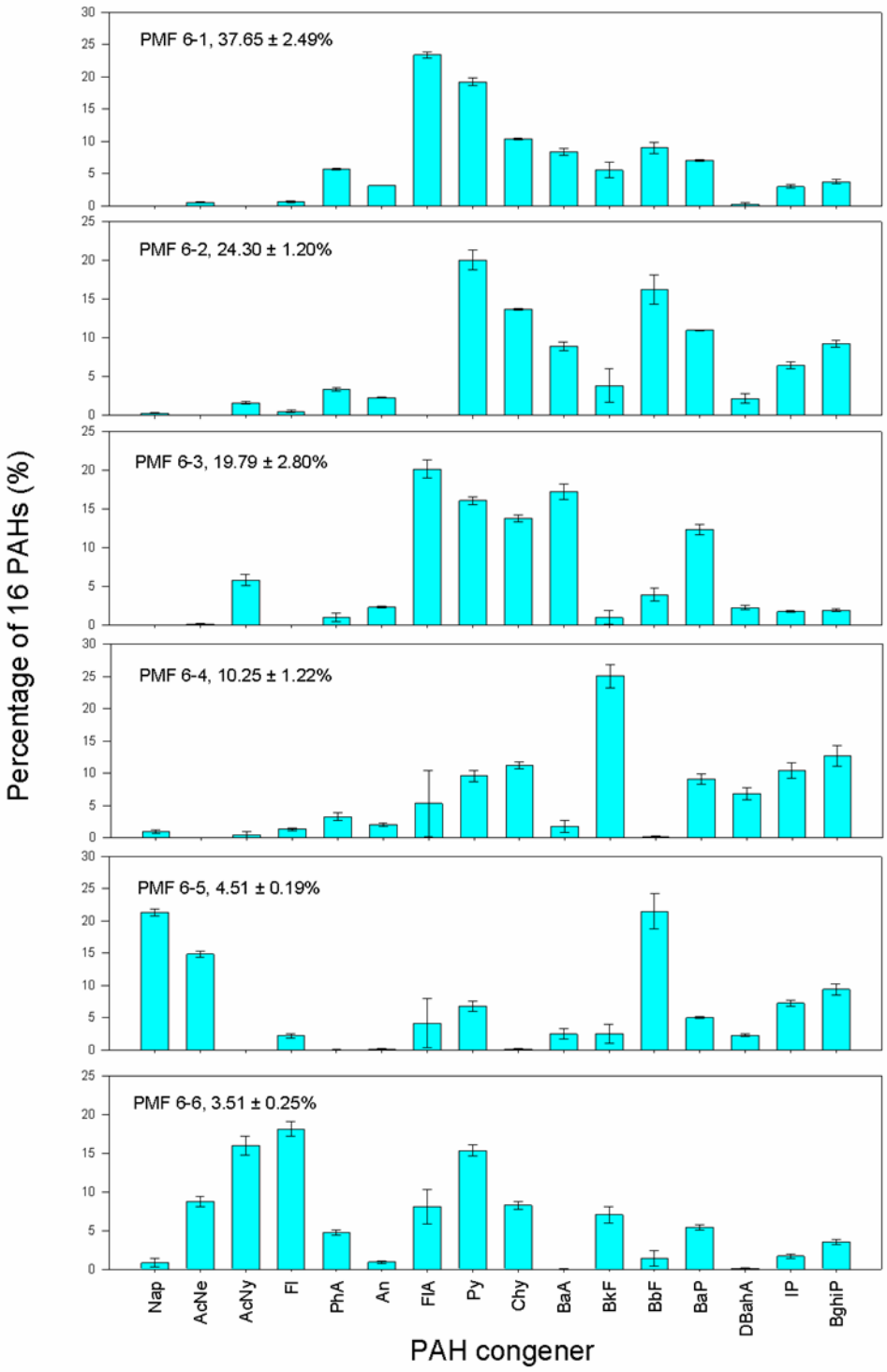

Figure E-3. PAH 6-factor fingerprints generated by PMF analysis.

APPENDIX F: PMF Extracted Metal Fingerprints

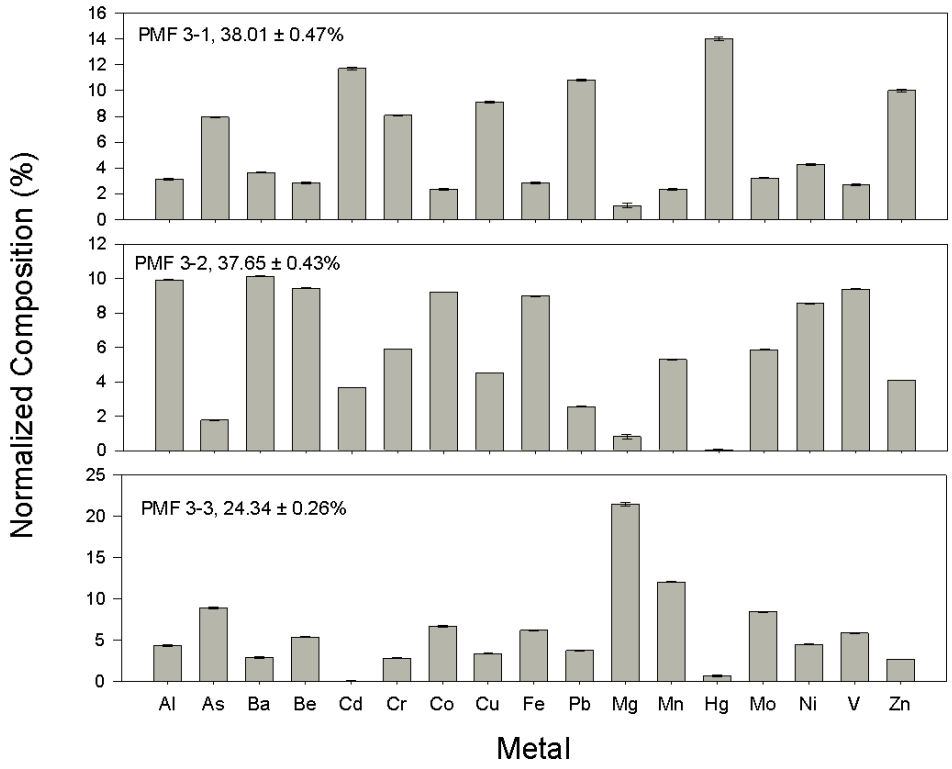

Figure F-1. Metal 3-factor fingerprints generated by PMF analysis.

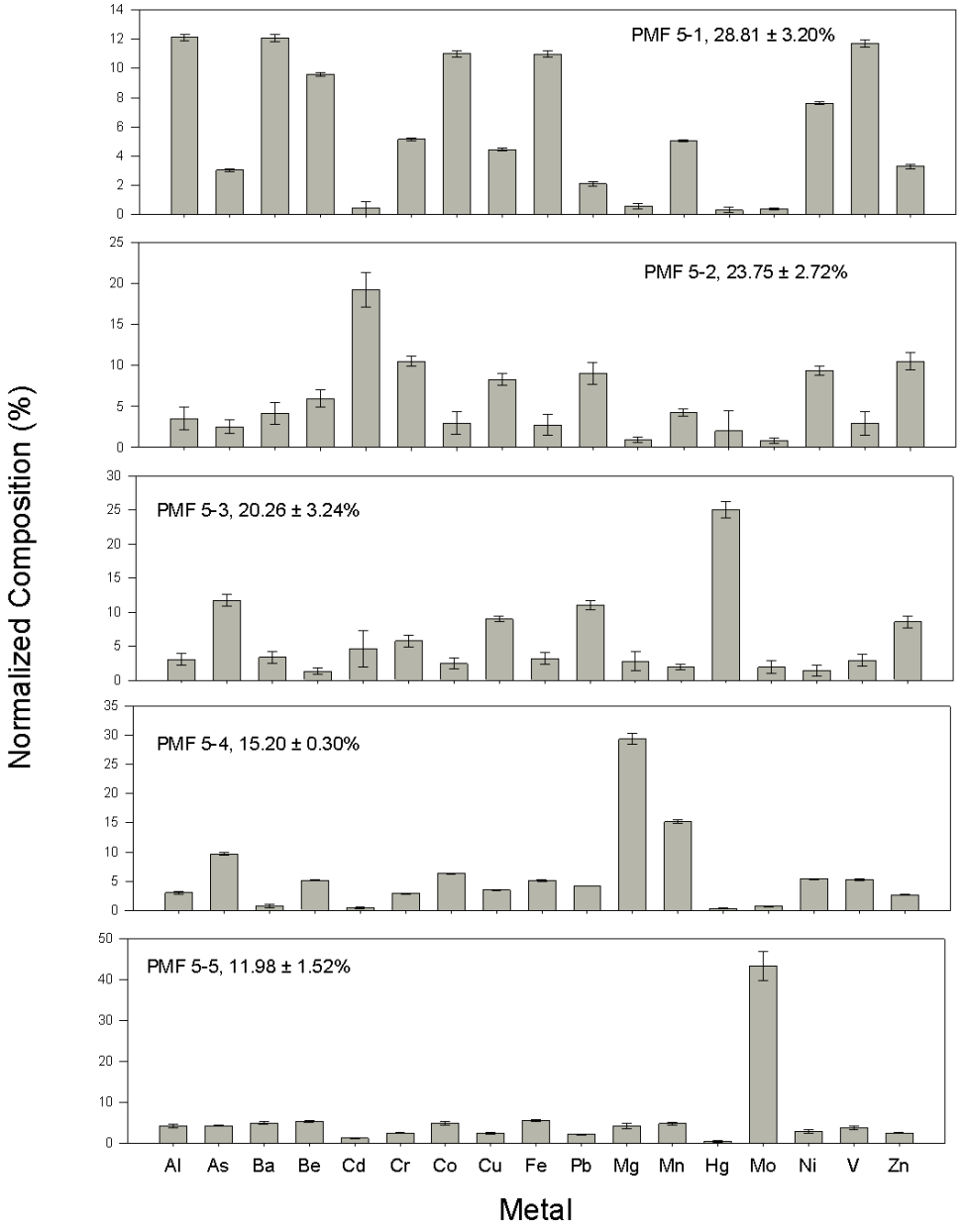

Figure F-2. Metal 5-factor fingerprints generated by PMF analysis.